Plastic shrinkage cracking in conventional and low volume fibre reinforced concrete

by
Riaan Combrinck

Thesis presented in partial fulfilment of the requirements for the degree
Master of Science in Engineering at the
University of Stellenbosch

Supervisor: Dr William Peter Boshoff
Faculty of Engineering
Department of Civil Engineering

March 2011

Declaration

By submitting this dissertation electronically, I declare that the entirety of the work contained therein is my own, original work, that I am the owner of the copyright thereof (unless to the extent explicitly otherwise stated) and that I have not previously in its entirety or in part submitted it for obtaining any qualification.

March 2011

Signature:

Summary

Plastic shrinkage cracking (PSC) is the cracking caused by the early age shrinkage of concrete within the first few hours after the concrete has been cast. It results in unsightly surface cracks that serve as pathways whereby corroding agents can penetrate the concrete which shortens the expected service life of a structure. PSC is primarily a problem at large exposed concrete surfaces for example bridge decks and slabs placed in environmental conditions with high evaporation rates.

Most precautionary measures for PSC are externally applied and aimed to reduce the water loss through evaporation. The addition of a low dosage of polymeric fibres to conventional concrete is an internal preventative measure which has been shown to reduce PSC. The mechanisms involved with PSC in conventional and low volume fibre reinforced concrete (LV-FRC) are however not clearly understood. This lack of knowledge and guidance leads to neglect and ineffective use of preventative measures. The objective of this study is to provide the fundamental understanding of the phenomena of PSC. To achieve the objective, an in depth background study and experiments were conducted on fresh conventional concrete and LV-FRC.

The three essential mechanisms required for PSC are: 1→ *Capillary pressure* build-up between the particles of the concrete is the source of shrinkage. 2→ *Air entry* into a concrete initiates cracking. 3→ *Restraint* of the concrete is required for crack forming.

The experiments showed the following significant findings for conventional and LV-FRC: PSC is only possible once all the bleeding water at the surface has evaporated and once air entry has occurred. The critical period where the majority of the PSC occurs is between the initial and final set of concrete. Any preventative measure for PSC is most effective during this period. The bleeding characteristics of a mix have a significant influence on PSC. Adding a low volume of polymeric fibres to concrete reduces PSC due to the added resistance that fibres give to crack widening, which increases significantly from the start of the critical period.

The fundamental knowledge gained from this study can be utilized to develop a practical model for the design and prevention of PSC in conventional concrete and LV-FRC.

Opsomming

Plastiese krimp krake (PSK) is die krake wat gevorm word a.g.v. die vroeë krimping van beton binne die eerste paar ure nadat die beton gegiet is. Dit veroorsaak onooglike oppervlak krake wat dien as kanale waardeur korrosie agente die beton kan binnedring om so die dienstydperk van die struktuur te verkort. Dit is hoofsaaklik ’n probleem by groot blootgestelde beton oppervlaktes soos brug dekke en blaaie wat gegiet is in klimaat kondisies met hoë verdamping tempo’s.

Meeste voorsorgmaatreëls vir PSK word ekstern aangewend en beperk die water verlies as gevolg van verdamping. Die byvoeging van ’n lae volume polimeriese vesels is ’n interne voorsorgmaatreël wat bekend is om PSK te verminder. Die meganismes betrokke ten opsigte van PSK in gewone beton en lae volume vesel versterkte beton (LV-VVB) is vaag. Die vaagheid en tekort aan riglyne lei tot nalatigheid en oneffektiewe aanwending van voorsorgmaatreëls. Die doel van die studie is om die fundamentele kennis oor die fenomeen van PSK te gee. Om die doel te bereik is ’n indiepte agtergrond studie en eksperimente uitgevoer op gewone beton en LV-VVB.

Die drie meganismes benodig vir PSK is: 1→ *Kapillêre druk* tussen die deeltjies van die beton is die hoof bron van krimping. 2→ *Lugindringing* in die beton wat krake inisieer. 3→ *Inklemming* van die beton is noodsaaklik vir kraakvorming.

Die eksperimente het die volgende noemenswaardige bevindinge opgelewer: PSK is slegs moontlik indien al die bloeiwater van die beton oppervlakte verdamp het en indien lug die beton ingedring het. Die kritiese periode waar die meerderheid van die PSK plaasvind is tussen die aanvanklike en finale set van die beton. Enige voorsorgmaatreël vir PSK is mees effektief gedurende die periode. Die bloei eienskappe van ’n meng het ’n noemenswaardige effek op die PSK. Die byvoeging van ’n lae volume polimeriese vesels tot beton verminder die PSK deur die addisionele weerstand wat die vesels bied teen die toename in kraakwydte. Die weerstand vergroot noemenswaardig vanaf die begin van die kritiese periode.

Die fundamentele kennis wat in die studie opgedoen is, kan gebruik word vir die ontwikkeling van ’n praktiese model vir die ontwerp en verhoed van PSK in gewone beton en LV-VVB.

Acknowledgements

I would like to thank the following people for the assistance and support during this study.

- My promoter, Dr Billy Boshoff for allowing sufficient space to grow and learn, by giving guidance when needed and for continuous support.

- The staff in the laboratory and workshop at the Civil Engineering Department of the University of Stellenbosch, for their assistance and time during the experimental work.

- Marko Butler, Rabea Barhum and Frank Altmann at TU-Dresden in Germany for their hospitality and assistance during my stay in Dresden.

- My parents for their unconditional support.

- My fiancé, Maretha van Zyl, for her support, love, friendship and needed distraction during this time.

- Finally, my Creator, for giving me the opportunity and ability to complete this study.

Contents

List of figures

List of tables

List of appendices

Notations and acronyms

Notations:

d	Fibre diameter
ER	Evaporation rate [kg/m^2/h]
F	Average maximum pullout force
L	Fibre length
Le	Fibre embedment length
P	Capillary pressure
R_1	Maximum radius of water meniscus
R_2	Minimum radius of water meniscus
r	Relative humidity [%]
T_a	Air temperature [°C]
T_{AE}	Time of air entry
T_{BE}	Time when bleeding measurements ended
T_c	Concrete temperature [°C]
T_{CS}	Time of crack stabilization
T_D	Drying time
T_{FS}	Final setting time
T_{IS}	Initial setting time
T_{OC}	Time of crack onset
V	Wind velocity [km/h]
V_f	Volume fraction of fibres added to mix
τ	Interfacial shear bond stress
σ	Surface tension
σ_c	Ultimate bridging stress over unit crack area

Acronyms:

ASTM	American Standard Testing Methods
COV	Coefficient of variance
FPP	Fluorinated polypropylene

GPa	Gigapascal
LV-FRC	Low volume fibre reinforced concrete
MPa	Megapascal
M1A	Mix 1 Accelerated
M1FPP	Mix 1 Fluorinated Polypropylene
M1B	Mix 1 Bleeding
M1PES	Mix 1 Polyester
M1PP	Mix 1 Polypropylene
M1R	Mix 1 Retarded
M1S	Mix 1 Standard
M2FPP	Mix 2 Fluorinated Polypropylene
M2PES	Mix 2 Polyester
M2PP	Mix 2 Polypropylene
M2S	Mix 2 Standard
NRMCA	National Ready Mixed Concrete Association
OPC	Ordinary Portland Cement
PSC	Plastic shrinkage cracking
PES	Polyester
PP	Polypropylene
PVC	Polyvinylchloride
SANS	South African National Standards

1. Introduction

Plastic shrinkage cracking (PSC) is the early age shrinkage of concrete due to evaporation. PSC occurs within the first few hours after the concrete has been cast and results in unsightly surface cracks. These cracks are not only unsightly, but also serves as pathways whereby corroding agents such as water, chloride and oxygen can penetrate the concrete. This accelerates the corrosion of the reinforcing steel and hereby brings into question the structural integrity of a structure. PSC is primarily a problem for large exposed concrete surfaces like bridge decks and building slabs placed in environmental conditions with high evaporation rates.

The long term cracking of concrete through shrinkage is unavoidable and is a big source of durability and maintenance problems associated with a concrete structure. The earlier the cracking occurs the shorter the expected service life of any given structure. Cracking is caused by several mechanisms, each of which has a pronounced effect at a certain time during a concretes lifespan. PSC is the earliest form of cracking in concrete. The correct building practices can in most cases prevent PSC, especially since PSC occurs in a relatively short time period. However, these practices are often neglected or ineffective due to the lack of knowledge and guidance.

Most precautionary measures for PSC are externally applied and aimed to reduce or control the water loss through evaporation. The addition of a low dosage of polymeric fibres to conventional concrete, normally in the order of 0.1 % to 0.2 % by volume, is an internal preventative measure which has been shown to reduce PSC (Illston et al., 2001:420 and Wongtanakitcharoen, 2005:2). The mechanisms involved with PSC in conventional and low volume fibre reinforced concrete (LV-FRC) are however not clearly understood. This lack of knowledge and guidance leads to neglect and ineffective use of preventative measures.

This study forms an integral part of a larger research project and has the following ***objectives***:

- To provide a fundamental understanding of the phenomena of PSC
- To shed light on the principles involved for the improved performance of LV-FRC compared to conventional concrete with regards to PSC.
- To serve as fundamental basis from where guidelines for the application of LV-FRC can be developed.

The following ***methodology*** was adopted to achieve the objectives of this study:

1. Gain a fundamental understanding of PSC in conventional concrete. This involved a broad background study that covers PSC in general, the mechanisms causing PSC as well as the factors influencing PSC.
2. The background study served as a basis to identify, propose and test certain phenomena and theses associated with PSC in conventional concrete. The main emphasis was on gaining knowledge in order to identify the time when PSC starts and ends. This is key information needed for preventing PSC. Furthermore, the experiments conducted in this study were aimed at investigating the validity of these proposed theses.
3. Once PSC was fundamentally understood in conventional concrete the influence of a low volume addition of polymeric fibres on PSC was investigated. This involved a background study on LV-FRC and experiments where fibres were added to the same mixes used for the experiments on conventional concrete.
4. Finally, single fibre pullout tests of fibres from fresh concrete paste were conducted to investigate the resistance that fibres give to crack widening as a function of time.

To conduct the experiments on PSC in conventional and LV-FRC a climate chamber setup was purposefully developed for creating the ideal conditions for PSC in concrete.

In terms of ***research significance***, this study is an in depth study on PSC which aims to give a fundamental understanding of the phenomena of PSC in conventional concrete and LV-FRC. The fundamental understanding of PSC will facilitate the development of practical guidelines

for the prevention of PSC in a South African context. The problem of PSC is related to harsh drying conditions which is typical for the South African climate. The guidelines will be the first of its kind not only in South Africa but also internationally. It will enable contractors, engineers and concrete suppliers to assess the potential for PSC for a specific circumstance, followed by the appropriate guidance of the needed preventative measure. This will lead to concrete structures with much higher quality, durability and performance, which reduces maintenance and construction cost in the long term. With the current drive towards infrastructure spending in South Africa it is extremely important to construct durable infrastructure since less or little maintenance will be required over the lifespan of the infrastructure. It will also create safer, more usable and aesthetical pleasing structures which can only result in a positive effect on economic growth.

The report has the following basic ***layout***:

- In *Chapter 2* a theoretical background is given on PSC. First, PSC in conventional concrete is considered in terms of precautionary measures, mechanisms and influencing factors. Finally, LV-FRC is also considered.
- In *Chapter 3* the experimental framework is explained in terms of setup, objectives, materials, mix proportions and testing procedures for the PSC and single fibre pullout experiments.
- In *Chapter 4* the results of the experiments are given.
- In *Chapter 5* the results are discussed.
- In *Chapter 6* the final conclusions are drawn and possible future prospects are set out.
- The *Appendices* contains all the detail of the climate chamber design and performance as well as complete summaries of all the experimental results.

2. Background study on plastic shrinkage cracking (PSC)

This chapter reports the fundamental knowledge required to understand plastic shrinkage cracking (PSC) in freshly cast concrete. It begins with an introduction as overview and various precautionary methods for PSC. This is followed by sections about the mechanisms needed to cause cracking and all the factors that can influence PSC. Finally, low volume fibre reinforced concrete (LV-FRC) is discussed.

2.1. *Introduction to PSC*

The term: *plastic shrinkage cracking (PSC) of concrete,* can be explained by looking at the definition of the individual words.

PSC occurs in *concrete*, where concrete is a mixture of cement, water, fine aggregate (sand) and coarse aggregate (gravel or crushed rock) in which the cement and water have hardened by a chemical reaction called hydration (Illston et al., 2001:93).

Plastic refers to the state of matter in which the concrete finds itself. A material capable of being moulded or shaped is plastic (Powers, 1968:446) and behaves similar to a fluid or liquid. A plastic concrete is still in the liquid or fluid phase which occurs only for a few hours after water has been added to the rest of the concrete constituents. The plastic phase ends when the concrete becomes unworkable, which means that concrete placement, compaction and finishing becomes difficult. This point in time is called the initial set of concrete (Garcia et al., 2008:446).

Shrinkage refers to a volume reduction. The volume reduction of the concrete during the plastic phase is mainly caused by the loss of water due to evaporation.

Finally, *cracking* occurs in the concrete due to the restrained shrinkage or volume reduction. The cracks can only form if the concrete is restrained and if no restraint is present the concrete will shrink freely with no cracks (Addis, 1998:15).

In this study the term *plastic shrinkage cracking (PSC)* refers to the entire phenomena of shrinkage of concrete and the associated cracking in the plastic phase. The term *plastic shrinkage* refers only to the shrinkage and does not necessarily lead to cracks.

PSC is mainly a problem with large exposed surfaces for example bridge decks and building slabs placed in environmental conditions with a high evaporation rate. The faster the water evaporates from the concrete surface the more shrinkage occurs, which relates to a larger potential for cracking. A high evaporation rate is caused by conditions with high temperature (often associated with direct sunlight), high wind speeds and low relative humidity (Addis, 1998:15). The potential for PSC is also high for mixes with a high fine content, for example ultra high performance concrete and self compacting concrete.

From an aesthetical point of view PSC results in unsightly surface cracks which give a non-uniform appearance of the concrete surface. In some cases cracks can penetrate the full depth of the concrete slab (Addis, 1998:15).

More importantly, PSC results in serious durability issues due to the possibility of corroding agents infiltrating the concrete through the cracks. This accelerates the reinforcing steel corrosion and the concrete deterioration that consequently gives a reduction in the performance, serviceability and durability of the concrete structure (Deif et al., 2009:1110 and Wongtanakitcharoen, 2005:1). Furthermore, cracks formed during the plastic stage of the concrete may later lead to large shrinkage cracks during the long-term drying of the hardened concrete structure, which again results in durability issues (Slowik et al., 2009:476).

Other issues, such as the abrasion resistance and curling of floors are normally not influenced by PSC. Abrasion is the deterioration of a floor surface due to the rolling and sliding of objects across it. The quality of the concrete surface is mainly influenced by the quality of the concrete, surface finishing, curing, choice of coarse aggregates and surface treatments. In general, high amounts of bleeding water degrades the quality of the concrete surface and results in a low abrasion resistance, whereas low amounts of bleeding water

results in a high quality concrete surface with high abrasion resistance (Marias et al., 1993:111). Since PSC is mainly a problem for concrete mixes with low amounts of bleeding water, it is concluded that the abrasion resistance of such concrete surfaces is normally sufficient. Curling of floors is typically caused by differential drying shrinkage which occurs when the top and bottom surfaces of a concrete floor is subjected to different drying conditions. This mainly occurs during the drying of hardened concrete, long after the plastic stage of the concrete (Marias et al., 1993:57). Therefore, PSC seldom causes the curling of floors.

2.2. *Precautionary measures for PSC*

Since the ideal conditions for PSC are common in South Africa, it is essential to be aware of the possible preventative measures. The standard precautions used to minimize PSC can be divided into two groups: the external and the internal precautionary measures.

External precautionary measures (Uno, 1998:374 and NRMCA, 2006:2):

- Temporary wind breaks are used to reduce the air flow over the concrete surface which hinders rapid evaporation
- Casting of concrete early in the morning, late in the afternoon or at night as well as using sunshades and adding ice to the mixing water, all minimizes the concrete temperature which reduces evaporation
- Curing the concrete surface during the plastic stage with a fog spray, liquid membrane curing compound or covering the surface with wet burlap or polyethylene sheeting also reduces evaporation
- Using evaporative retarders such as aliphatic alcohols
- Lightly moistening the sub-grade and formwork prior to casting will minimize their water absorption which reduces water loss

Internal precautionary measures (Uno, 1998:374):

- Adding random distributed synthetic fibres in the concrete mix reduces the size and distribution of PSC

- Avoid excess use of retarders which prolongs the setting time and therefore increases the risk for PSC
- Accelerators can be used to shorten the setting time which decreases the risk for PSC
- Avoid or limit excessive fine content (cement and cement replacement materials for example fly ash and silica fumes) which increase the risk for PSC by reducing the bleeding rate and increasing the shrinkage or volume reduction.

2.3. *Mechanisms causing PSC*

The focus of the following section is on the mechanisms causing PSC namely: capillary pressure, air entry and restraint. If one of these mechanisms is missing, no cracks will form.

2.3.1. Capillary pressure

The origin of plastic shrinkage is capillary pressure. This was confirmed by Wittman (1976:56) more than three decades ago. It is therefore safe to conclude that the main mechanism which causes plastic shrinkage is capillary pressure. Capillary pressure is caused by water evaporation from the concrete surface. The more water evaporates the more concave the water surfaces between the particles become. These concave water surfaces are called water menisci which causes a negative pressure in the capillary water.

According to the Gauss-Laplace equation (Equation 2.1), the pressure *P* is inversely proportional to the main radii of the water surface as well as the surface tension σ of the liquid. This pressure acts on the surrounding particles and tends to suck all these particles closer together (Slowik et al., 2008:558). This is called plastic shrinkage and is referred to as capillary shrinkage by some authors to avoid any confusion from the fact that plastic shrinkage is caused by capillary pressure. Figure 2.1 shows the meaning of the radii in Equation 2.1 and also shows the force acting on the particles due to the capillary pressure as well as the vertical and horizontal component of the force. The smaller the radii of the menisci, the larger the capillary pressure P.

$$P = -\sigma\left(\frac{1}{R_1} + \frac{1}{R_2}\right) \quad \text{..... (Equation 2.1)}$$

with:

P = capillary pressure

σ = surface tension

R_1= maximum radius of water meniscus

R_2= minimum radius of water meniscus

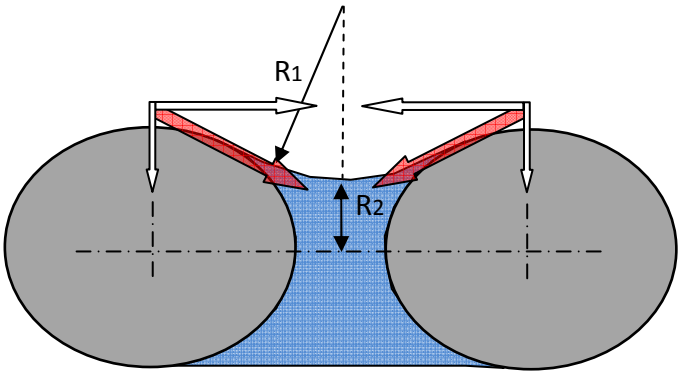

Figure 2.1: Meniscus forming in capillary pore

2.3.2. Air entry

Evaporation continuously decreases the main radii of the menisci between the solid particles at the concrete surface which causes a rising capillary pressure build-up. At a certain capillary pressure air enters the concrete surface at a local position and not simultaneously over the entire concrete surface because of the irregular arrangement of solid particles. The air enters because the radius of meniscus between the particles becomes too small to the bridge the gap between the particles. The system has now become unstable which causes a relocation of pore water. The positions where air entry has occurred are weak spots where cracks could form (Slowik et al., 2008:558).

This air entry pressure was first observed by Wittman (1976), followed by more research through Slowik et al. (2008), where it is stated that cracks are impossible to form without air entry into a drying surface. It can be concluded that the mechanism that initializes cracks associated with plastic shrinkage is air entry.

2.3.3. Restraint

The position where air entry has occurred does not immediately form a crack and is merely a pore filled with air instead of water. Plastic shrinkage alone will also not form any cracks, because the material will shrink uniformly with no cracking and just a change in volume

(shrinkage). The other mechanism needed to form a physical crack after the crack has been initialized by air entry is restraint (Addis, 1998:15). If the shrinkage is restrained, cracks could form to facilitate the change in volume of the material. The restraint is ever present and is a result of external and internal boundary conditions. See Section 2.4.4 for more details on restraint.

2.4. *Factors influencing PSC*

The factors that influence PSC are diverse and all seem to be interdependent. This means that by changing one aspect, you could have an influence on several other factors that also influences PSC. For example, the use of a different cement type changes the bleeding characteristics, capillary pressure build-up, paste mobility as well as the heat of hydration which influences the evaporation and setting times. The evolution of time complicates PSC even further as most of these factors changes continuously with time due to hydration. In the following sections, seven factors that influence PSC are highlighted.

2.4.1. Capillary pressure build-up

Since capillary pressure is the main mechanism that causes PSC it is important to know how it is influenced. The main factors which determine capillary pressure build-up are the rate of water loss, evaporation, bleeding and the material composition.

2.4.1.1. *Rate of water loss*

The rate at which water is lost from the surface of the concrete depends on the rate of evaporation and bleeding. Water that evaporates from the surface is constantly replenished by bleeding water from inside the concrete paste. Once the rate of water evaporation from the concrete surface exceeds the rate at which bleeding water is supplied to the surface PSC can be expected. The higher the rate of water loss from a concrete surface the faster the capillary pressure build-up.

2.4.1.2. *Evaporation*

Evaporation is the process by which a liquid is converted into a vapour or gas. The liquid molecules can escape the liquid as vapour through heat absorption or where the pressure above the liquid surface is less than in the liquid (Uno, 1998:368). Equation 2.2 was developed by Uno (1998:368) to calculate the evaporation from a concrete surface.

$$ER = 5([T_c - 18]^{2.5} - r[T_c + 18]^{2.5})(V + 4) \times 10^{-6}$$ ..... (Equation 2.2)

with:

ER = evaporation rate [kg/m^2/h]

T_c = concrete temperature [°C]

T_a = air temperature [°C]

r = relative humidity [%]

V = wind velocity [km/h]

The main conditions that determine the evaporation rate are: wind velocity, relative humidity, air temperature, concrete temperature and solar radiation. A discussion of these five conditions follows:

Wind

Wind accelerates the evaporation process by continually removing escaping water molecules from the liquid into the atmosphere (Uno, 1998:368-371). Protecting a freshly cast concrete specimen from wind, is considered to be one of the most effective ways to reduce PSC (Kwak et al., 2006:531). As higher wind speed dramatically increase the evaporation rate.

Relative humidity

The relative humidity refers to the combination of air temperature and water vapour in the air, i.e. that air with a certain temperature can only hold a certain amount of water vapour. The higher the air temperature the more water vapour can evaporate into the air. A 100 % relative humidity means that the air is fully saturated with water vapour and does not allow any additional evaporation (Uno, 1998:371). If the temperature increases suddenly it lowers the relative humidity for example from 100 % to 90 %, which now allows more water to evaporate into the air. The lower the relative humidity the faster water will evaporate.

Air temperature

Air temperature influences the relative humidity as well as the concrete temperature. It should be mentioned that air temperature does not include direct solar radiation (Uno, 1998:371). A higher air temperature increases the rate of water evaporation.

Concrete temperature

The concrete temperature is mostly influenced by the temperature of all the concrete material constituents (water, cement, fine and coarse aggregate) when mixed together as well as the air temperature, formwork or sub-grade temperature and the solar radiation after casting. The heat released by the hydration reaction between cement and water may also increase the concrete temperature. The higher the temperature of the concrete the faster water will evaporate. Reducing the temperature of freshly cast concrete is considered to be one of the most effective ways to reduce the evaporation rate (Kwak et al., 2006:531).

Solar radiation

Water surfaces exposed to direct sun rays (solar radiation) evaporate faster. This also applies for freshly cast concrete surfaces, but opinions still differ concerning its effect on PSC. Some researcher say shielding concrete specimens from the sun will reduce the evaporation rate, which in turn will reduce the risk for PSC. Other researchers found that although specimens exposed to direct sunlight had increased evaporation, they also showed an increased rate of hydration which shortens the time available for PSC and therefore reduced the risk (Uno, 1998:371-372).

However, it can be speculated that an increased evaporation rate due to direct sunlight will increase the risk for PSC, since these cracks normally occur within 2 to 3 hours after casting, when the degree of hydration is still low even with a possible increased rate of hydration. Furthermore, the extra hydration heat will increase the concrete temperature, which will further increase the evaporation rate.

2.4.1.3. *Bleeding*

To understand bleeding it is necessary to consider the nature and the composition of fresh concrete. A basic fresh concrete consists of water, cement, fine aggregate (sand) and coarse

aggregate (stone). The aggregate in concrete is dispersed by the cement paste (water and cement particles); and the cement particles are dispersed by water. The dispersion and suspension of all solids in fresh concrete occur during the mixing process. The initial state of freshly cast concrete is not stable, because the solids in the concrete are denser than water and tend to settle downwards due to gravitational forces. The settlement of solid particles will stop once equilibrium interparticle distance has been reached, which occurs when the combined forces of electrostatic repulsion and increased disjoining pressure of absorbed water are equal to the gravitational forces acting on the particle. As the solids settle downwards it displaces water upwards which accumulates at the surface of the concrete and is called bleeding water. Bleeding is therefore caused by the settlement of solid particles. The end of settlement can be caused by either the process of settlement ceasing mechanically, or due to the setting of the concrete which arrests the settlement by filling the interparticle gaps with hydration products (Powers, 1968:533-535).

Two types of bleeding can be distinguished: Normal bleeding and channel bleeding. Normal bleeding is caused by particle settlement due to gravitation as explained in the previous paragraph. Channel bleeding may occur in addition to normal bleeding. Channel bleeding occurs when a number of localized channels develop in the concrete whereby water as well as small solid particles can be transported from the interior of the concrete to the surface. The rate of channel bleeding is much higher than for normal bleeding and can be identified by the formation of small craters around the mouth of the channel. Channel bleeding normally occurs when mixes are too wet and lacks cohesion (Powers, 1968:533-535).

For normal bleeding there are two important aspects to consider: the rate of bleeding and the total amount of bleeding. The rate of bleeding under conditions with no capillary pressure can be divided into two periods: first a constant bleeding rate period, followed by a period where the rate diminishes gradually to zero (Powers, 1968:534-535). The following material properties and processes will influence the bleeding characteristics:

Permeability

The permeability of the fresh concrete has the biggest influence on the rate of bleeding. Permeability is the property that governs the rate of flow of a fluid into or through a porous solid (Mehta et al., 2006:126). Fresh concrete paste can be described as a porous material/solid consisting of dispersed solid particles with an interconnected pore system. As bleeding water is displaced upwards by particle settlement it needs to flow through the fresh concrete paste to reach the surface. The less permeable the concrete paste the slower the water flows through the concrete which leads to a lower bleeding rate.

The permeability of the concrete depends on the fines content. The bleeding rate decreases with an increase of fine content. Fines are mostly cement, fly ash and the dust content of the fine aggregates. The fines not only retards movement of water by making the paste less permeable but also settles slower due to a smaller gravitational force acting on them. This also causes a lower bleeding rate. The fines content are often increased due to an increase of cement particles which causes an increased hydration rate and more hydration products. This results in a less permeable paste and, in turn, also results in a lower bleeding rate (Suhr et al., 1990:38).

Water absorption

The internal absorption of water through unsaturated aggregate particles as well as the external absorption through unsaturated formwork or sub-grade will decrease the total amount of bleeding (Powers, 1968:535).

Aggregate content and degree of dispersion

Aggregate has relative densities of about 2.5-2.8 times that of water and hence it tends to subside to the bottom of freshly cast concrete, which displaces the water upwards. The heavier the aggregates the bigger the gravitational force acting on them. This results in more settlement which increases the total amount of bleeding. The bleeding amount increases with increasing aggregate size and quantity (Kwak et al., 2006:524).

The degree of dispersion of the aggregate is also important. If the aggregate is uniformly dispersed throughout the cement paste it will increase the bleeding amount, since the aggregate has sufficient space to settle unhindered by other aggregates. This is called a high degree of dispersion. A low degree of dispersion means that the aggregate is spaced unevenly and to close to each other in certain regions which decreases or hinders settlement and therefore the total amount of bleeding (Powers, 1968:535).

Unit water content

The total amount of bleeding increases with an increase in water content (Kwak et al., 2006:523-524).

Slab depth

The amount of bleeding water is proportional to the depth of the concrete specimen (Kwak et al., 2006:524-525). This means that a deeper concrete specimen will yield more bleeding as more particle settlement can occur.

Hydration

The filling of interparticle gaps by hydration products decreases the rate and the total amount of bleeding (Powers, 1968:535).

Capillary pressure

Capillary pressure starts to develop once the amount of water evaporated from the concrete surface exceeds the amount of bleeding water at the surface. As explained in Section 2.3.1, capillary pressure is caused by menisci forming between the solid particles which tend to suck the particles together. The force caused by the menisci has a vertical and a horizontal component as shown in Figure 2.1. The vertical component forces the particles downwards which displace water upwards. This relieves or decreases the capillary pressure because the additional water displaced upwards increased the radius of the menisci. Capillary pressure thus results in additional settlement of particles which results in an increase of bleeding rate and total amount of bleeding. The increase of bleeding rate due to capillary pressure can be as much as the evaporation rate or the rate needed to relieve the capillary pressure build-up (Powers, 1968:591).

Vibration

Vibration with a low intensity and short duration does not have a pronounced effect on the total bleeding amount. Prolonged vibration could however lower the degree of dispersion of the aggregate which will decrease the total bleeding amount. This is due to the fluidizing effect of vibration which allows the aggregate to settle through the paste. External vibration due to machinery or by other means may also increase the rate of bleeding (Powers, 1968:584).

2.4.1.4. *Material composition*

Material composition concerns the size and distribution of the small solid particles in a concrete paste for example: cement, fly ash and fine sand.

Size

Equation 2.1 shows that the capillary pressure increases with a decrease of the radii of the menisci. Smaller particles also have smaller meniscus radii between them. In general, the lower the average sizes of the solid particles in a concrete paste, the higher the capillary pressure build-up (Slowik et al., 2009:466-467).

Distribution

The distribution and quantity of the particle sizes through the concrete influence the magnitude of the capillary pressure values reached (Slowik et al., 2009:466-468). For example, if a certain volume of small particles are located next to one another at the surface of the concrete it will result in a high capillary pressure. This is due to the many small menisci between the small particles. The same volume filled with larger particles would have resulted in a much lower capillary pressure as the larger particles would be less over the same volume with larger menisci between them.

2.4.2. Air entry pressure

Air entry pressure is the second factor that influences PSC. When air enters into a concrete paste, the risk for cracking is assumed to be at its maximum, because the positions of air entry form weak points on the concrete surface (Slowik et al., 2008:558). It is important to

identify the time and position at which air enters the paste because it initializes cracking i.e. cracking can only start once air has penetrated the paste. Six different stages (A - F) during capillary pressure build-up, including air entry and cracking, are shown in Figure 2.2 and are explained as follows:

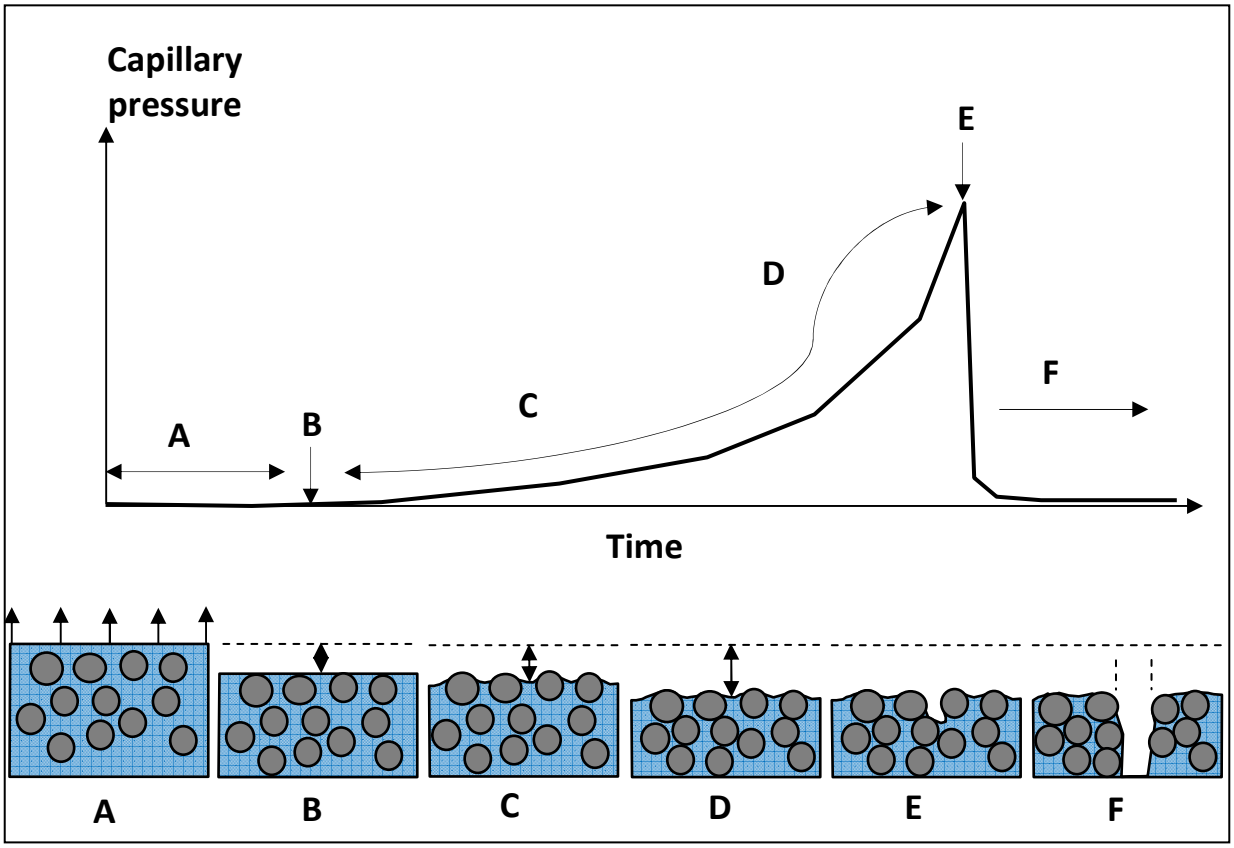

Figure 2.2: Stages during capillary pressure build-up

Stage A:

This is the stage directly after concrete casting during which a thin film of water is still present on the surface of the concrete paste. The rate of bleeding is initially more than the rate of evaporation for this stage.

Stage B:

This is the point when the amount of bleeding water that has come to the surface of the concrete as a result of particle settlement, is equal to the amount of water that has evaporated from the concrete surface. From this point forward capillary pressure develops.

Stage C:

During this stage the bleeding rate is less than the evaporation rate and menisci start forming between the particles which tends to pull the particles together. This results in the capillary pressure building up.

Stage D:

The capillary pressure has a vertical and horizontal component as shown in Figure 2.1. During this stage the vertical component of the capillary forces the particles downwards which displaces additional water upward that relieves the capillary pressure (Powers, 1968:585-590). Even though the capillary pressure is slightly relieved, the rate of capillary pressure build-up increases strongly due to the evaporation. This stage ends when the maximum vertical settlement is reached (Slowik et al., 2008:564).

Stage E:

This is the point in time where air enters into the concrete paste and normally coincides with the time of maximum vertical settlement (Slowik et al., 2008:564). Air entry occurs because the radii of the menisci become too small the bridge the gap between the particles. The positions where air enters are weak points on the concrete surface where cracks will form if capillary pressure continues building up. The positions of air entry are purely localized points on the surface of the concrete paste and do not occur simultaneously and uniformly over the entire concrete surface (Slowik et al., 2008:558).

The horizontal component of the capillary pressure now plays the dominant role and relieves the capillary pressure by reducing the radii of the menisci through horizontal shrinkage. The vertical component of the capillary pressure plays no significant role from this point onwards, because the maximum vertical settlement has already been reached. The work of Slowik et al. (2008) and Kronlöf et al. (1995) confirm this by indicating that pronounced horizontal shrinkage only started once considerable vertical settlement has occurred as shown in Figures 2.3 and 2.4.

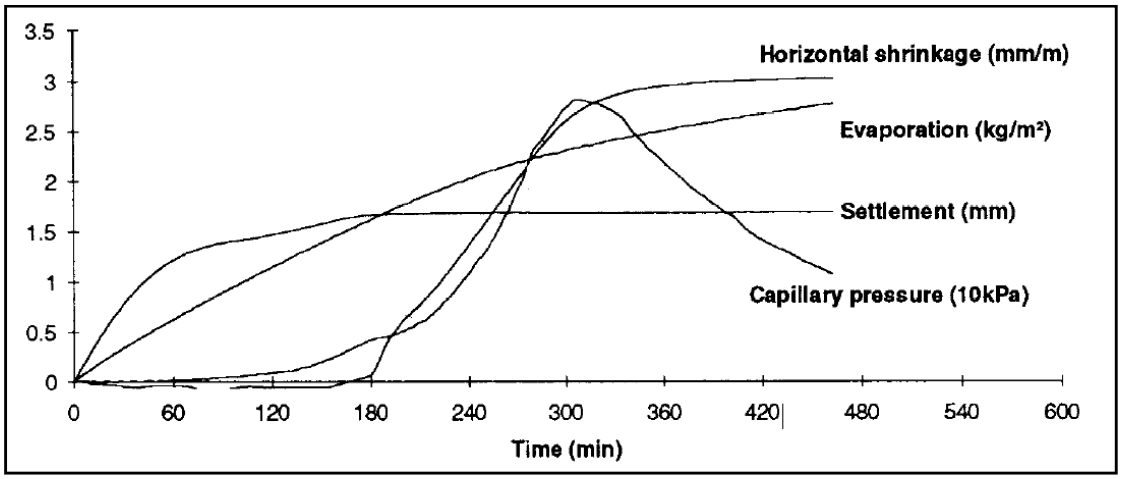

Figure 2.3: Graph of horizontal shrinkage and settlement (Kronlöf et al., 1995:1749)

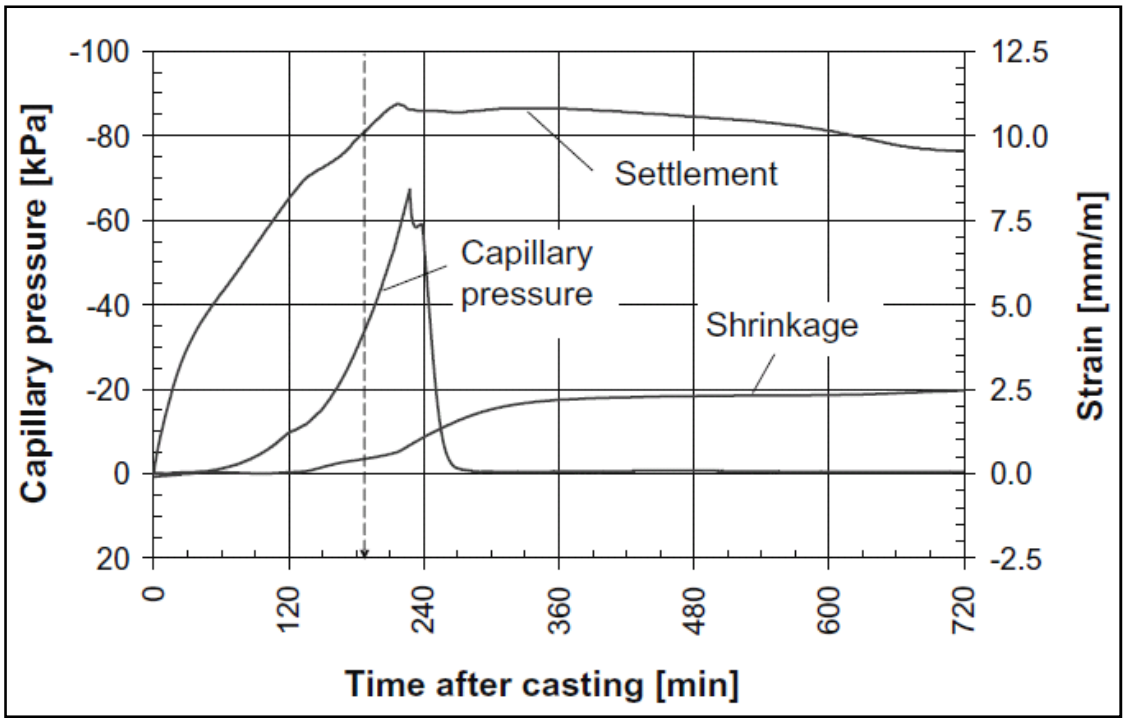

Figure 2.4: Graph of horizontal shrinkage and settlement (Slowik et al., 2008:563)

Stage F:

The capillary pressure continues to build up between the positions where air entry has occurred. The paste between positions of air entry starts to shrink horizontally to relieve the pressure build-up. This opens the air gap formed at the positions of air entry and is called a plastic shrinkage crack.

2.4.3. Paste mobility

Paste mobility is the third factor that influences PSC and is defined as the level of ease by which the material moves or deforms when subjected to a force. For a concrete paste to be mobile, the particles need to be able to move easily in relationship to each other. The mobility depends on the properties of the solid particles as well as the water to solid ratio and is explained in the following sections.

2.4.3.1. *Solid particle properties*

Solid particle properties concern the physical properties of the particle, i.e. the shape, size and self-weight.

Shape

Maximum mobility is achieved with smooth spherical particles. Anything less spherical or with a rougher surface is less mobile. Weathered aggregates are normally more mobile than crushed aggregates.

Size and relative density

The mobility of particles in a concrete paste increases with a decrease in particle size and relative density due to the smaller gravitational force acting on the particles. This increases the particles susceptibility to the horizontal component of the capillary pressure (Slowik et al., 2009:467). In general, the finer the particles in the concrete paste, the higher the mobility of the paste.

2.4.3.2. *Water to solid ratio*

In this study solid refers to any solid in the concrete mixture, especially the hydration products that form with time due to the hydration reaction of cement with water. The higher the degree of hydration, the more hydration products have formed and the less mobile the concrete paste becomes as the hydration products gives concrete a solid skeleton which resists movement. A solid skeleton refers to the increasing connections between particles in the concrete paste by hydration products.

2.4.4. Restraint

Restraint is the fourth factor that influences PSC and is responsible for cracking by restricting free shrinkage. This restraint can be defined as internal or external.

2.4.4.1. *Internal restraint*

The internal restraint is a result of a differential volume reduction. This occurs when the upper part of the concrete experiences more shrinkage due to the evaporation at the surface compare to the lower part of the concrete. The free shrinkage of the upper part of the concrete is restraint by the underlying concrete, which results in cracking on the concrete surface (Addis, 1998:15).

2.4.4.2. *External restraint*

External restraint of the concrete is always present through physical boundary conditions which have a restraining effect on the concrete. Irregular shapes and rough surface finishes of the formwork or the sub-grade on which the concrete is cast increases the concrete restraint. Large quantities and irregular layouts of the reinforcing steel also increase the concrete restraint. In general, cracking is increased with increased restraint.

2.4.5. Setting time

Setting time is the fifth factor that influences PSC. The reaction between cement and water is called hydration and is the primary cause of concrete setting. The two defined times with regard to concrete setting are called the initial setting time and the final setting time. At the initial setting time the concrete paste can still be easily be moulded into almost any shape by hand without visible damage to the paste structure. However, the same cannot be accomplished at the final setting time without visibly destroying the paste structure.

This is demonstrated in Figure 2.5 which shows pictures of a concrete paste at the initial and final setting times as well as the attempts to manually shape the paste into a sphere.

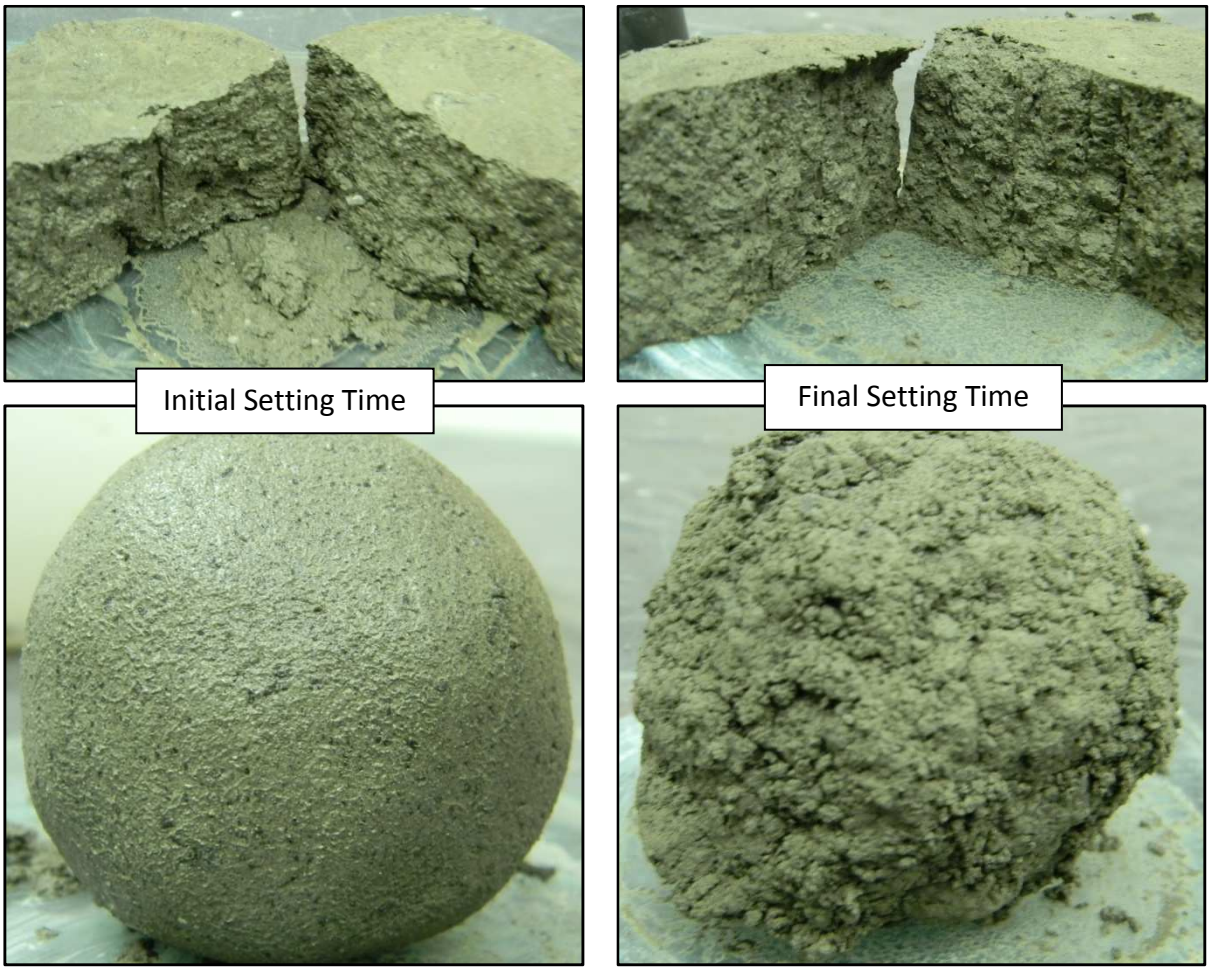

Figure 2.5: Pictures of a concrete paste at the initial and final setting times

The initial and final setting times are important when investigating PSC because as it can be used to distinguish between the three stages of fresh concrete, namely: stiffening, solidification and hardening (Mehta et al., 2006:223).

Figure 2.6 shows the three different stages graphically, where the round particles represent the aggregates and the gray parts the hydration products. It also shows the change in the relative amount of the permeability, porosity and strength of the concrete with time.

The hydration of cement, the three stages of fresh concrete and the factors that influence the setting times are explained in the following sections.

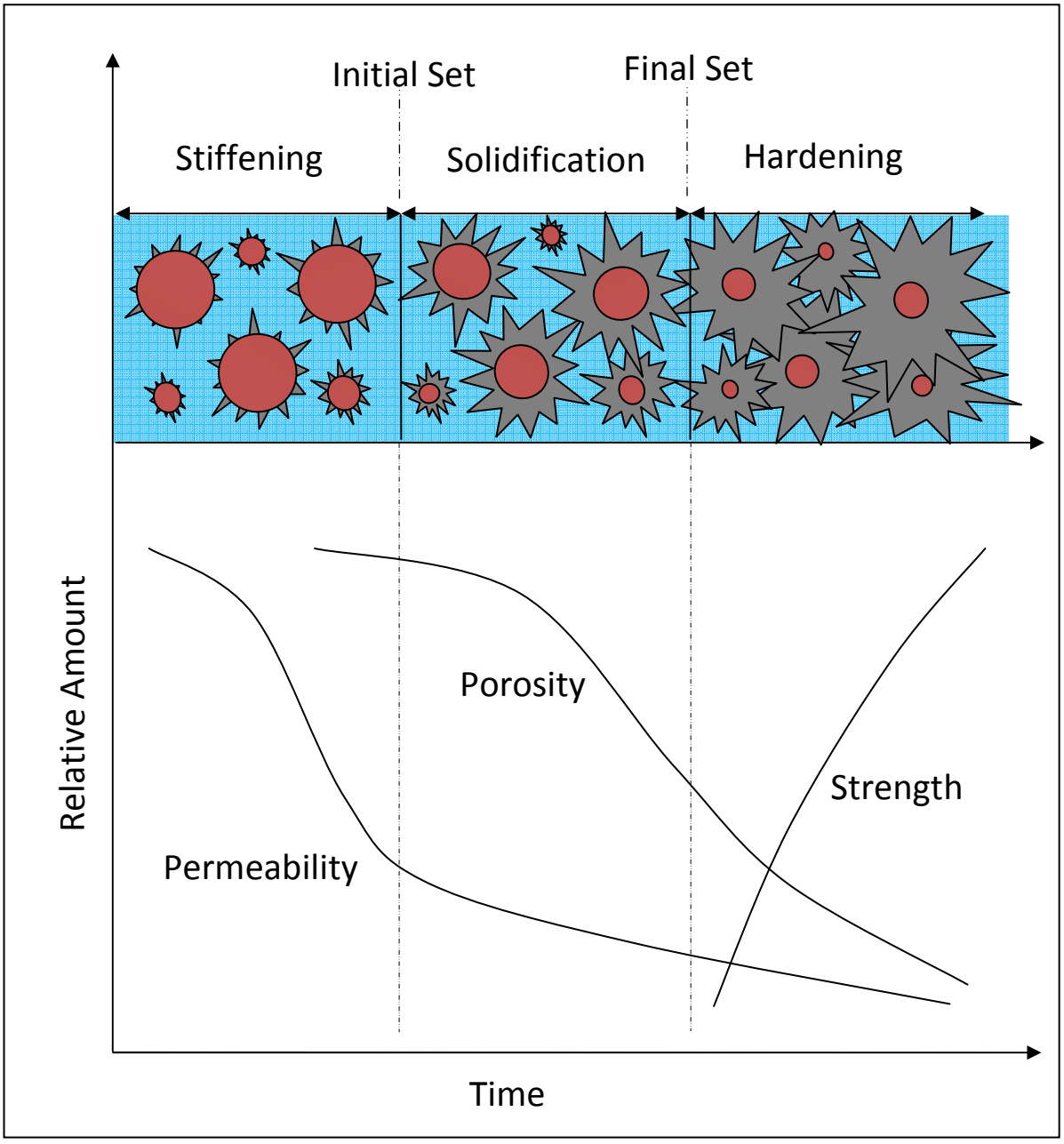

Figure 2.6: Three stages of fresh concrete (Mehta et al., 2006:223)

2.4.5.1. *Cement hydration*

Hydration is the chemical reaction between water and cement to form a rock-like material. The two constituents of Portland cement which have the biggest influences on hydration are called the aluminates (C_3A) and the silicates (C_3S and C_2S). The aluminates hydrate at a much faster rate than the silicates and mainly influence the stiffening and solidification stages of fresh concrete. The silicates which are normally 75% of ordinary Portland cement, hydrates

much slower than the aluminates and play a dominate role during the hardening stage of fresh concrete. The silicates are therefore mainly responsible for the strength of concrete (Mehta et al., 2006:214).

2.4.5.2. *Stiffening*

Stiffening is the first stage of fresh concrete and occurs directly after the concrete has been cast. It can be explained as the loss of consistency, i.e. the loss of workability and plasticity. Since free water gives the paste its plasticity, it can be concluded that the loss of water causes the paste to lose its plasticity. The water is lost due to evaporation, absorption by unsaturated aggregates, formwork or sub-grade as well as the formation of hydration products which composes mainly of aluminates (C_3A) hydration products during this stage (Mehta et al., 2006:222).

2.4.5.3. *Solidification*

Setting refers to the solidification of the cement paste through hydration. Solidification is the second stage of fresh concrete and starts at the initial set of concrete and ends with the final set of concrete. The initial setting time is defined as the time when the concrete ceases to be liquid and becomes unworkable. Beyond this point in time concrete placement, compaction and finishing operation becomes difficult. The point in time where complete solidification occurs is called the final set of concrete and signifies the time when hardening begins. The concrete has little or no strength at this point as the final set only represents the beginning of strength gain through the silicates (C_3S and C_2S) hydration. Solidification of the concrete paste does not occur suddenly but requires considerable time to become fully rigid (Mehta et al., 2006:222-223).

2.4.5.4. *Hardening*

Hardening is the third stage of fresh concrete and is the stage where the concrete starts to gain strength. The silicate hydration (C_3S and C_2S) plays the dominate role in the rate of strength development and continues rapidly for several weeks if free water is available (Mehta et al., 2006:223).

2.4.5.5. *Setting measurement*

The initial and final setting times are defined times after water comes in contact with the cement particles which are measured with penetration resistance methods as discussed in

Section 3.1.2.6. These times do not mark a specific or sudden change in the physical or chemical characteristics of the cement paste, but purely gives functional points in time. The initial setting time defines the limits of handling and the final setting time defines the onset of significant mechanical strength development (Mehta et al., 2006:367).

2.4.5.6. *Factors influencing setting time*

Any factor that influence the water-cement ratio of concrete will also influence the setting times, because setting is basically the filling of interparticle gaps with hydration products formed between water and cement. The factors discussed in Section 2.4.1.2 which increase water loss through evaporation will also decrease the setting times. The amount and type of cement also influences the setting times and generally an increase of the cement content decreases the setting time. If more heat is released during hydration the setting times will decrease. The heat of hydration differs for each type of cement, generally the finer the cement the more heat it releases during hydration (Mehta et al., 2006:368). Admixtures may also influences the setting times and are discussed in Section 2.4.6.

2.4.5.7. *Setting time importance*

The setting times of concrete can be influenced by many factors. The results obtained from any of the measuring techniques used to determine the setting times should by no means be accepted as the absolute correct time. It should only be used as an indication of when setting occurs. This is even more emphasized by the fact that the transition from one stage to another is gradual and not sudden. The setting times therefore only give an approximate indication of the current stage of the concrete paste. The stage of a concrete paste does however give information about what stress the paste can resist as well as how the paste will react to this applied stress. In other words, the setting times gives a measure of the strength and stiffness of the concrete paste.

2.4.6. Admixtures

Admixtures are the sixth factor that influence PSC and are normally liquid substances added in small amounts to concrete during mixing. Admixtures modify the properties of the concrete which can offer great advantages in terms of concrete performance and versatility if used correctly. The commonly used admixtures that play a role in PSC are discussed in the following sections.

2.4.6.1. *Plasticizers*

Plasticizers are also known as water reducers, which means that less water can be used in a mix while still retaining the same level of workability. Plasticizers work by physically dispersing the cement particles by given the particles a negative charge which causes mutual particle repulsion (Addis, 1998:95). This releases any water that may have been trapped by flocculated cement particles. Plasticizer also acts as retarders by delaying the setting of concrete. They can also entrain air in the form of air bubbles (Illston, 2001:110).

2.4.6.2. *Superplasticizers*

The action of superplasticizers is similar to that of plasticizers but with much greater effect. They can be used to give the high workability needed for self compacting concrete as well as the normal workability for high strength concrete with a low water-cement ratio (Addis, 1998:96). Superplasticizer used up to 1 % by weight of cement normally does not result in excessive bleeding or set retardation (Mehta et al., 2006:289).

2.4.6.3. *Accelerators*

Accelerators increase the rate of cement hydration, which increase the early strength gain of concrete (Illston, 2001:112). Calcium chloride ($CaCl_2$) is generally used effectively as an accelerator and also decreases the amount of bleeding as well as the setting time of the concrete. However, since the chloride content accelerates the corrosion of steel reinforcement, it is not suitable for use in reinforced concrete (Powers, 1968:562).

2.4.6.4. *Retarders*

Retarders delays the setting time of concrete by physically inhibiting the hydration of cement. It may also increase the amount of bleeding (Addis, 1998:98). In general, retarders contain significant amounts of sugar.

2.4.6.5. *Air entraining agents*

Air entraining agents are organic materials which entrains air in the concrete paste by dispersing microscopic bubbles through the concrete paste. These bubbles cannot be removed by vibration. The main advantages are improved workability and increased resistance to freezing and thawing cycles which lead to concrete deterioration. Entrained air is distinctly different from entrapped air that results from incomplete compaction. Large

quantities of entrained air may decrease the amount of bleeding and delay the setting times of concrete (Mehta, 2006:287).

2.4.7. Building procedures

Building procedures is the seventh and final factor that can have a significant influence on PSC. Simple techniques for example casting during favourable environmental conditions and proper curing can reduce PSC in most cases.

Modern day building practices seldom allows for concrete to be mixed on site and cast directly afterwards. Most of the concrete is supplied by ready-mix companies and sometimes mixes can spend hours in a mixing truck before being cast. This could influence the setting time and other aspects of concrete performance including PSC. Although this aspect requires further investigation it was not considered in this study.

2.5. *Low volume fibre reinforced concrete (LV-FRC)*

Low volume fibre reinforced concrete (LV-FRC) refers to conventional concrete which contains less than 0.2 % fibres as a percentage of the total volume of the concrete. Normally, only synthetic fibres such as polypropylene, polyethylene and polyester are added at these low volumes to concrete. Synthetic fibres are man-made and generally have a low modulus of elasticity and high percentage of elongation. They are produced by chemical processes developed in the petrochemical and textile industries and are mainly available in two forms, monofilament fibres or film (fibrillated) fibres (Hannant, 1978:81).

In this study only monofilament fibres with a circular cross sections are considered. Although the addition of a low volume of synthetic fibres to conventional concrete improves the performance of the material as discussed in the following section, it should be mentioned that the tensile strength of LV-FRC is never more than for conventional concrete without fibres. As for all fibre reinforced concretes the additional tensile strength due to fibres only contributes once cracking has occurred. For LV-FRC the magnitude of the tensile strength added by fibres after cracking is small in comparison with the tensile strength of the concrete and does not contribute to the structural integrity of a structure.

2.5.1. Advantages of LV-FRC

The addition of a low volume of randomly distributed synthetic fibres to conventional concrete has numerous advantages. In the hardened state it improves mechanical properties for example: ductility, post-cracking behaviour and toughness. Although a low volume of fibres does not increase the tensile strength of concrete, it does reduce and control crack growth. In the fresh state synthetic fibres also reduces PSC (Illston et al., 2001:420 and Wongtanakitcharoen, 2005:2).

An added advantage of adding synthetic fibres to concrete is the increase fire resistance of concrete, especially high strength concrete. The heat of a fire turns the moisture in the concrete to steam which expands rapidly if it cannot escape. The rapid expansion causes spalling of concrete which exposes the steel reinforcement to the fire. This may lead to a catastrophic structural failure, because steel loses its strength at high temperatures. When fibre reinforced concrete is exposed to heat, the synthetic fibres combust which creates small tunnels whereby the expanding steam can escape. This prevents the spalling of concrete and therefore the exposing of reinforcing steel (Zeiml et al., 2006:929-930).

2.5.2. LV-FRC and PSC

The addition of synthetic fibres to concrete has been shown to control PSC (Illston et al., 2001:420 and Wongtanakitcharoen, 2005:2). The extent of this control is however not clearly understood.

From a mechanical point of view the most common explanation is that the fibres reduces PSC by given an additional tensile strength to the concrete paste by holding or stitching the concrete surface together after cracking has occurred. The additional tensile strength is mainly caused by the bond between the concrete paste and the fibres, called the interfacial shear bond stress (Hannant, 1978:3). The bond is especially low within the first few hours after the concrete has been cast (Wongtanakitcharoen, 2005:131), but it is believed to increase steadily with time as solid contact points between the fibre and concrete paste increases due to hydration. The time when fibres start giving meaningful resistance to cracking is investigated in this study.

From a material point of view the addition of fibres may influence the settlement and bleeding of the concrete through added stiffness and cohesion or change in permeability. This in turn influences the capillary pressure which causes PSC as well as the air entry that initiates cracking.

The time when cracking is initiated also influences the effect that fibres will have on PSC, since fibres only start working once cracking has occurred. Furthermore, the resistance of fibres to PSC depends on the bond strength between the fibres and concrete paste which also varies with time.

It is therefore not elementary to identify why, when and to what degree fibres control PSC, since various mechanisms can be involved simultaneously. The pullout mechanism of fibres, the post-cracking behaviour of LV-FRC and the influence of fibres on bleeding are discussed in the following sections.

2.5.2.1. *Pullout mechanisms of fibres*

Once fibres bridge a crack it can resist further crack widening until the fibres are pulled out or ruptured. For fresh concrete paste the fibres never reach their ultimate stress capacity and therefore crack widening results from fibre pullout. The pullout characteristics of a fibre are influenced by the fibre shape, fibre length, fibre diameter, fibre surface properties and the properties of the concrete paste such as fineness, strength and rate of hydration. Friction, adhesion and mechanical anchorage can influence the pullout mechanisms of fibres (Wongtanakitcharoen, 2005:18). The synthetic fibres used in this study are generally smooth, straight fibres with no irregular deformities and results in no mechanical anchorage within the concrete paste. The pullout mechanisms involved with these fibres are mainly adhesion and friction, each may have a predominant contribution to the pullout resistance of the fibre at a specific time.

Adhesion is described as the sticking or joining together of two surfaces and can be normal adhesion between the fibre and concrete paste or chemical adhesion. Normal adhesion results from the attractive forces between different molecules. For example, water drops cleaving to the surface of a leave. Chemical adhesion occurs if the fibre surface absorbs

water which is later involved in the chemical reaction of hydration (Wongtanakitcharoen, 2005:44). Interfacial friction between the concrete paste and fibre is caused by the solid contact points between them. Furthermore, hydration increases the friction by increasing the physical contact points of the concrete paste with the fibre surface. The magnitude of the influence of each mechanism at a certain time is unknown. Although this requires further research it was not explicitly investigated in this study.

2.5.2.2. *Post-cracking behaviour of LV-FRC*

Once cracking has been initiated by air entry, fibres are the only additional internal resistance to crack widening. The extent to which these fibres can bridge a crack depends on the magnitude of the interfacial shear bond stress between the fibre and the fresh concrete paste, which increases with time. Hannant (1978:24) proposed Equation 2.3 to calculate the ultimate stress sustained by a unit area of a composite after cracking i.e. the stress that can be bridged across a unit crack area by fibres. It accounts for the volume fraction, length and diameter of the fibres and the interfacial shear bond stress between the fibre and the concrete paste.

$$\sigma_c = \frac{1}{2}\tau V_f \left(\frac{L}{d}\right) \quad \text{..... (Equation 2.3)}$$

with:

σ_c = Ultimate bridging stress over unit crack area

τ = Interfacial shear bond stress

V_f = Volume fraction of fibres added to mix

L = Fibre length

d = Fibre diameter

It should be mentioned that this equation was developed for cracking in hardened fibre reinforced concrete, however since the shear bond between the fibre and the concrete paste is present for both fresh and hardened concrete the author believes that this equation is also applicable for fresh concrete paste. Although the magnitude of the mechanisms that

contributes to the interfacial shear bond stress may differ for fresh concrete paste as discussed in Section 2.5.2.1, it remains the main factor controlling the performance of a fibre reinforced concrete with regards to crack propagation (Hannant, 1978:3). The equation by Hannant (1978:22-24) assumes the following:

- all the fibres remain straight,
- all the fibres pulls out without fracture and
- all the fibres are straight with no hooks.

2.5.2.3. *Influence of fibres on bleeding*

In general, the addition of synthetic fibres to concrete reduces the bleeding rate of concrete (Uno, 1998:374). Fibres normally increase the stiffness of a concrete mix which reduces the settlement (Qi et al., 2003:390). Since settlement causes bleeding, it can be assumed that less settlement will cause less bleeding. The increased fibre surface area could also explain the reduction in bleeding (Uno, 1998:374), especially if the fibre is hydrophilic and can absorb quantities of concrete mixing water.

It should also be mentioned that in certain cases fibres may increase the bleeding rate of a concrete mix, by acting as channels where by water can move to the surface (Qi et al., 2003:390).

Depending on the effect of the fibres on the bleeding of concrete, the capillary pressure will also be influenced. If the fibres reduce the bleeding, the rate of capillary pressure build-up will increase as well as the risk for PSC, therefore counteracting to an extent the reduced risk of PSC due to the addition of fibres.

2.5.3. Fibre types

The synthetic polymeric fibres used in this study are a polyester fibre and two polypropylene fibres. Table 2.1 summarises the typical properties of the fibre types.

The different fibre types used in this study are discussed in the following sections.

Table 2.1: Typical mechanical properties of fibres (Addis et al., 2001:250)

Fibre type	Fluorinated polypropylene	Polypropylene	Polyester
Surface treatment	Fluorinated	Untreated	Untreated
Density [g/cm³]	0.91	0.91	1.38
Melting point [°C]	165	165	260
Modulus of elasticity [GPa]	3.5 - 4.8	3.5 - 4.8	4 - 14
Tensile strength [MPa]	140 - 700	140 - 700	230 - 1100
Chemical stability in concrete	Stable	Stable	Unstable
Water absorption [%]	0	0	0.4

2.5.3.1. *Polypropylene fibres*

Polypropylene fibres are chemically inert and stable in the alkaline concrete environment. They have a hydrophobic surface, which means they do not absorb water. This reduces the possibility of chemical adhesive to the concrete paste once the cement hydrates with water. The bond between the concrete paste and the fibres is mainly through interfacial friction. In general, the fibres have a smooth surface which results in a relatively poor bond with the concrete paste. The fibres have a low modulus of elasticity and are sensitive to sunlight and oxygen (Wongtanakitcharoen, 2005:44).

2.5.3.2. *Fluorinated polypropylene fibres*

Fluorinated polypropylene fibres are modified by the chemical process of fluorination, which is the treatment of a material with fluorine gas (F_2). The treatment results in an atom exchange on the polymer surface, which changes the molecular structure, polarity and the micro surface texture of the material. The change in polarity increases the water absorption of the fibre surface which results in improved adhesive characteristics (Forrester, 2004:8-9). This may possibly lead to a higher bond strength between the fibre and the concrete paste, due to the hydration of the absorbed water with cement. The rest of the fibre properties are similar to untreated polypropylene fibres.

2.5.3.3. *Polyester fibres*

Polyester fibres have a higher tensile strength and modulus of elasticity than the polypropylene fibres. Polyester is not resistance to strong alkalis, like concrete, and does tend to decompose under these conditions over long time periods. A higher temperature increases the rate of decomposition (Zheng et al., 1995:203). Polyester fibres are primarily used for crack reduction during the early ages of concrete and cannot

guarantee any long term advantages like impact resistance or additional flexural strength. These fibres are however suited to control PSC that occurs within the first few hours after concrete has been cast, which is long before any significant decomposition of fibres have occurred (Boghossian et al., 2008:930).

2.6. *Concluding summary*

In this chapter, the mechanism that causes PSC was identified as capillary pressure. The important principles of air entry and restraint were highlighted as added mechanisms needed for PSC. The factors that influence PSC were discussed in detail, where the importance of determining the concrete setting times was emphasized. The influence of adding a low volume of synthetic fibres to conventional concrete on PSC was also considered.

The experimental framework for PSC in conventional concrete and LV-FRC together with the single fibre pullout tests are discussed in the following chapter.

3. Experimental framework

In this chapter the setup, objectives, programme, procedures and materials that were used for the plastic shrinkage cracking (PSC) and single fibre pullout experiments are discussed. The objectives of the experiments are to investigate fundamentally the phenomena of PSC in conventional concrete and in low volume fibre reinforced concrete (LV-FRC). This was achieved through a series of experiments firstly on conventional concrete, where the emphasis was on the determination of the time when PSC starts and ends. This knowledge is of vital importance if PSC is to be reduced or prevented. Once the basic principles and factors that influence PSC are understood, the influence of fibres can be investigated. This was done by performing tests on LV-FRC as well as single fibre pullout tests from conventional concrete.

3.1. *Plastic shrinkage cracking (PSC) experiments*

PSC experiments refer to the tests that were conducted with concrete in controlled environmental conditions where the evaporation, bleeding, capillary pressure, setting times and crack growth were measured.

3.1.1. Test setup of climate chamber

The climate chamber shown in Figure 3.1 was designed to simulate ideal conditions for the formation of PSC i.e. conditions of extreme heat, low relative humidity and high wind speeds. The temperature and relative humidity can be controlled electronically to preset values with a heating element and a dehumidifier respectively. Axial fans circulate the air within the climate chamber to create airflow.

The climate chamber can create a stable extreme environmental condition with temperatures of up to 50 °C, relative humidity as low as 10 % and uniform wind speeds of up to 70 km/h. The details about the design and performance of the climate chamber are discussed in Appendix A.

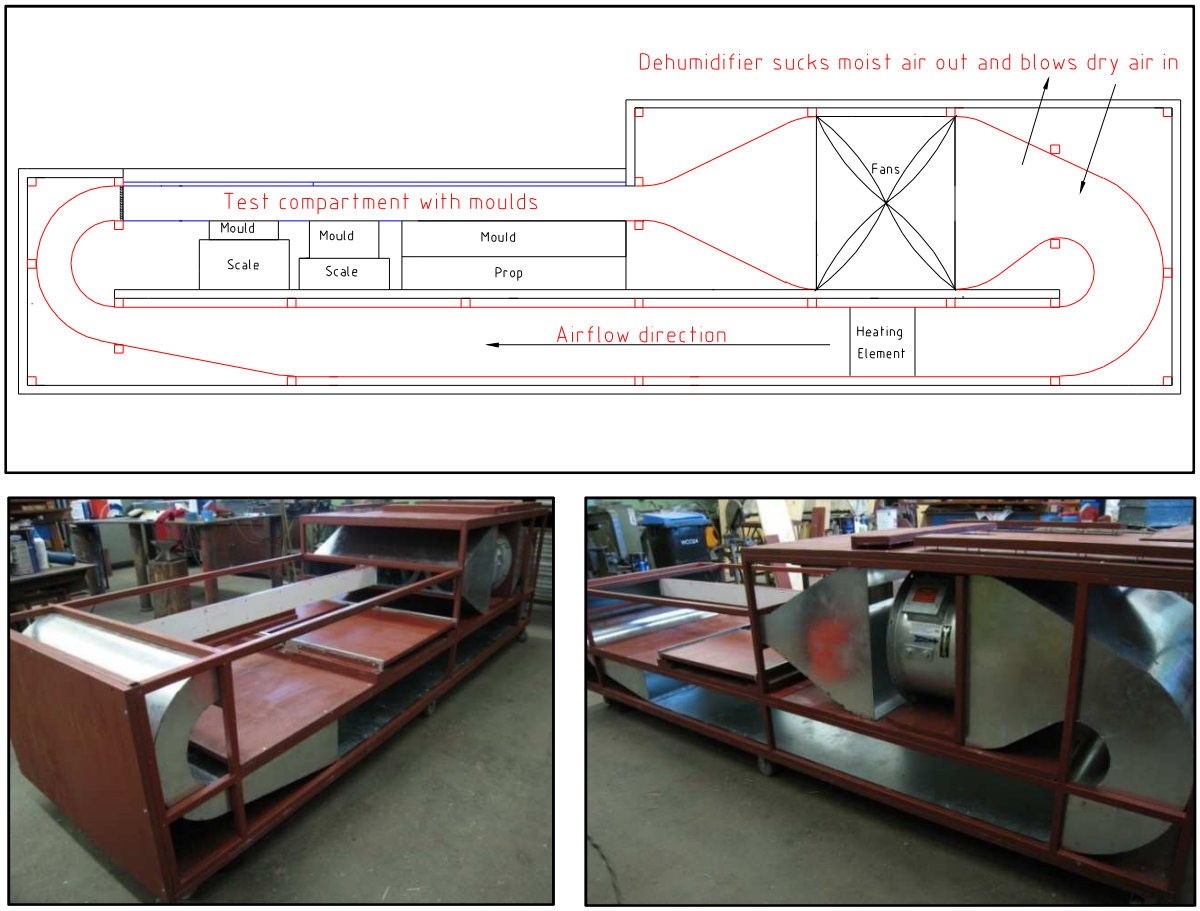

Figure 3.1: Climate chamber layout

The PVC moulds that were used for crack measurements are shown in Figure 3.2. The moulds are based on the layout proposed for fresh concrete testing by ASTM C 1579 (2006). In this study these moulds are referred to as PSC moulds. The PSC moulds are 600 x 200 x 100 mm (length x width x height) in size with three triangular shapes spaced at the bottom. The centre triangle creates a weak spot to enforce a single crack while the other two triangles act as the horizontal restraint required for the cracking.

Two square PVC moulds and two circular metal pans were used to measure the water evaporation from the concrete and normal water evaporation respectively with electronic scales as shown in Figure 3.5. All the moulds were placed into the test compartment of the climate chamber as shown in Figure 3.3. The entire test compartment can be viewed through Perspex covers.

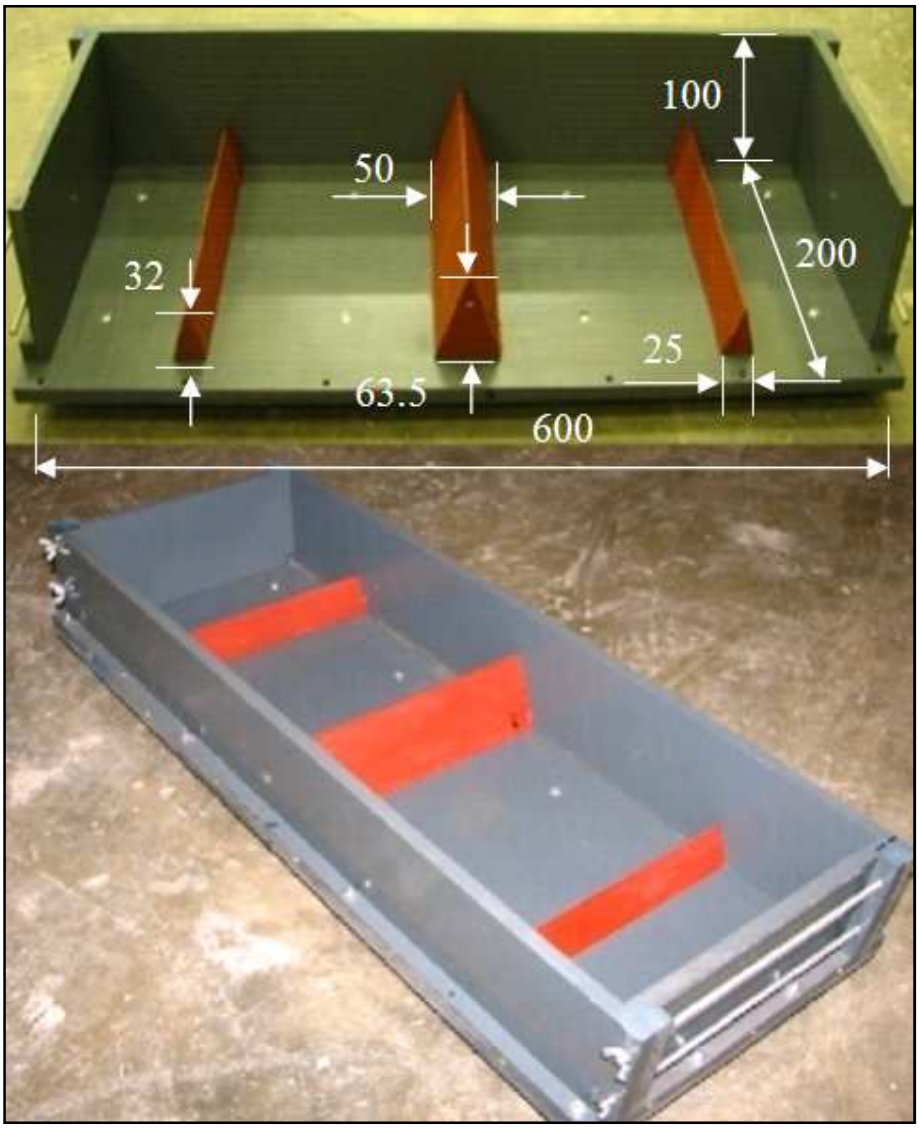

Figure 3.2: PSC moulds used for crack measurement

Figure 3.3: Test compartment with Perspex covers and PVC lining inside

3.1.2. Test measurements

All the measurements except the bleeding measurements were conducted in the climate chamber. The apparatus used for each measurement are discussed in the following sections.

3.1.2.1. *Wind Speed*

The wind speed was measured with a hand held anemometer with a rotary fan as shown in Figure 3.4. The anemometer has an accuracy of ± 3 % up to 150 km/h.

Figure 3.4: Hand held anemometer for wind speed measurements

3.1.2.2. *Evaporation*

The water and concrete water evaporation were measured with electronic scales that log the data points on a computer. The moulds and the scales are shown in Figure 3.5.

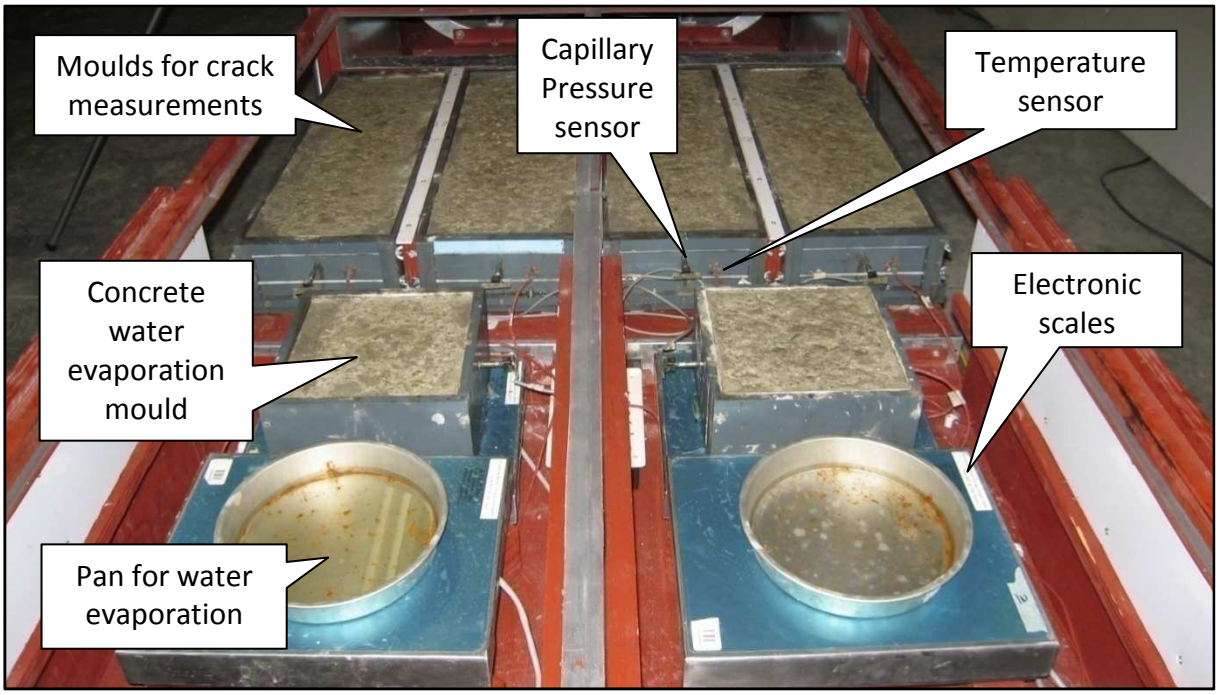

Figure 3.5: Layout of moulds and measuring equipment in test compartment

3.1.2.3. *Concrete temperature*

The temperature was measured in all the concrete specimens with temperature sensors (called PT 100) that log the data points on a computer. To prevent the sensors from bonding to the hydrated concrete they were inserted into copper sleeves which were imbedded into the concrete specimen as shown in Figure 3.6.

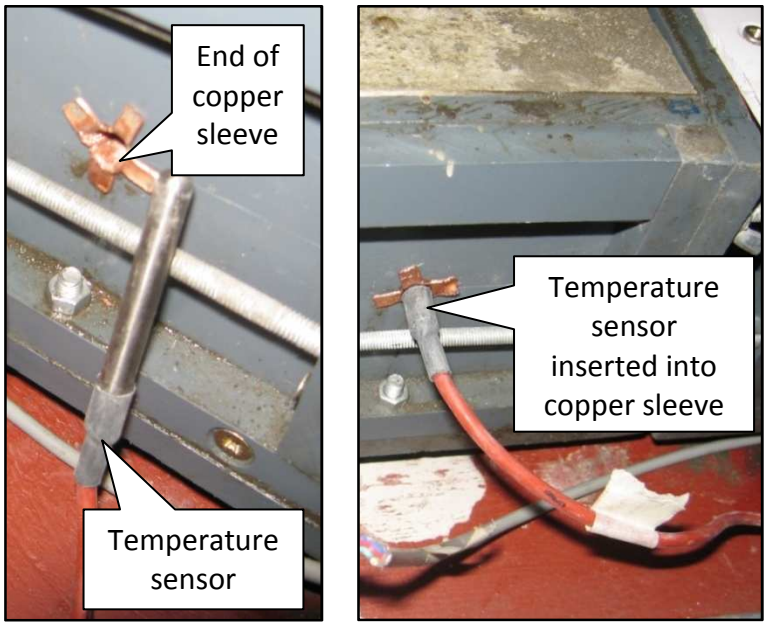

Figure 3.6: Temperature sensor and copper sleeve

3.1.2.4. *Capillary pressure*

The method of the capillary pressure measurement was adopted from Slowik et al. (2008:560). Small electronic pressure sensors were connected to the pore system of each concrete specimens by long metal tubes which have an inside diameter of approximately 3 mm. Figure 3.7 shows the capillary pressure sensor and the metal tube separately as well as the thread on both these elements that allow them to be connected. The figure also shows a connected capillary pressure sensor and metal tube which has been inserted into a concrete specimen.

Before inserting the metal tube into the concrete specimen both the tip of the capillary pressure sensor and the metal tube was filled with distilled water after which they were connected to each other. A small sponge was also inserted into the tip of the metal tube to prevent small solid particles from the concrete paste to enter the tube. The tubes were

inserted horizontally 35 mm beneath the surface of the concrete specimen. This was achieved by first filling the specimen with fresh concrete up to the level of the metal tube. The metal tube with capillary sensor was then inserted, after which the specimen was filled completely. This depth of measurement is sufficient since water pressure within the interconnected pores is almost uniformly distributed up to a depth of 100 mm from the surface during the plastic phase (Slowik et al., 2009:462). The tips of the tubes where the capillary pressure was measured were located just above the centre triangular restraint of the PSC moulds, since this is where the crack will form.

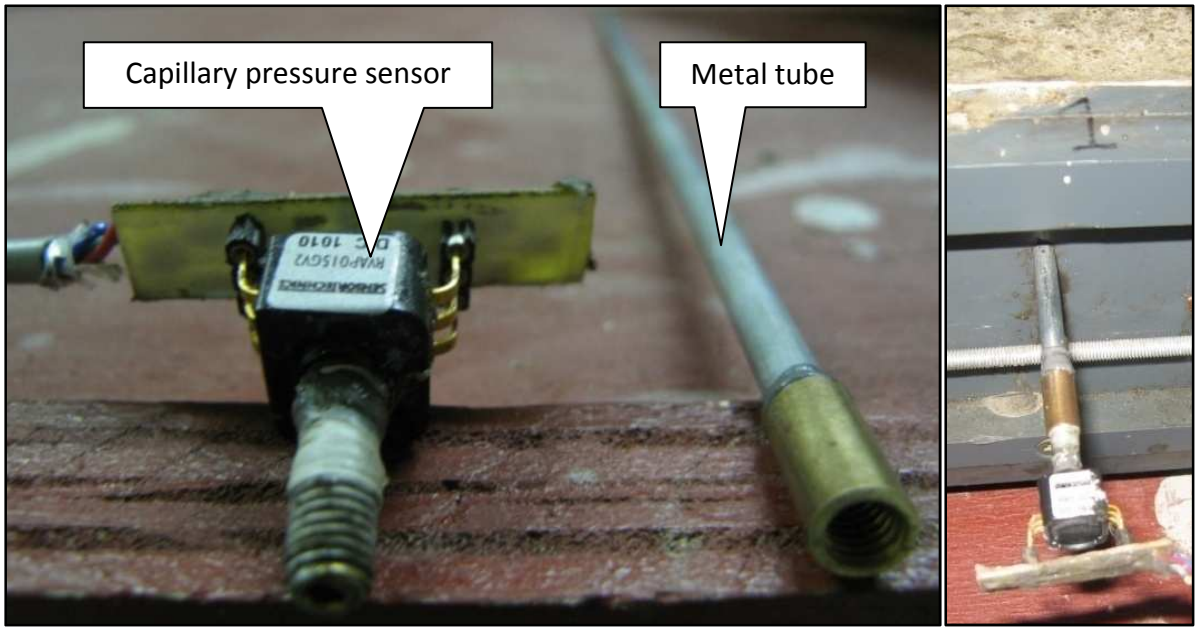

Figure 3.7: Capillary pressure sensor and metal tube

3.1.2.5. *Crack growth*

The crack area was used as an indicator of crack growth. Crack area combines the crack length and average crack width and hereby gives a measure of the severity of the crack over the entire concrete element. If only average crack width was considered the severity of the crack may have been lost. For example, a crack with a length of 10 mm and average width of 0.1 mm is must less severe than a crack with a length of 100 mm with the same average width. Crack area therefore gives an adequate assessment of the crack damage in a concrete element and was determined as follows:

A high resolution picture of the crack as shown in Figure 3.8 was taken every 20 minutes. These pictures were scaled in CAD software by using the known length of the ruler in each picture. The crack length was measured with 10 mm line segments of which the width was also measured. The author conducted all the crack measurements with the same consistent procedure and method. The crack area was then calculated with Equation 3.1.

$$Crack\ Area\ [mm^2] = Average\ crack\ width\ [mm]\ x\ number\ of\ line\ segments\ x\ 10\ [mm] \quad \text{..... (Equation 3.1)}$$

It is acknowledged that although these measurements do not give the precise crack area, it succeeds in given a good indication of how the crack area develops with time.

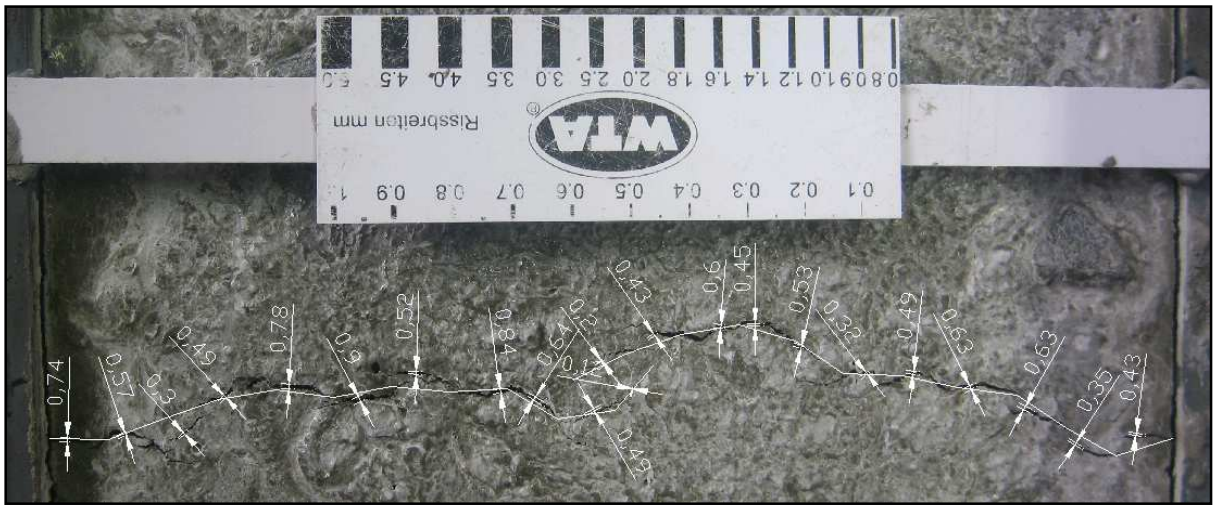

Figure 3.8: Example of picture used for crack area measurements

3.1.2.6. *Setting time*

The importance of the initial and final setting times were highlighted in Section 2.4.5.7. Normal penetration tests with a Vicat apparatus, moulds and penetration needles (shown in Figure 3.9) were used to determine both setting times in accordance with SANS 50196-3 (2006:9-14). The initial setting time is reached when the tip of the standard 1.1 mm diameter initial setting time penetration needle measures a distance of 6 ± 3 mm from the base plate. The final setting time is reached when the ring attachment of the standard final setting time penetration needle fails to create a mark on the surface of the specimen.

The fresh concrete was sieved trough a 4.75 mm sieve, which left a mortar suitable for penetration resistance testing (Ahmadi, 2000:512). The moulds were closed to the atmosphere with covers which avoided any evaporation and were placed in the climate chamber outside the area of direct wind. It should be mentioned that the Vicat apparatus is intended to find the initial and final setting times of cement paste with a standard consistency under standard climate conditions, therefore the use of the Vicat apparatus on mortars with varying climate conditions only serves as an indication or measure of the strength development of the concrete paste.

Figure 3.9: Vicat penetration apparatus

3.1.2.7. *Bleeding*

The method used for measuring the concrete bleeding was developed by Josserand et al. (2004). Two cylindrical PVC moulds with a diameter of 120 mm and a height of 120 mm were used for the measurements. The concrete depths in the bleeding moulds were a 100 mm which was identical to the depths of all the other concrete specimens used for testing. This ensured that the bleeding, concrete water evaporation and crack growth measurements were comparable, since the depth of a concrete specimen influences the bleeding amount (see Section 2.4.1.3). The three triangular shapes which has been added to the PSC mould as shown in Figure 3.2 have minimum effect on the comparison of the previously mentioned results. Although they change the depth of the concrete specimen at their locations, they have an insignificant influence on the bleeding of the entire specimen, since they only fill 4 % of the entire volume of the specimen. The bleeding will therefore only slightly be influenced near the triangles and this will have almost no influence on the crack growth, since the

cracks are formed due to the contraction of the entire specimen and not just the regions above the triangles. Considering the fact that the majority of the bleeding in the concrete specimen is not influenced by the triangles and that it is especially the contraction of the concrete in the region where no triangles are present, it is assumed that the small difference in bleeding due to the triangles has minimum influence on the crack measurements.

The bleeding was measured in a controlled environmental room with a constant temperature of between 20 and 25 °C, a relative humidity of between 50 and 60 % and no wind. This environment is called Climate 3 as shown in Table 3.2. Although this climate is different than Climates 1 and 2 used for the evaporation and crack measurement, the results remain comparable since bleeding is caused by the particle settlement due to gravitational forces acting on the particles. Bleeding is therefore mainly influenced by the composition of the concrete paste and not the climate conditions. Furthermore, the proposed method of bleeding measurement required a more stable and less extreme environmental condition to ensure accurate results. In addition to the lower temperature and higher relative humidity, the bleeding mould was also covered to minimize the evaporation of bleeding water between measurement intervals. The volume of air in the bleeding mould after it has been filled with concrete is less than 17 % of the total volume of the mould which, together with the less severe climate, further reduced the amount of bleeding water which could evaporate. The amount of bleeding water which evaporated was measured as proposed by Josserand et al. (2004) and was found to be insignificant when compared to the measured bleeding amount.

There are however limitation in choosing two different climates for these measurements. The different temperatures influences the rate of hydration which may influence the bleeding, but since the majority of the bleeding occurs before pronounced hydration has occurred it is believed to result in relatively small differences. Furthermore, the measurement of bleeding with the proposed method only accounts for normal bleeding due to particle settlement through gravitation and neglects the additional bleeding that results from the vertical component of the capillary pressure which forces the solid particles downwards as explained in Section 2.4.1.3. This limits the accuracy of the bleeding results after the drying time has been reach, since capillary pressure may cause additional bleeding.

The drying time is once all the bleeding water that has come to the surface of the concrete has evaporated and will differ for each environmental condition and concrete mix. A more advanced method of bleeding measurement needs to be develop which allows more precise and comprehensive measurement at extreme environmental conditions. However, the proposed method used in this study is sufficient, since the measurements will mainly be used to determine the drying time which occurs long before any pronounced hydration or bleeding due to capillary pressure has occurred. A discussion about the test procedures and equipment used follows:

A device was used to create tracks on the concrete surface where bleeding water can accumulate. A 10 ml syringe was used to extract the bleeding water accumulating in the tracks. The water extracted by the syringe contained many small cement and sand particles which would increase the weight of the bleeding water. To remove the solid particles the bleeding water was measured using two small plastic containers. The water extracted by the syringe was first injected into one container, which was then emptied into the second container. All the solid particles cleaved to the sides of the first container and only the water was transferred to the second container which was weighed with an electronic scale every 20 minutes to obtain the bleeding water mass. The bleeding moulds were closed to the atmosphere with covers to limit evaporation between measurements. Figure 3.10 shows the two bleeding moulds, the device used to create the tracks and the syringe used to extract the bleeding water.

Figure 3.10: Bleeding moulds, syringe and device used to create tracks

3.1.3. Test objectives

The background study on PSC revealed various theses or statements regarding PSC, which are assumed to be true without proper experimental prove. Several preliminary tests on PSC also resulted in observations on when PSC starts and ends (Combrinck et al., 2010). The experiments on PSC were set up to determine whether these theses and observations are valid. The main objective of the theses and the observations rests on obtaining information on when and why PSC occurs. A discussion of the theses and observations as well as how the experiments were set up to prove them follows:

Thesis 1

PSC can only occur once the total volume of water evaporated from the concrete surface exceeds the volume of bleeding water at the surface, called the drying time (T_D) in this study. This statement can be found in virtually any literature or book concerning PSC (Illston et al., 2001:138 and Powers, 1968:599 and Kwak et al., 2006:518).

Thesis 2

No cracks will form before air entry has occurred (Slowik et al., 2008:559). Air entry is characterized by a significant drop in capillary pressure after a period of steady pressure build-up.

Experiments for proving Theses 1 and 2

To prove these theses the amount and rate of bleeding of concrete was changed by using different sand types. The evaporation rate was also varied by changing the wind speed. The objective was to investigate the effect the changes in bleeding and evaporation characteristics of concrete have on the relationship between the time of first crack appearance and the times of air entry as well as the drying time.

Observation 1

The time of first crack appearance is near or just after the initial set of concrete (Combrinck et al., 2010).

Observation 2

No plastic shrinkage cracks will start after the final set of concrete. In fact the time where PSC stops is somewhere between the initial and final set of concrete and coincides with the time of crack growth stabilization (Combrinck et al., 2010).

Experiments for proving Observation 1 and 2

To prove these observations the initial and final setting times of concrete was altered by adding retarders and accelerators respectively. The objective was to investigate the effect that different concrete setting times have on the time of first crack appearance and time of crack growth stabilization.

The final objective of the experiments was to investigate what influence the addition of a low volume of synthetic fibres has on the PSC.

3.1.4. Experimental test programme

Two standard mixes were used for the PSC experiments. The details of the materials and proportions used for the mixes are discussed in Section 3.1.5. The first mix is similar to mixes frequently used by local ready-mix companies for industrial floor slabs, which are the concrete elements mainly prone to PSC. The variations, in terms of bleeding and evaporation characteristics of concrete as well as the setting times of concrete, for proving the theses and observations were only implemented on the first mix.

The second mix was designed to give significant PSC by choosing a low water-cement ratio of 0.4 and reducing the average sand particle size by sieving a crushed sand through a 2 mm sieve. Both of these factors not only decreases the concretes permeability which results in a lower bleeding rate, but also increases the risk for PSC by increasing the mobility of the concrete paste as well as the magnitude of the capillary pressure.

Low volumes of polyester, polypropylene and fluorinated polypropylene fibres were added to the standard Mixes 1 and 2 respectively. Table 3.1 summarises the name, definition and characteristic of every mix used in the experiments.

Table 3.1: Name, definition and description of mixes

Mix	Name	Definition	Description
1	M1S	Mix 1 Standard	Frequently used for slabs
	M1R	Mix 1 Retarded	Retarded setting times
	M1A	Mix 1 Accelerated	Accelerated setting times
	M1B	Mix 1 Bleeding	Increased bleeding by using Malmesbury sand
	M1PES	Mix 1 Polyester	Added polyester fibres
	M1PP	Mix 1 Polypropylene	Added polypropylene fibres
	M1FPP	Mix 1 Fluorinated Polypropylene	Added fluorinated polypropylene fibres
2	M2S	Mix 2 Standard	High PSC risk
	M2PES	Mix 2 Polyester	Added polyester fibres
	M2PP	Mix 2 Polypropylene	Added polypropylene fibres
	M2FPP	Mix 2 Fluorinated Polypropylene	Added fluorinated polypropylene fibres

The environmental conditions used for the PSC experiments are shown in Table 3.2. Climate 1 was chosen as an extreme environmental condition ideal for PSC. The placing temperature of the concrete mixes was between 21 °C and 25 °C for all the PSC experiments. The temperature change within the concrete spesimen once placed into the climate chamber is due to the difference between the concrete placing temperature and the temperature of Climates 1 and 2 in the climate chamber. This will influence the setting times and water evaporation of the concrete. The measurement of these factors within the climate chamber directly accounts for the influence of the mentioned temperature change. The calculated evaporation rate for Climate 1 is 1.04 kg/m²/h if calculated with Equation 2.2 in Section 2.4.1.2 with concrete placing temperatures in the range of 21 °C to 25 °C. An evaporation rate of 1 kg/m²/h is considered to be an extreme condition and precautions should be taken to avoid PSC (Uno, 1998:372). Climate 2 has a much lower wind speed and evaporation rate than Climate 1 and assist with the verification of Theses 1 and 2. Climate 2 was utilized only for M1S and M1B and Climate 1 for the rest of the tests. Climate 3 was used for the bleeding measurements and single fibre pullout tests.

Table 3.2: Environmental conditions

Condition	Climate 1	Climate 2	Climate 3
Relative Humidity [%]	20	20	55
Air temperature [°C]	40	40	22.5
Wind speed [km/h]	33	4	0
Concrete temperature [°C]	23	23	23
Calculated evaporation rate (Equation 2.2) [kg/m²/h]	1.04	0.23	0.10

The setting time, bleeding as well as crack growth measurements were conducted every 20 minutes. For all the variations of Mix 1 the tests were ended at least 40 minutes after the final setting time of the concrete has been reached and for all the variations of Mix 2 the test were ended after 24 hours. More details on the testing procedure are discussed in Section 3.1.6.

3.1.5. Materials and mix proportions

The materials used in the mixes as well as the mix proportions are discussed in the following sections.

3.1.5.1. *Aggregates*

The grading of four sand types used in the concrete mixes is shown in Figure 3.11 and was determined in accordance with SANS 1083 (2002:2-4).

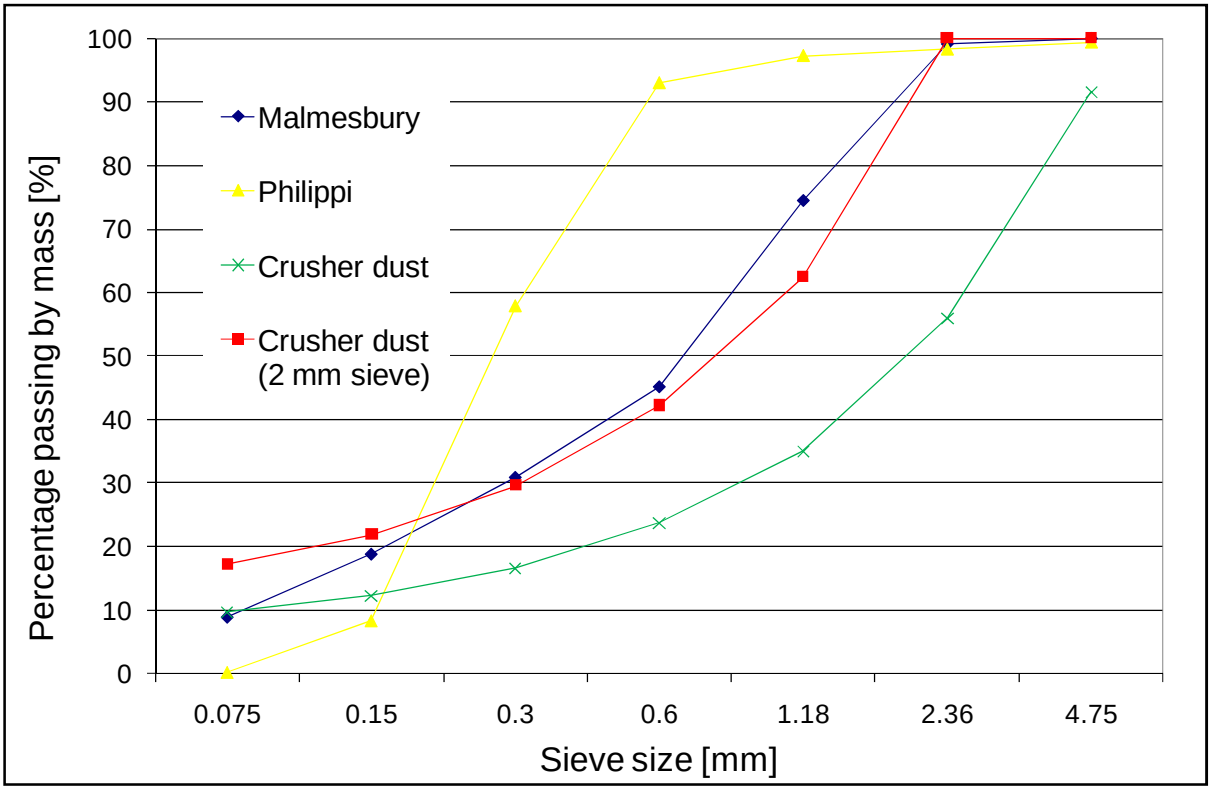

Figure 3.11: Grading of sand

Table 3.3 gives the properties of the aggregates. The sands known locally as Philippi and Malmesbury sand were formed by the natural disintegration of rock, while the Greywacke crusher dust was a by-product of the mechanical crushing of Malmesbury shale.

The stone was graded in accordance with SANS 1083 (2002) with a nominal size of 19 mm and was produced by the mechanical crushing of Malmesbury shale and is known locally as Greywacke stone.

Table 3.3: Aggregate properties

Material	Fineness modulus - FM	Relative density - RD [kg/m³]	Particle shape
Malmesbury sand	2.3	2.69	Round
Philippi sand	1.5	2.71	Round
Greywacke crusher dust	3.6	2.60	Angular
Greywacke crusher dust (2 mm sieve)	2.4	2.60	Angular
19 mm Greywacke stone	-	2.72	Angular

3.1.5.2. *Cement and admixtures*

The cement used was CEM I 42.5N and was supplied by PPC (Pretoria Portland Cement Co. Ltd.). The admixtures were supplied by Chryso SA (Pty) Ltd. The following description of the admixtures was taken from their general catalogue (Chryso SA, 2007).

- Plast 500 is a chloride free water-reducing admixture and is classified as a normal plasticizer. It disperses the fine particles in the concrete mix, which improves the workability of the concrete for the same water content.
- Plast Activator is a set accelerator which gives better cement hydration and increased setting times. It consists of a chloride formulation and should not be used in the presence of steel reinforcement due to the added corrosion potential of the chloride-ions.
- Tard CE is a set retarder that delays the initial set of concrete by modifying the hydration reactions. It does not increase the time between the beginning and end of setting, and allows the concrete to harden normally once the setting starts. There are no surface tension effects or changes in the consistency of the concrete.

The properties of the cement and the admixtures are given in Table 3.4.

Table 3.4: Cement and admixture properties

Material	Relative density - RD [kg/m³]	Recommended dosage [litre / 100kg of cementitious material]
Cement (CEM I - 42.5N)	3.14	-
Plasticizer (Plast 500)	1.20	0.16 to 0.42
Accelerator (Plast activator)	1.12	0.20 to 0.80
Retarder (Tard CE)	1.25	0.30 to 2.0

3.1.5.3. *Fibres*

Polyester, polypropylene and fluorinated polypropylene fibres were added to the standard Mixes 1 and 2 and were supplied by Hosaf Fibres (Pty) Ltd. South Africa, Sapy (South African Polypropylene Yarns) (Pty) Ltd. and Chryso SA (Pty) Ltd. respectively. The fibre dosage was 0.9 kg per cubic meter of concrete, which is normally specified as the dosage of fibres needed to prevent PSC (Illston et al., 2002:420). The fibres have a length of 12 mm and can be classified as short fibres. The addition of such a small amount of short fibres to concrete, classifies the concrete as a low volume fibre reinforced concrete (LV-FRC), since the volume fraction of fibres as percentage of total concrete volume is less that 0.2 %.

Table 3.5 summarises the important information of the short fibres added to Mixes 1 and 2 for PSC experiments. Pictures of the different short fibre types (12 mm in length) were taken with an electron microscope to verify the fibre diameter, as shown in Figure 3.12.

Table 3.5: Properties of short fibres

Fibre type	Relative density - RD [kg/m³]	Dosage [kg/m³]	Volume fraction [%]	Length [mm]	Diameter [µm]
Polyester (PES)	1.38	0.9	0.07	12	18
Polypropylene (PP)	0.91	0.9	0.10	12	30-40
Fluorinated polypropylene (FPP)	0.91	0.9	0.10	12	30-40

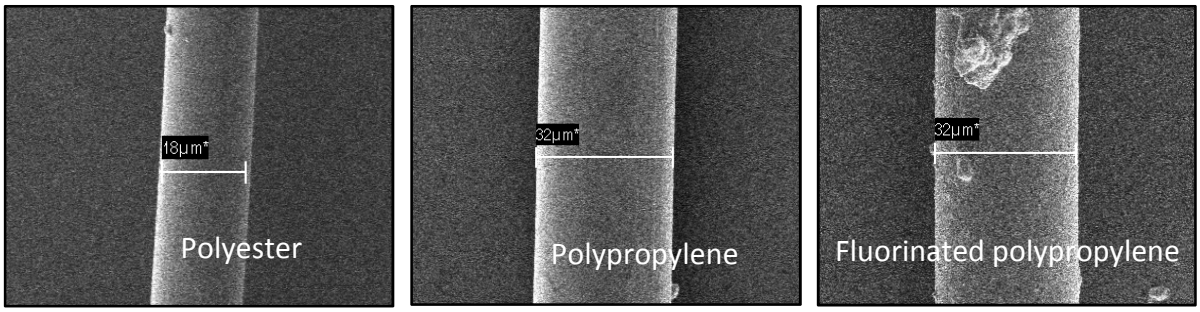

Figure 3.12: Electron microscope pictures of short fibre types

3.1.5.4. *Mix proportions*

All the variations of Mix 1 have a constant water-cement ratio of 0.7 and showed no segregation as well as good workability and cohesion. The tested slump values were all in the range of 75 ± 20 mm and the 28 day compression strength was on average 31.4 MPa. The slump and compression tests were conducted to verify the quality of the concrete mixes. The proportions of the different Mix 1 variations are shown in Table 3.6.

Table 3.6: Proportions of Mix 1 variations

Mix 1	**M1S**	**M1A**	**M1R**	**M1B**	**M1PES**	**M1PP**	**M1FPP**
Content	**[kg/m³]**						
Philippi sand	503	503	503	-	503	503	503
Greywacke crusher dust	506	506	506	506	506	506	506
Malmesbury sand	-	-	-	486	-	-	-
19 mm Greywacke stone	950	950	950	950	950	950	950
Cement (CEM I - 42.5N)	270	270	270	270	270	270	270
Water	190	190	190	190	190	190	190
Plasticizer	1	1	1	-	1	1	1
Accelerator	-	1.51	-	-	-	-	-
Retarder	-	-	1.7	-	-	-	-
Polyester fibres	-	-	-	-	0.9	-	-
Polypropylene fibres	-	-	-	-	-	0.9	-
Fluorinated polypropylene fibres	-	-	-	-	-	-	0.9
Total content	2420	2422	2422	2402	2421	2421	2421

All the variations of Mix 2 showed no segregation and good cohesion. However, it showed poor workability due to a low water-cement ratio of 0.4 and high fine content of the sand. Since the purpose of this mix was to result in pronounced PSC, the workability was of minor importance. The slump values were between 5 mm and 10 mm and the 28 day compression

strength was on average 65.3 MPa. The proportions of the different Mix 2 variations are shown in Table 3.7.

Table 3.7: Proportions of Mix 2 variations

Mix 2	**M2S**	**M2PES**	**M2PP**	**M2FPP**
Content	**[kg/m³]**			
Greywacke crusher dust sieved (2 mm)	579	579	579	579
19 mm Greywacke stone	1018	1018	1018	1018
Cement (CEM I - 42.5N)	573	573	573	573
Water	229	229	229	229
Polyester fibres	-	0.9	-	-
Polypropylene fibres	-	-	0.9	-
Fluorinated polypropylene fibres	-	-	-	0.9
Total content	2399	2400	2400	2400

3.1.6. Test procedures

The climate chamber was switched on at least 2 hours before the test commenced to allow the environmental conditions to stabilize. Two different mixes were placed in the climate chamber for each test. The mixes were prepared one at a time after which the slump test was carried out in accordance with SANS: 5862-1 (2006:3). The concrete as well as the capillary pressure sensors were then placed into the two PSC moulds and one square evaporation mould. A thin layer of mould oil was applied to the insides of the moulds to create a frictionless surface as well as assist with demolding after tests have finished.

After the moulds were filled with concrete they were vibrated on a table vibrator until all the entrapped air had escaped. The metal pan was also filled with water and the Vicat mould was filled with a concrete mortar which was collected by sieving the concrete through a 4.75 mm sieve. All the aforementioned moulds were then placed in the climate chamber and all the sensors were connected to the computer. This procedure was then repeated for the second mix. The bleeding moulds were also filled and placed in the controlled environmental room. The measurement of the bleeding, setting times and crack growth were conducted in 20 minute intervals.

3.2. *Single fibre pullout experiments*

Single fibre pullout experiments refer to the repeated physical pullout of different synthetic fibres from a fresh concrete paste. These experiments were conducted separately from the PSC experiments.

3.2.1. Test setup

The length of the fibres used in this study is 12 mm as shown in Table 3.5. However, conducting pullout tests from fresh concrete paste with 12 mm fibres was cumbersome and problematic. Furthermore, the embedment lengths achievable with 12 mm fibres were believed to be too small to give quantitative results for pullout test from fresh concrete paste. This problem was overcome by using uncut yarns of the fibres and a fibre embedment length of 20 mm was chosen.

A special mould was designed to perform the single pullout tests of fibres from fresh concrete paste. The design was optimized through various preliminary trial and error experiments to give a repeatable and stable testing procedure which causes minimum disturbance of the fibre and paste interface. The setup consists of a rectangular PVC mould with a depth of 20 mm. There are 22 holes at the bottom of the mould with a diameter of 1 mm each. The mould has a bridge structure above it to which 22 small metal plates can be screwed. The fibres must be threaded through the holes and are held in place above the concrete paste by the metal plates to which the fibres are glued.

The bridge structure has special screw adjusters which allow the bridge to be raised and lowered. The metal plates have holes at the top which allows the plates to be screwed to a fitting that is attached to a 10 Newton load cell. Once the metal plates are connected to the load cell via the special fitting, they can be unscrewed from the bridge structure. Each fibre can then be pulled freely from the concrete paste. More details on the testing procedure are discussed in Section 3.2.5. Figure 3.13 shows the fibre pullout setup.

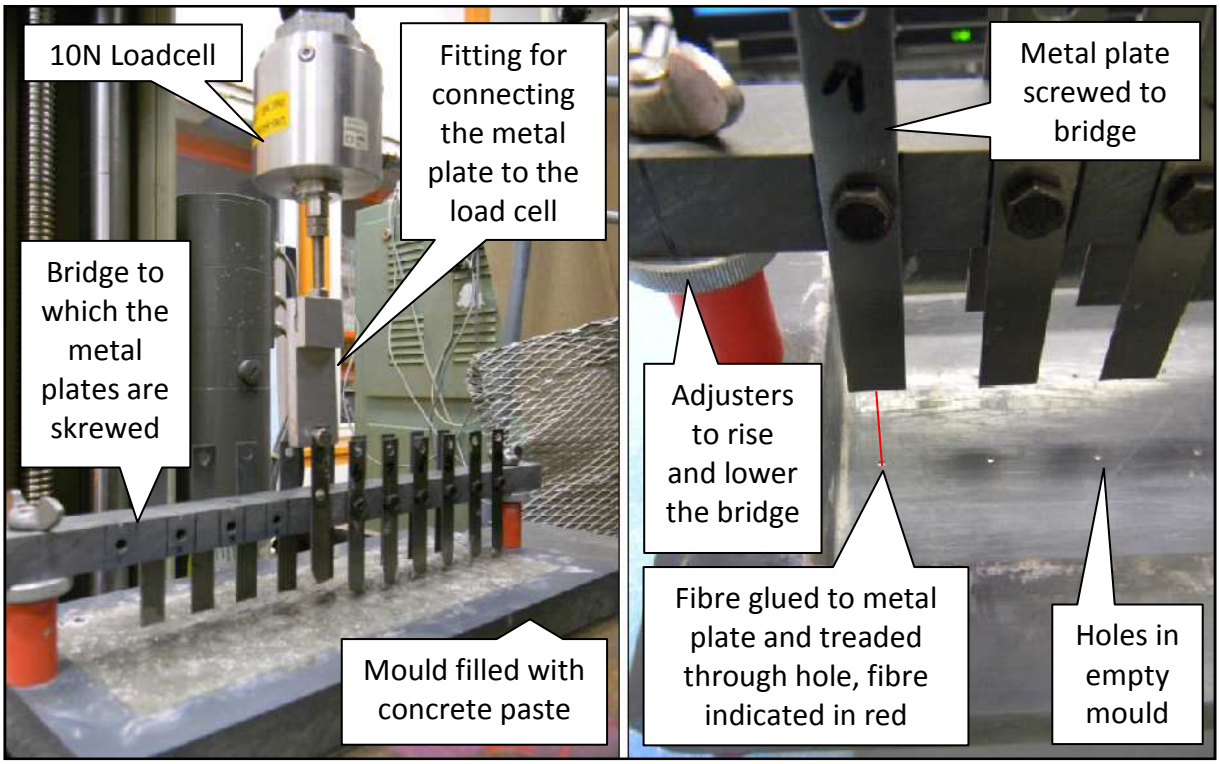

Figure 3.13: Pictures of a fibre pullout setup

3.2.2. Test objectives

The mechanical advantages of fibres in any fibre reinforced concrete only become apparent once cracking occurs. The fibre can bridge the crack which reduces further crack growth. Once a fibre bridges a crack it can only fail through pullout or rupture. For fresh concrete paste rupture is unlikely and crack widening proceeds mainly through fibre pullout. The force required to pull a fibre out depends on the interfacial shear bond stress between the fibre and the concrete paste. The structure of the concrete paste changes continuously in fresh concrete due to hydration, which will influence the magnitude of the interfacial shear bond stress.

The objective of the single fibre pullout test was to determine the interfacial shear bond stress between the fibre and the concrete paste and how this bond stress increases with time.

3.2.3. Experimental test programme

To achieve the objective it was aimed to conduct at least five pullout tests from the fresh concrete paste for every hour after the concrete paste has been cast. The tests were ended after the final setting time of the concrete paste has been reached. The standard Mixes 1 and 2 (M1S and M2S) that were used for the PSC experiments were also used for the fibre pullout experiments. No stone was added to the mixes which ensured an undisturbed fibre and concrete paste interface. The same polyester, polypropylene and fluorinated polypropylene fibres that were used for the PSC experiments were also used for the single fibre pullout tests.

The force required to pull the fibre out of the concrete paste and the displacement was logged on a computer. A constant pullout speed of 0.05 mm/s was chosen. The pullout tests were conducted in a controlled environmental room. The temperature was kept constant between 20 °C and 25 °C and the relative humidity between 50 % and 60 %. No wind was present during testing. The setting times were also measured under these environmental conditions which is called Climate 3 in this study. The setting times were determined as explained in Section 3.1.2.6.

3.2.4. Materials and mix proportions

The uncut polypropylene and fluorinated polypropylene fibres used for the pullout tests unfortunately had diameters of 20 µm which differs from the equivalent short fibres that were used for the PSC experiments. This was confirmed by measurements with an electron microscope as shown in Figure 3.14. The properties of the uncut fibres are shown in Table 3.8.

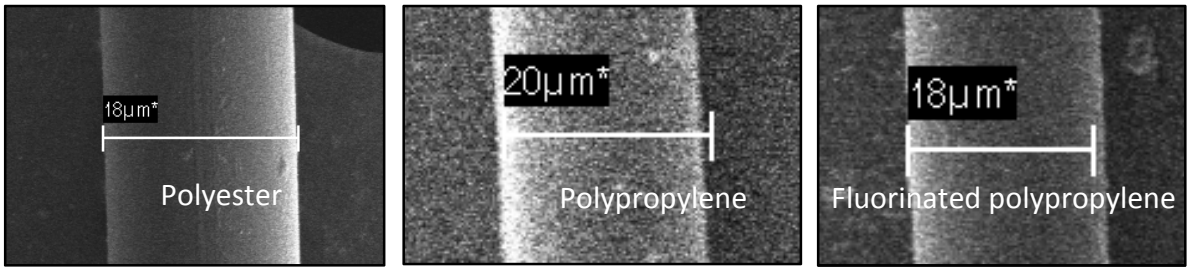

Figure 3.14: Electron microscope pictures of uncut fibre types

Table 3.8: Properties of uncut fibres

Fibre type	Relative density - RD [kg/m³]	Diameter [µm]
Polyester (PES)	1.38	18
Polypropylene (PP)	0.91	20
Fluorinated polypropylene (FPP)	0.91	20

The standard Mixes 1 and 2 were used as shown in Tables 3.6 and 3.7 except that no stone was added.

3.2.5. Testing procedures

Uncut yarns of the fibres were used to simplify the preparation producers. The fibre yarns were first glued to the rectangular metal plates and were then treaded through the holes at the bottom of the mould once the glue had sufficient time to harden. The fibres were kept straight by a small clay weight hanging from the fibre beneath the mould. The metal plates were then connected to the bridge with screws. The mix was then prepared and carefully added to the mould after mixing thoroughly for at least 2 to 3 minutes with a Hobart type mixer. The free length of the fibres above the concrete paste was 2 mm at this stage. The mould was vibrated on a table vibrator to allow entrapped air to escape from the concrete.

After vibrating the mould, the fibres were cut at the bottom of the moulds and were then pulled 3 mm upwards by raising the bridge with the screw adjusters. This ensured that the fibres were only embedded in the concrete paste and not in the holes at the bottom of the mould. Each fibre had a straight free length of 5 mm above the paste at this stage. The mould was then moved to the controlled environmental room where the tests were conducted. The bridge was lowered by 2 mm just before the first test, which kept the free length of the fibres at 5 mm but curved as shown in Figure 3.15. This ensured no accidental pullout of the fibres during the connection of the metal plate with fitting below the load cell. The fibres were then pulled out one at a time after screwing the metal plates to the fitting below the load cell and unscrewing them at the bridge.

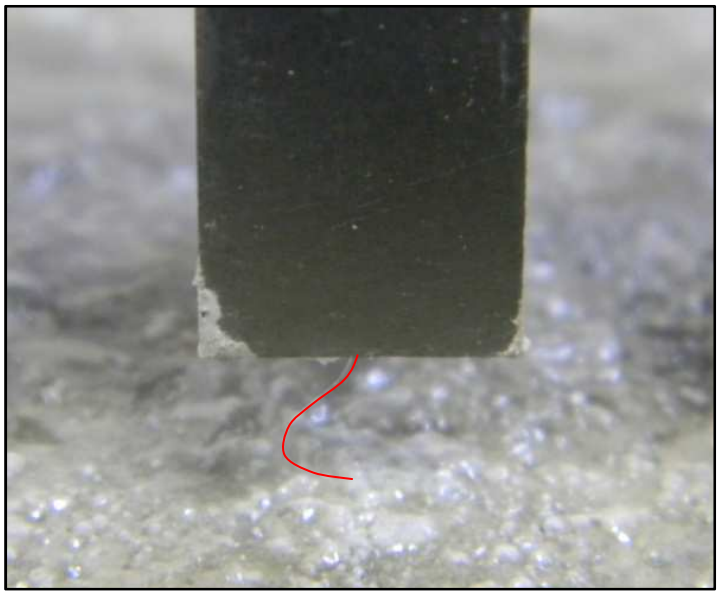

Figure 3.15: Curved fibre before pullout, with the fibre indicated in red

3.3. *Concluding summary*

In this chapter, the framework of both the PSC and single fibre pullout experiments were presented. The PSC test consisted of numerous measurements on conventional fresh concrete mixes. Most of the measurements were conducted in the climate chamber which was manufactured as part of this study. The main objective was to gain knowledge on when and why PSC occur. This knowledge is important if PSC is to be reduced or prevented. The PSC experiments also included several tests on LV-FRC. The pullout tests comprised of several single synthetic fibres being pulled out individually from fresh concrete paste at different times. The objective was to ascertain the resistance that fibres give to pullout as a function of time, which is valuable information to aid in explaining the reduction of PSC due to fibres.

The results of the PSC experiments and the single fibre pullout experiments are presented in the next chapter.

4. Experimental results

In this chapter the experimental results of the plastic shrinkage cracking (PSC) and single fibre pullout experiments are presented. The complete sets of the results are given in Appendixes B and C for the PSC and fibre pullout experiments respectively.

4.1. *Plastic shrinkage cracking experiments*

In the following sections the result of a specimen from each mix on which PSC experiments were conducted are summarised in separate graphs. This includes all the mixes with and without fibres as well as mixes which were tested at different climate conditions. The name, definition and characteristic of every mix used is summarised in Table 3.1.

The graph of each specimen shows the following:

- The cumulative bleeding and evaporation amounts of the concrete specimen.
- The crack area growth.
- The capillary pressure build-up.
- The initial and final setting times of the concrete.
- The time of crack onset (T_{CO}) which is defined as the time when the first crack is observed and is indicated on each graph with a vertical black dotted line.
- The time of crack stabilization (T_{CS}) which is defined as the time where a clear decrease in the rate of crack area growth can be identified. This is always after a period of rapid crack growth and is indicated with a vertical dotted blue line on each graph.
- The time of air entry (T_{AE}) which can be identified by the significant drop in capillary pressure after a period of steady pressure build-up.

Although each mix had two specimens and therefore two graphs, only one graph per mix is presented in this chapter. The results of both specimens where used for analysis and there was no basis on which a specimen was chosen for presentation, either would be acceptable. The results of all the specimens are shown in Appendix B. The summary of the results for the bleeding and average crack growth for all mixes are also shown in the following sections.

4.1.1. Results of mixes without fibres

Figure 4.2 shows the results of M1S and M1B at Climates 1 and 2 which were conducted to investigate Theses 1 and 2 as discussed in Section 3.1.3. The figure also indicates the drying time (T_D) which is defined as the time once all the bleeding water at the surface of the concrete has evaporated.

Figure 4.3 shows the results of all the variations of Mix 1 without fibres at Climate 1 which were conducted to investigate Observations 1 and 2 as discussed in Section 3.1.3. The figure also indicates the general shape of the crack area growth line with time as a stretched out S-shape, which is characterized with no cracks in the beginning, followed by a sudden increase in crack area just after the time of air entry and normally stabilizes before the final setting time is reached.

4.1.2. Results of mixes with and without fibres

Figure 4.4 shows the results of the standard Mix 1 with and without fibres at Climate 1. It is shown that no cracks were observed for the mixes containing fibres. This was undesirable since the results needed to give a measureable comparison between a mix with and without fibres. To avoid the same result for tests with the second mix an additional restraint was added to the PSC moulds in the form of two steel bars as shown in Figure 4.1. The details of the added restraint are discussed in Appendix A.5.7.

Figure 4.5 shows the results of the standard Mix 2 with and without fibres at Climate 1 that were conducted in the PSC moulds with the additional restraint. It should be mentioned that the results of crack initiation and growth for the variations of Mixes 1 and 2 are not directly comparable since they were conducted at different levels of restraint.

Figure 4.1: PSC mould with steel bars for additional restraint

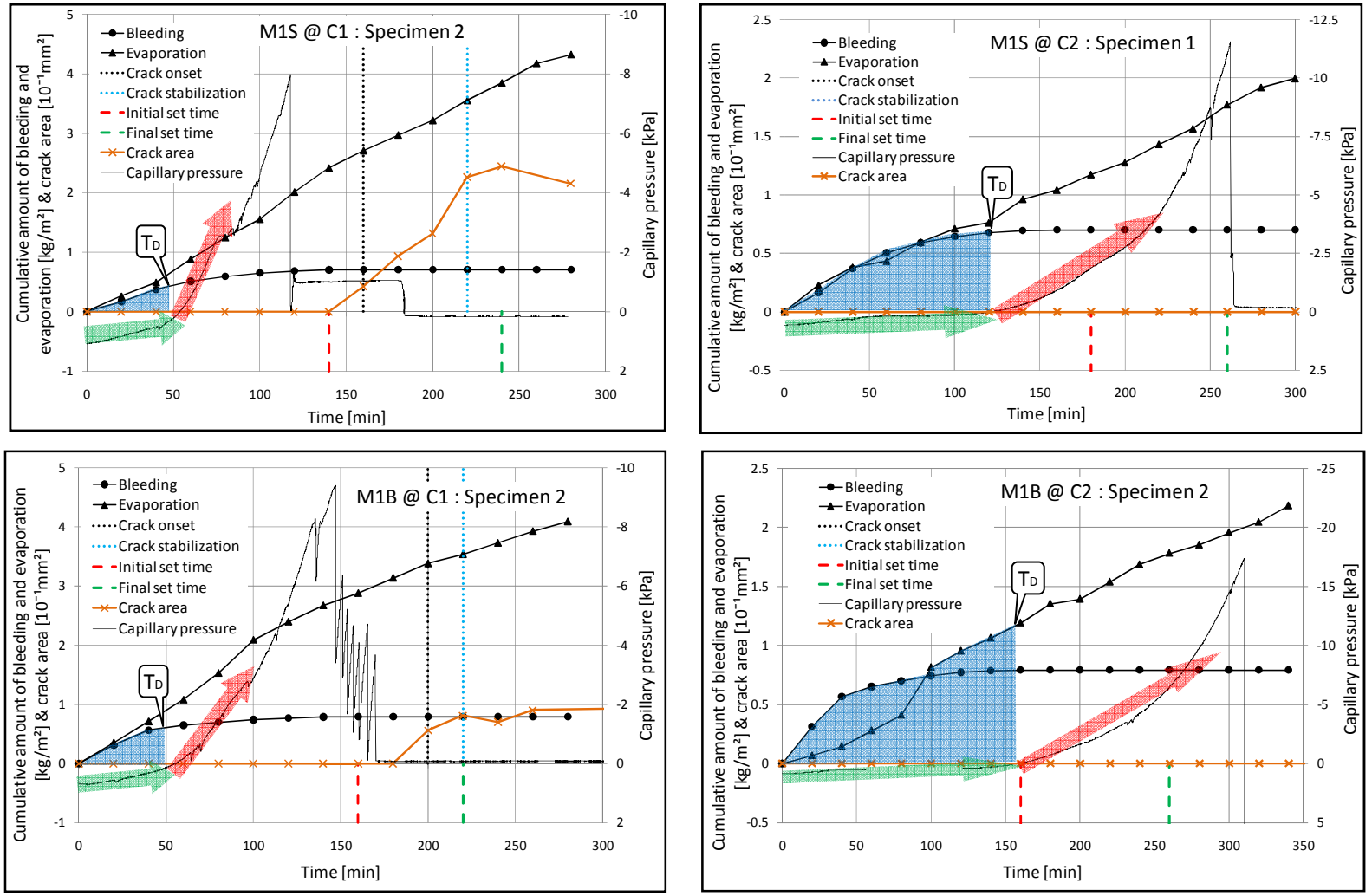

Figure 4.2: Results of M1S and M1B at Climates 1 and 2. The blue shading illustrates the time when the amount of bleeding water that has come to the surface is equal to the to the evaporated amount of bleeding water, called the drying time and is indicated with a marker labelled T_D. The green and red arrows illustrate the start of capillary pressure build-up once the drying time is reached.

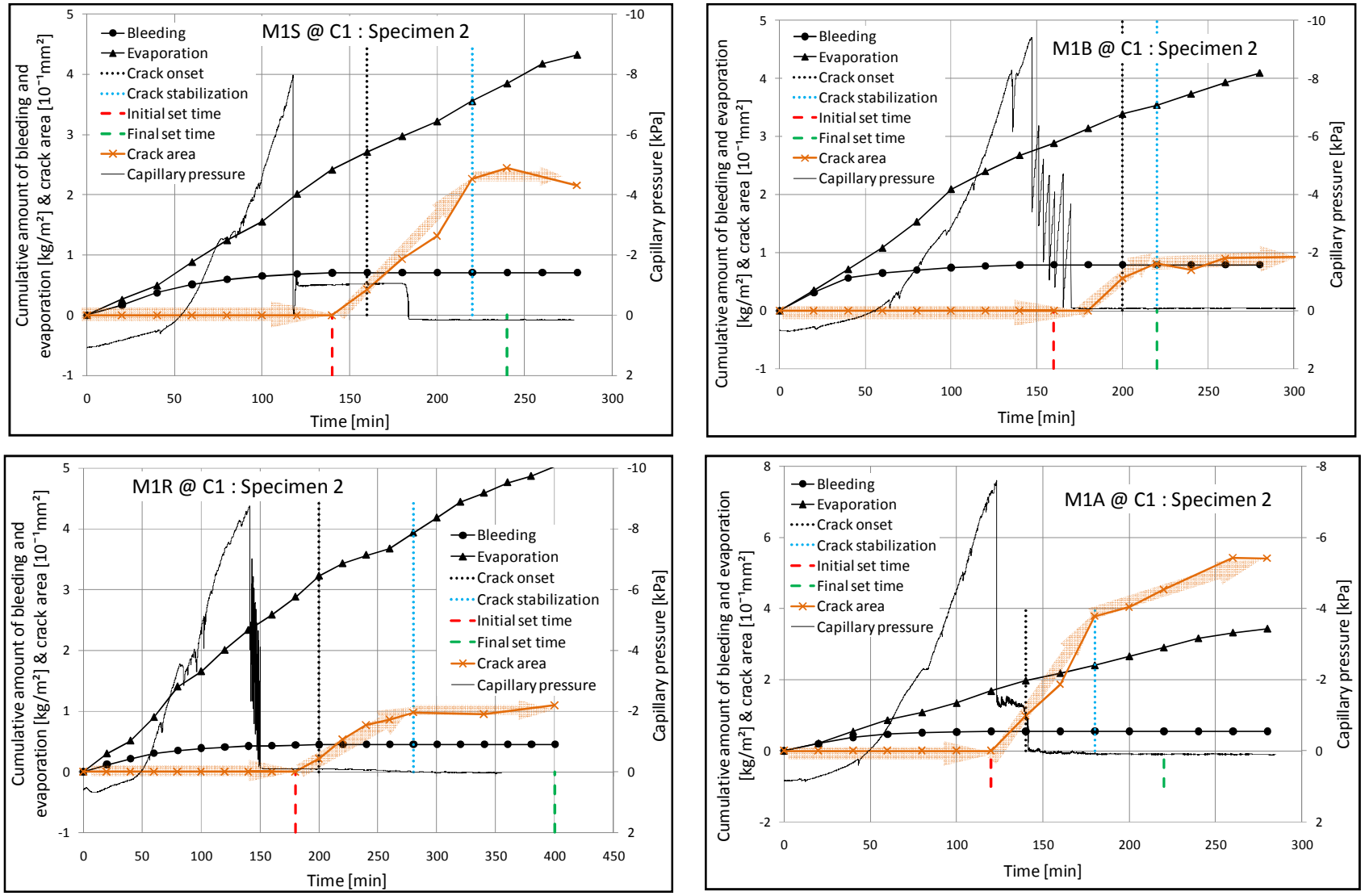

Figure 4.3: Results of the variations of Mix 1 without fibres at Climate 1. The orange arrows illustrate the rapid growth of the crack before stabilization.

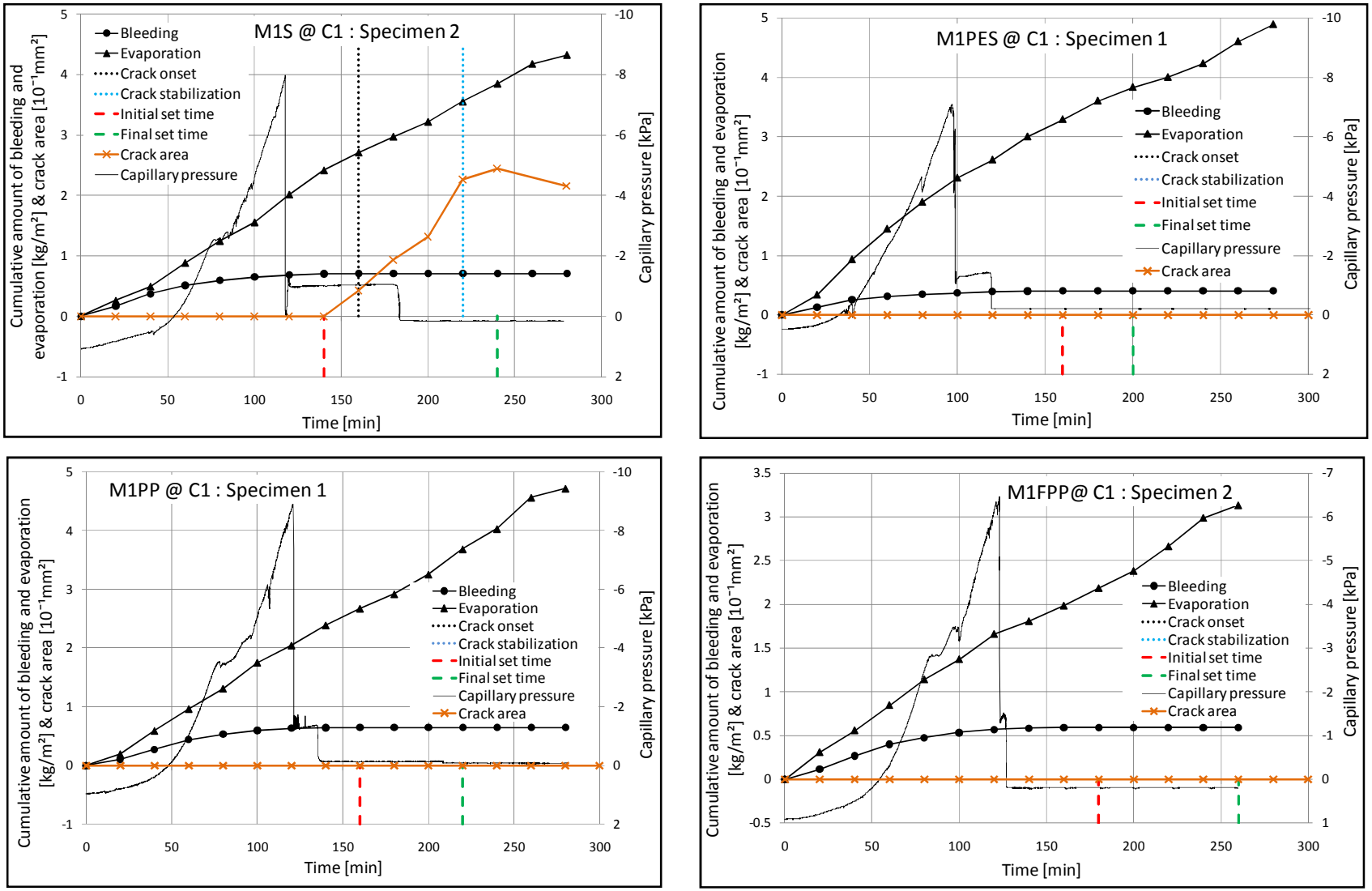

Figure 4.4: Results of the standard Mix 1 with and without fibres at Climate 1

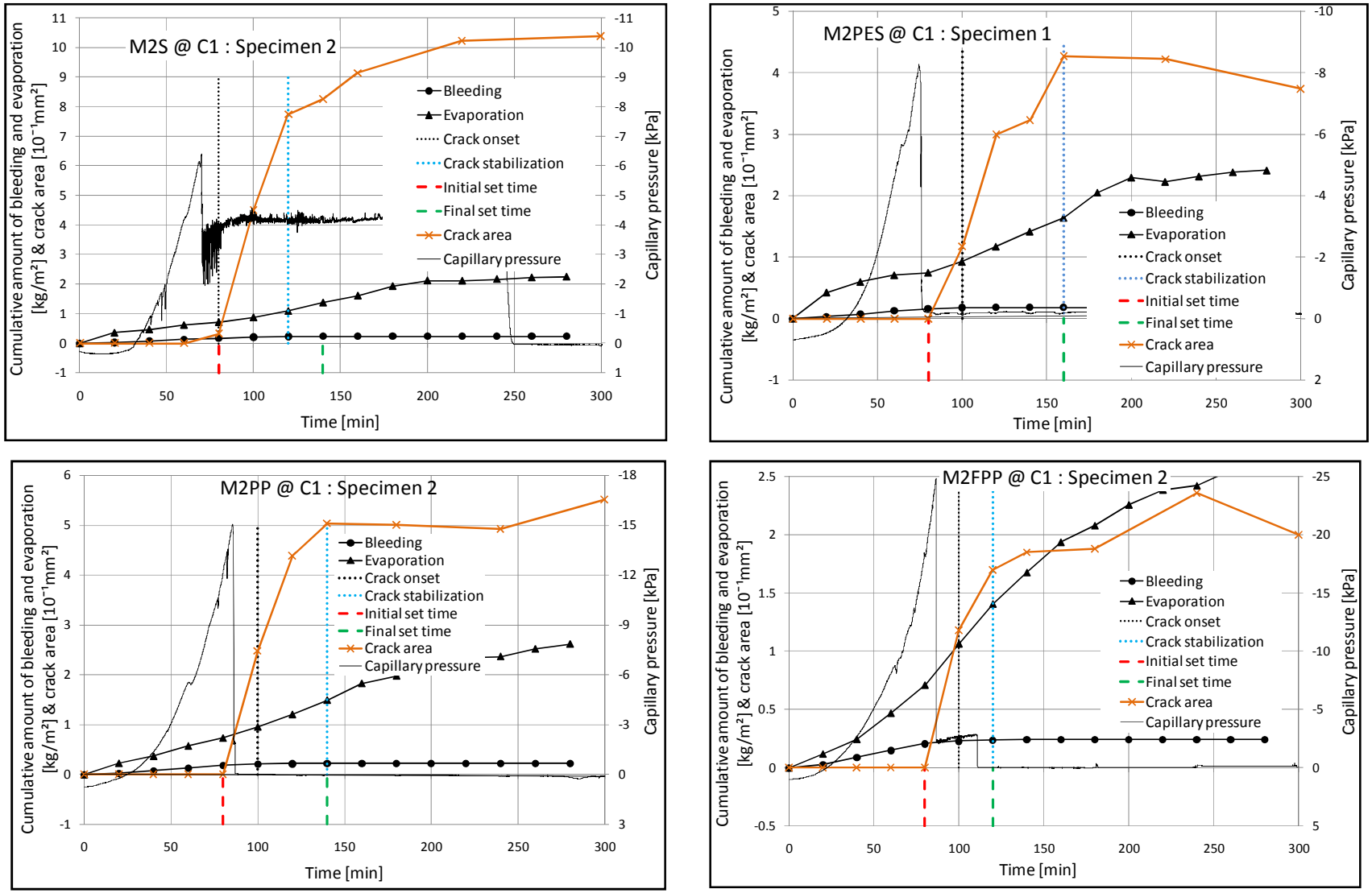

Figure 4.5: Results of the standard Mix 2 with and without fibres at Climate 1 with added restraint

4.1.3. Crack growth results

Figures 4.6 to 4.9 show the results of the average crack area and the rate of average crack area growth with time for the variations of Mixes 1 and 2. The crack areas as indicated in these figures were calculated as the average of the two specimens of a specific mix.

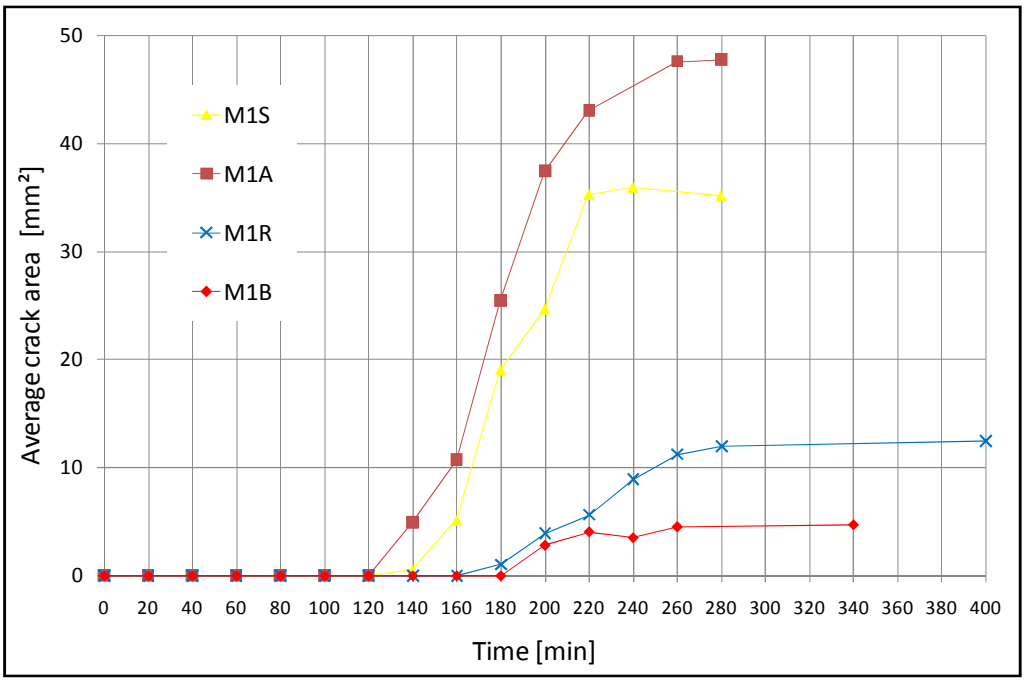

Figure 4.6: Average crack area of the variations of Mix 1 without fibres at Climate 1

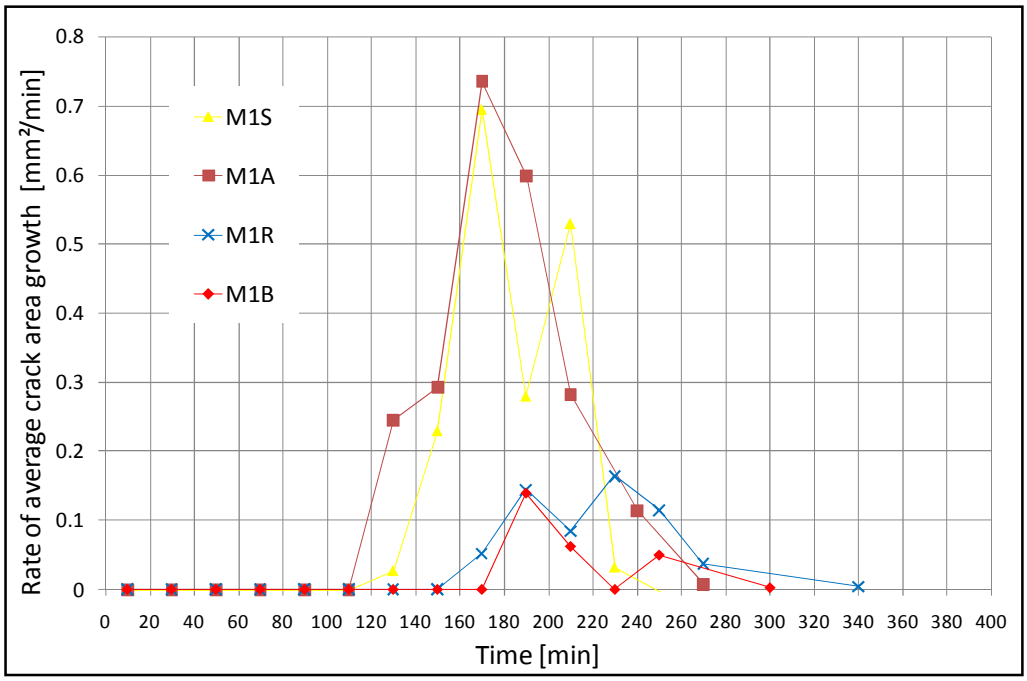

Figure 4.7: Rate of average crack area growth of the variations of Mix 1 without fibres at Climate 1

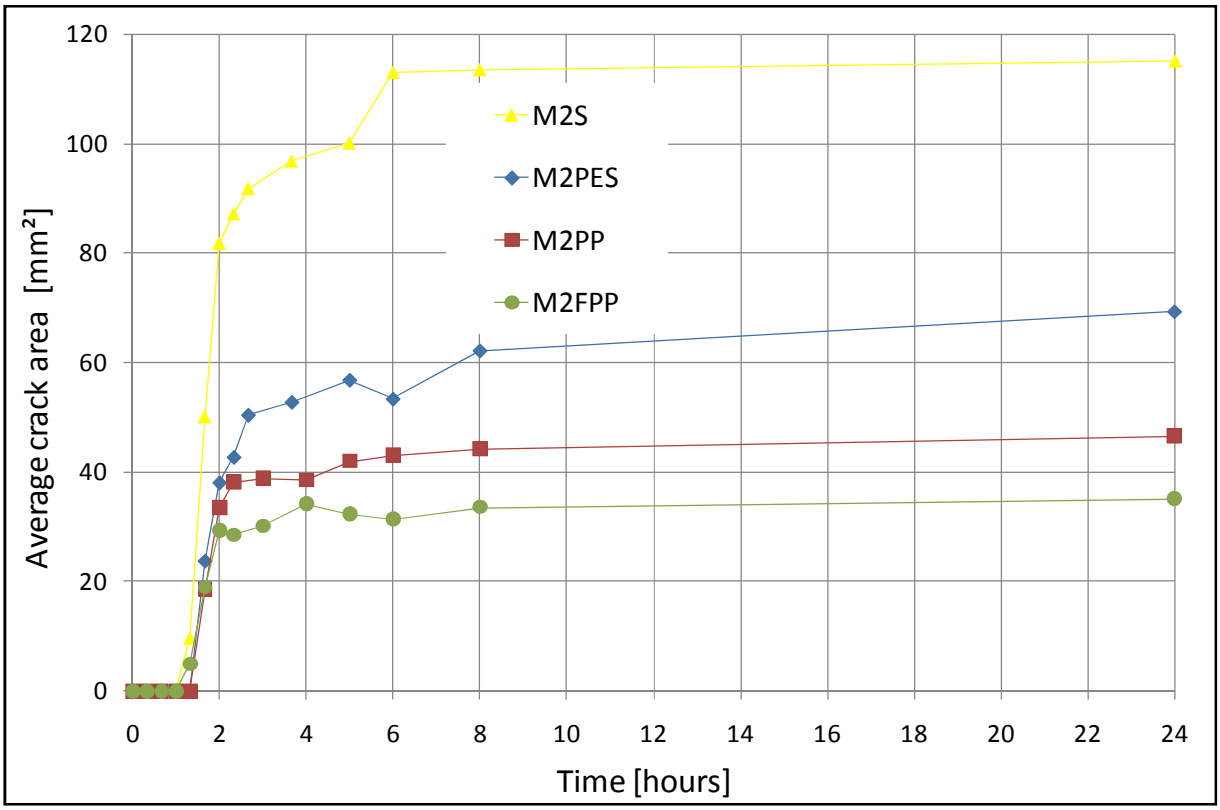

Figure 4.8: Average crack area of the standard Mix 2 with and without fibres at Climate 1

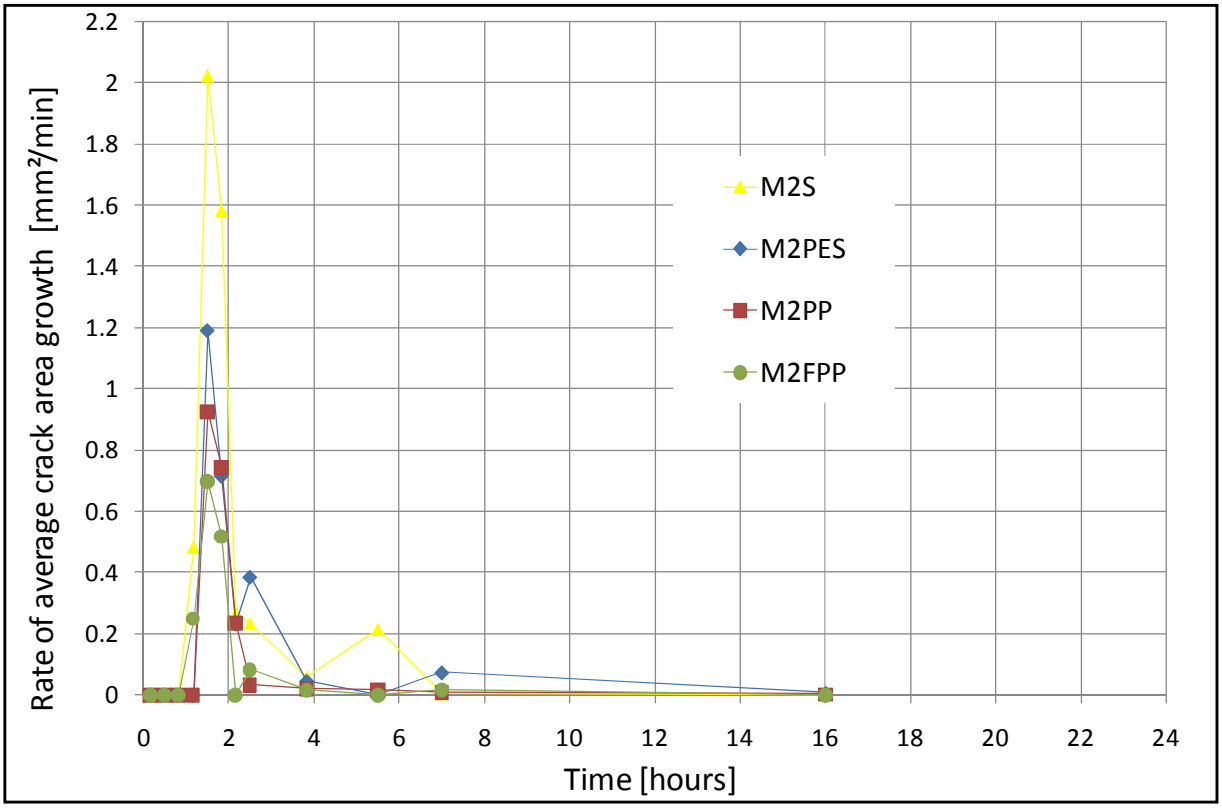

Figure 4.9: Rate of average crack area growth of the standard Mix 2 with and without fibres at Climate 1

4.1.4. Bleeding results

Figures 4.10 and 4.11 show the results of the cumulative bleeding amount and the rate of bleeding respectively of all the mixes without fibres.

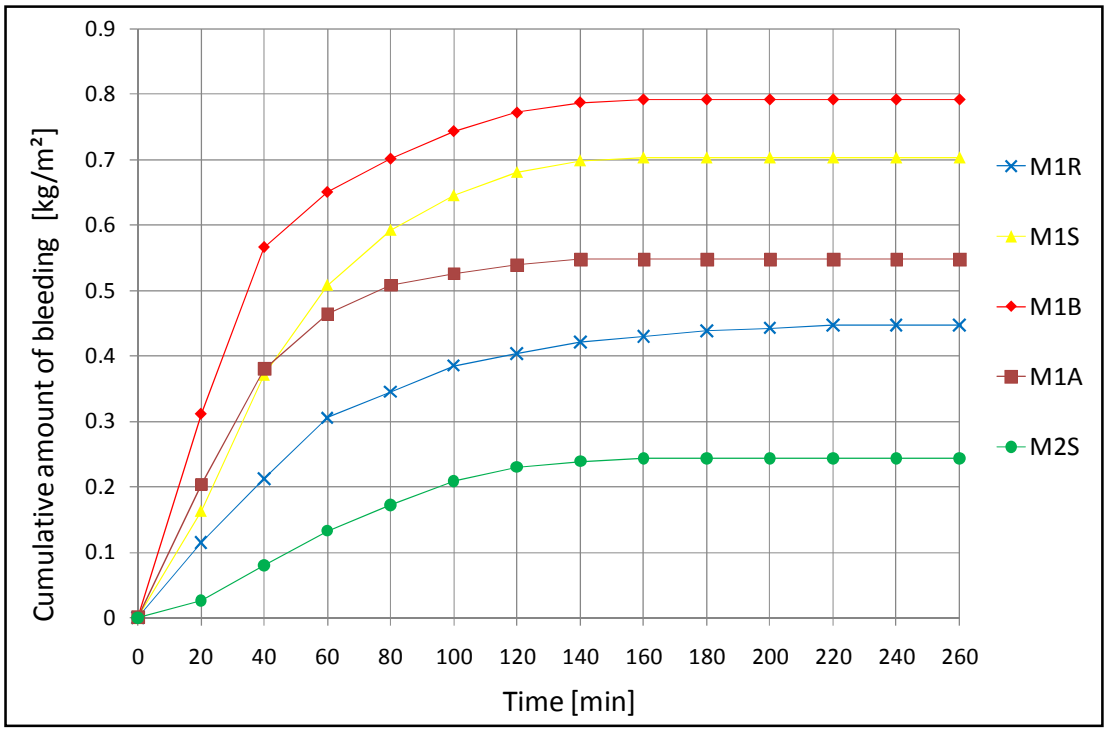

Figure 4.10: Cumulative bleeding amount of mixes without fibres

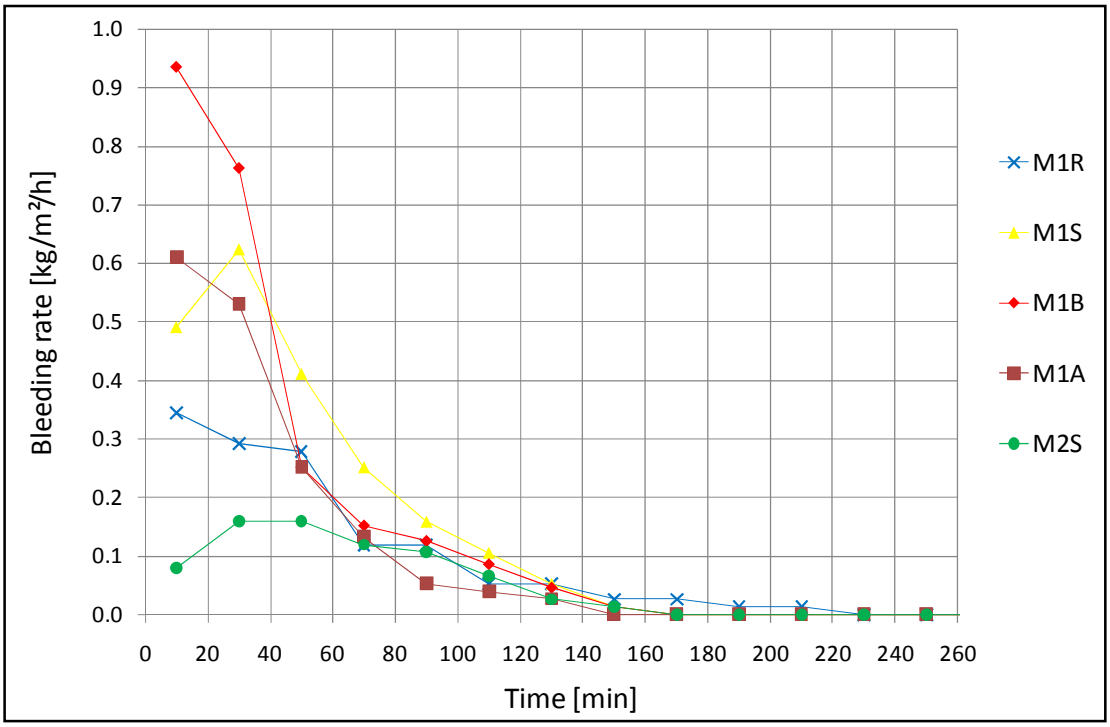

Figure 4.11: Bleeding rate of mixes without fibres

Figures 4.12 and 4.13 show the results of the cumulative bleeding amount and rate of bleeding respectively of the standard Mixes 1 and 2 with and without fibres.

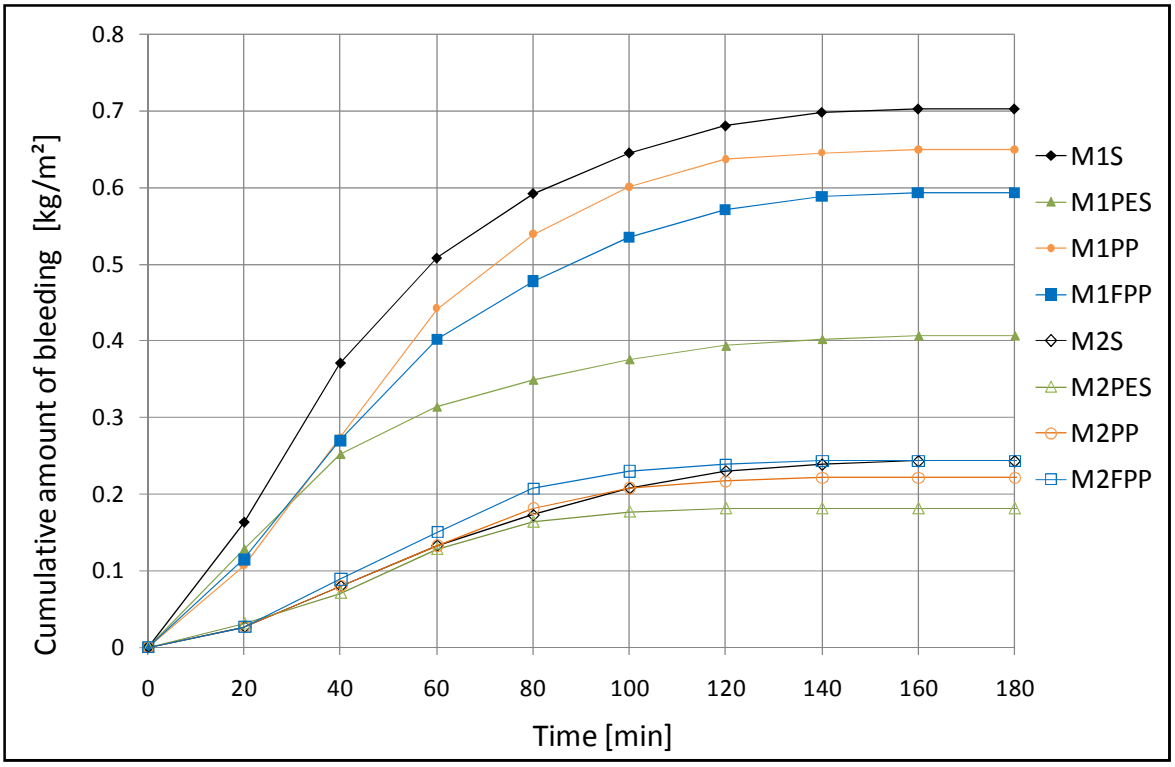

Figure 4.12: Cumulative bleeding amount of the standard Mixes 1 and 2 with and without fibres

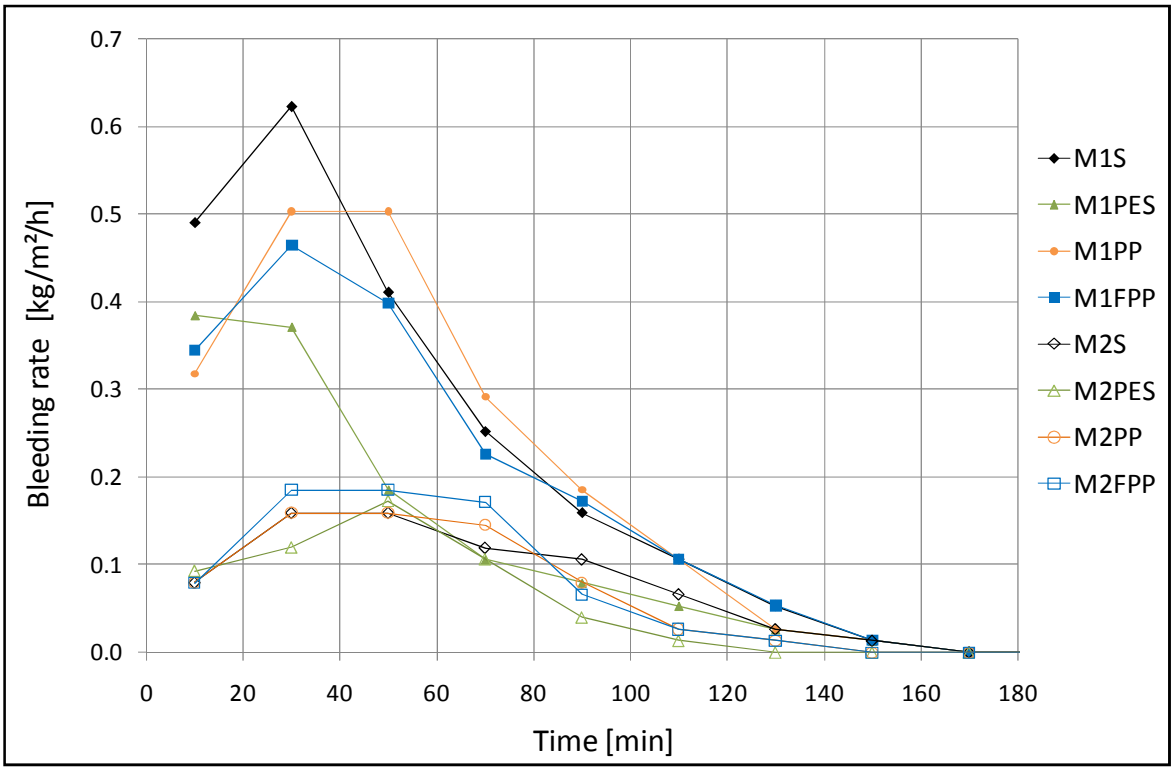

Figure 4.13: Bleeding rate of the standard Mixes 1 and 2 with and without fibres

4.2. *Single fibre pullout experiments*

Figure 4.14 shows the results of a typical single fibre pullout test from fresh concrete paste. The experiments were set up in such a way that the fibre only started pulling out of the concrete paste after the cross head of the testing machine has displaced approximately 2 mm. This enabled the clear identification of the zero reading from the load cell, which is very sensitive at low forces. The arrows in the figure show the expected behaviour of a single fibre pullout test from fresh concrete paste. It consists of an increase to maximum pullout force followed by a gradual decrease to zero. The first peak value is the force required to completely debond the fibre from the concrete paste. This value was identified for each pullout test as the first stable peak value reached and was used for calculations and comparisons, since it is the initial force required for crack widening with the presence of fibres in concrete. In other words, it is the force bridged by a fibre across a crack.

Figure 4.14 also shows that additional peaks and troughs may occur after the first stable peak. This is a result of the non-homogenous nature of the fibre-paste interface that is caused for example by the air bubbles in a concrete paste, aggregate particles disturbing the fibre-paste interface, slight skew fibre pullout as well as possible mechanical anchorage through a wedge shaped fibre end caused by cutting. Furthermore, the author believes that the crosshead movement can directly be linked to the fibre pullout displacement, due to the relative low magnitude of the forces and the stiffness of the setup, which reduces the influence that the free length of the fibre has on the displacement.

The aim was to conduct a minimum of five tests for each mix and fibre type up to at least the point where the final setting time has occurred. An exception was made for the first 3 hours of M1S where only two tests per hour were performed. This was done as these values were found to be close to zero during preliminary tests. Three pullout tests were also conducted at 12 hours and 24 hours for M1S. This was done to get an indication of the pullout force some time after the final setting time. The aim of a minimum of five tests was not always achieved due to experimental errors and time constraints. The experimental errors occurred due to the small size of the test setup and fibres which led to obvious human induced errors during preparation and testing.

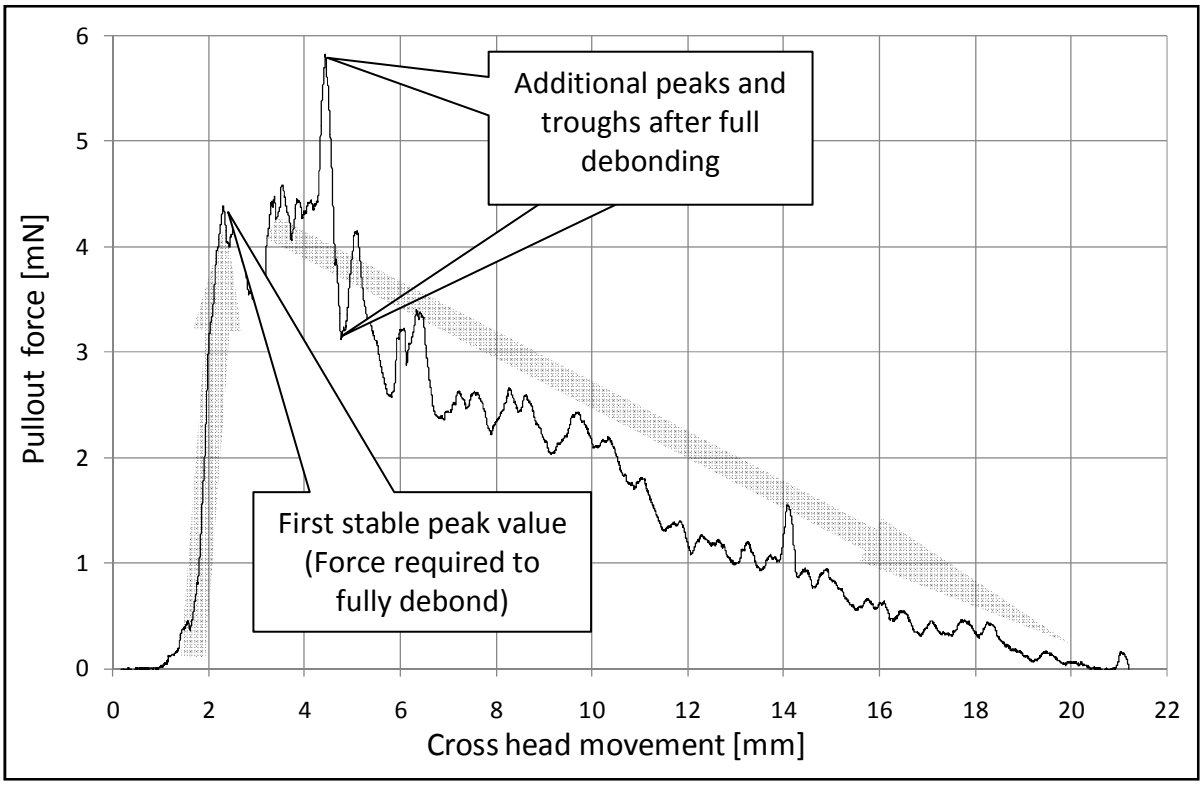

Figure 4.14: Typical result of a single fibre pullout test

Tables 4.1 and 4.2 show the number of test results which could be used for calculations. Tables that summarise all the results and additional calculations of the single fibre pullout tests are shown in Appendix C.

Table 4.1: Number of useable single fibre pullout results for M1S

M1S – Standard Mix 1 used frequently in slabs							
Time	1h & 2h & 3h	4h	5h	6h	7h	12h	24h
Polyester (PES)	6	7	7	7	5	3	3
Polypropylene (PP)	6	6	5	7	7	3	3
Fluorinated polypropylene (FPP)	6	7	7	7	7	3	3

Table 4.2: Number of useable single fibre pullout results for M2S

M2S – Standard Mix 2 with high risk for PSC					
Time	1h	2h	3h	4h	5h
Polyester(PES)	5	4	5	5	4
Polypropylene (PP)	5	5	5	5	3
Fluorinated polypropylene (FPP)	5	5	5	5	5

4.2.1. Average pullout force results

Figures 14.15 to 14.17 show the results of fibre pullout tests from M1S and M2S. The figures show the average pullout force for each fibre type, mix and time which was calculated as the average of the usable single fibre pullout results. The single fibre pullout results were obtained by identifying the force required to fully debond the fibre from the concrete paste for each pullout test as shown in Figure 4.14.

The figures also indicate the coefficient of variance (COV) of the pullout force for each set of pullout results. The COV is the standard deviation divided by the mean of the data set and is express as a percentage. The initial and final setting times of the concrete paste are also shown on the figures.

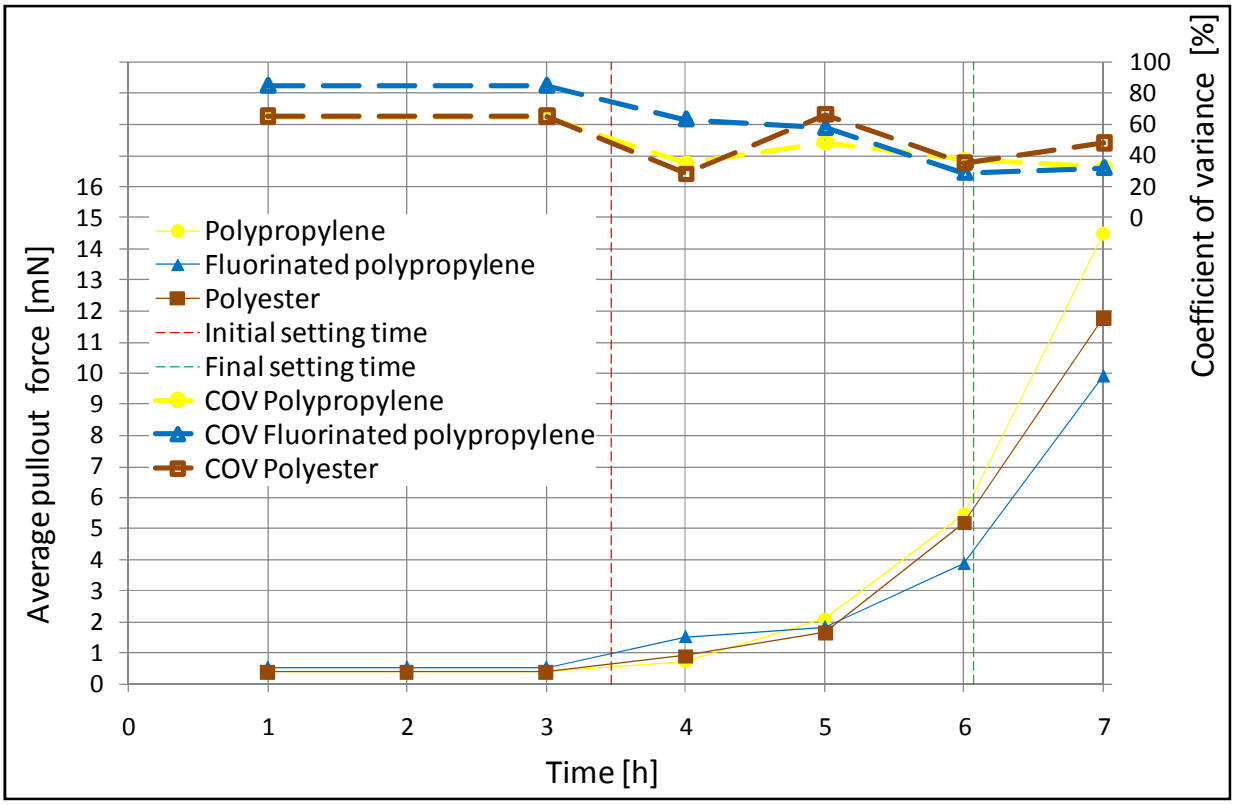

Figure 4.15: Average and COV of fibre pullout force from M1S up to 7 hours

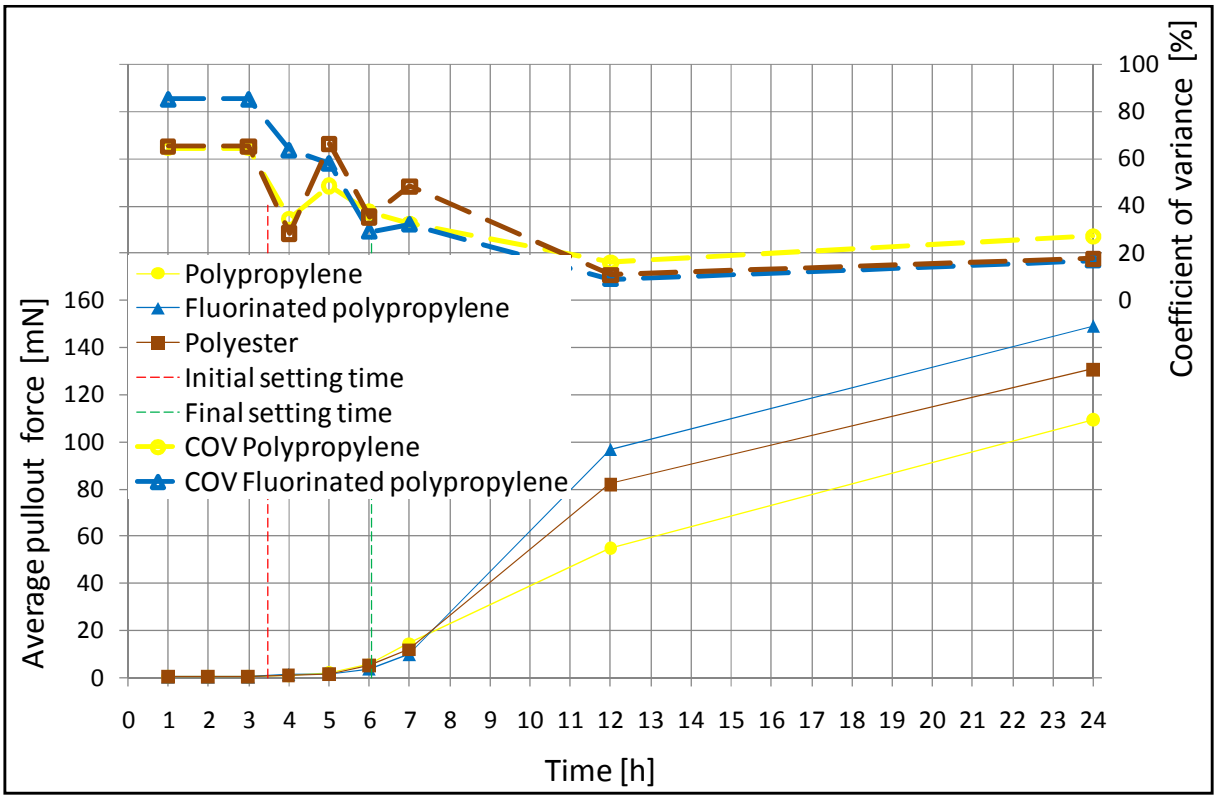

Figure 4.16: Average and COV of fibre pullout force from M1S up to 24 hours

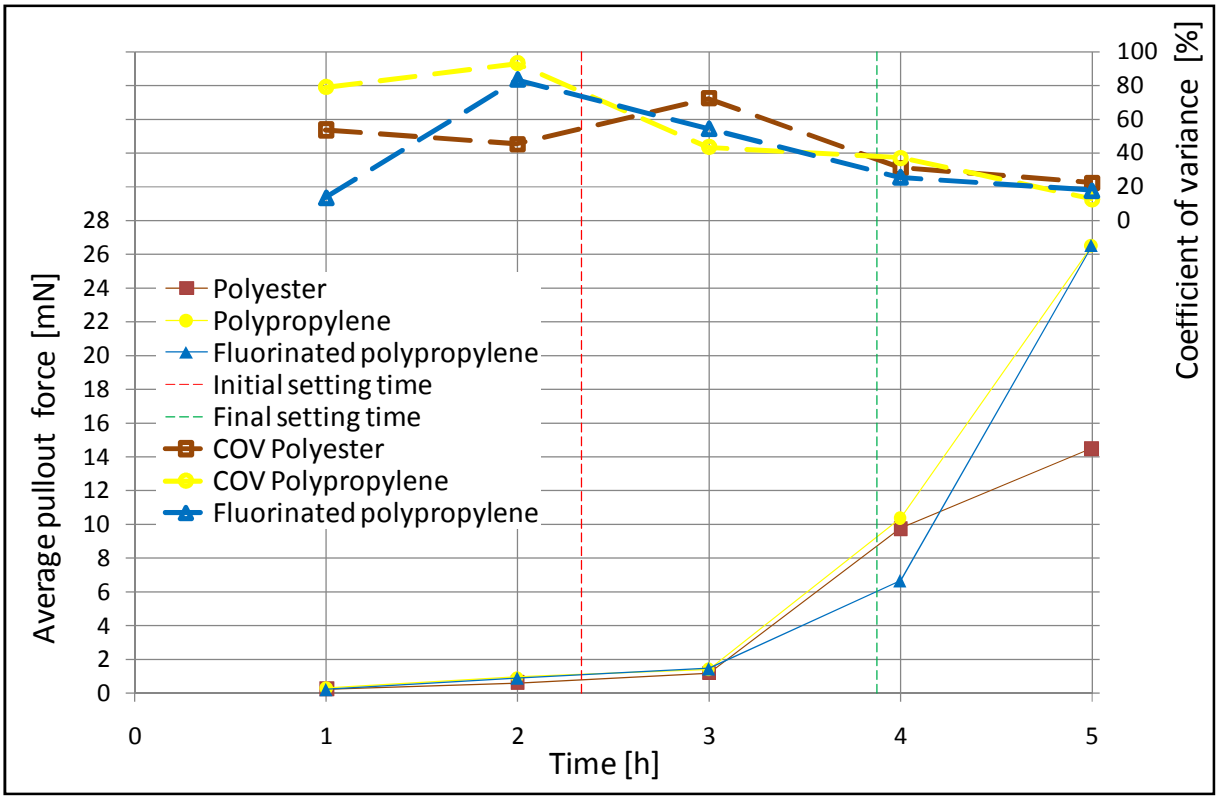

Figure 4.17: Average and COV of fibre pullout force from M2S up to 5 hours

4.2.2. Interfacial shear bond stress results

Figures 14.18 to 14.20 show the results of fibre pullout tests from M1S and M2S in terms of the interfacial shear bond stress between the fibre and the concrete paste.

The average maximum pullout force (F) as shown in Figures 14.15 to 14.17 was used to calculate the interfacial shear bond stress (τ) with Equation 4.1. This allows for a comparison between the results of the different fibres types and diameters.

$$\tau = \frac{F}{\pi \cdot d \cdot Le} \quad \text{..... (Equation 4.1)}$$

with:

τ = Interfacial shear bond stress

F = Average maximum pullout force

Le = Fibre embedment length

d = Fibre diameter

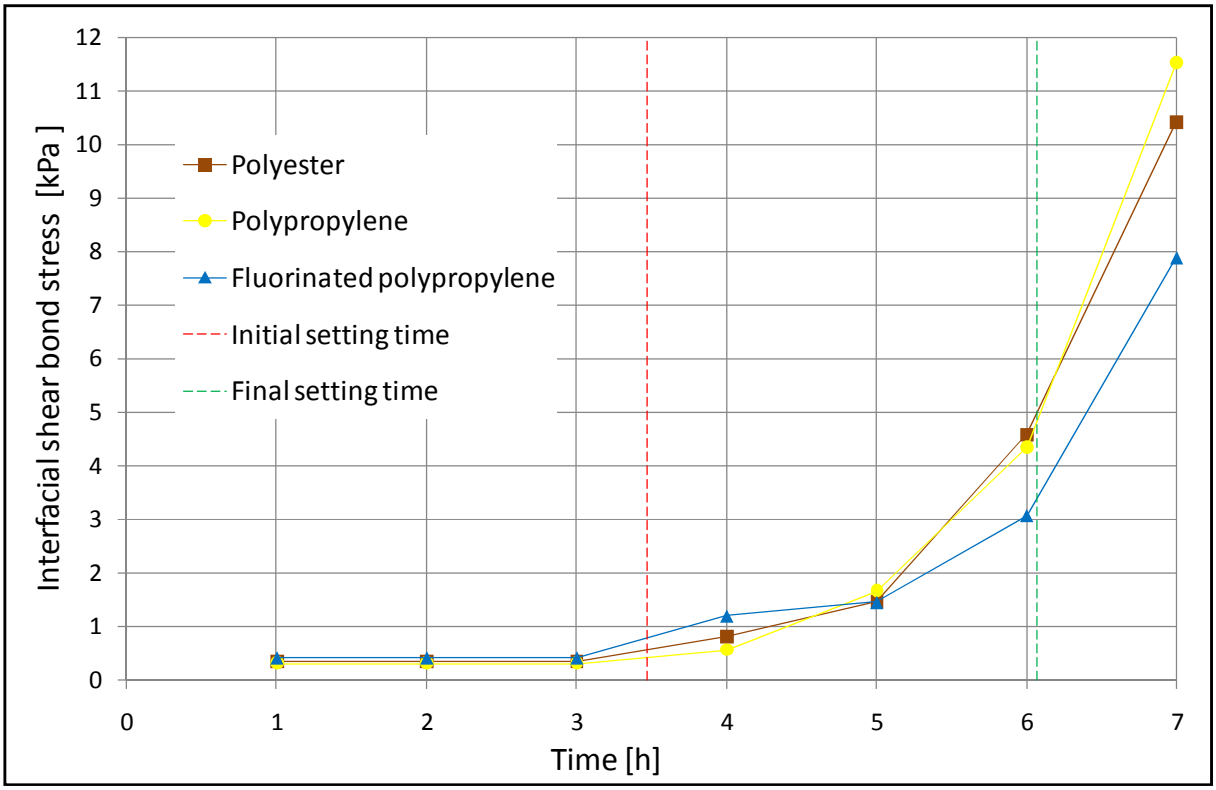

Figure 4.18: Interfacial shear bond stress of fibres from M1S up to 7 hours

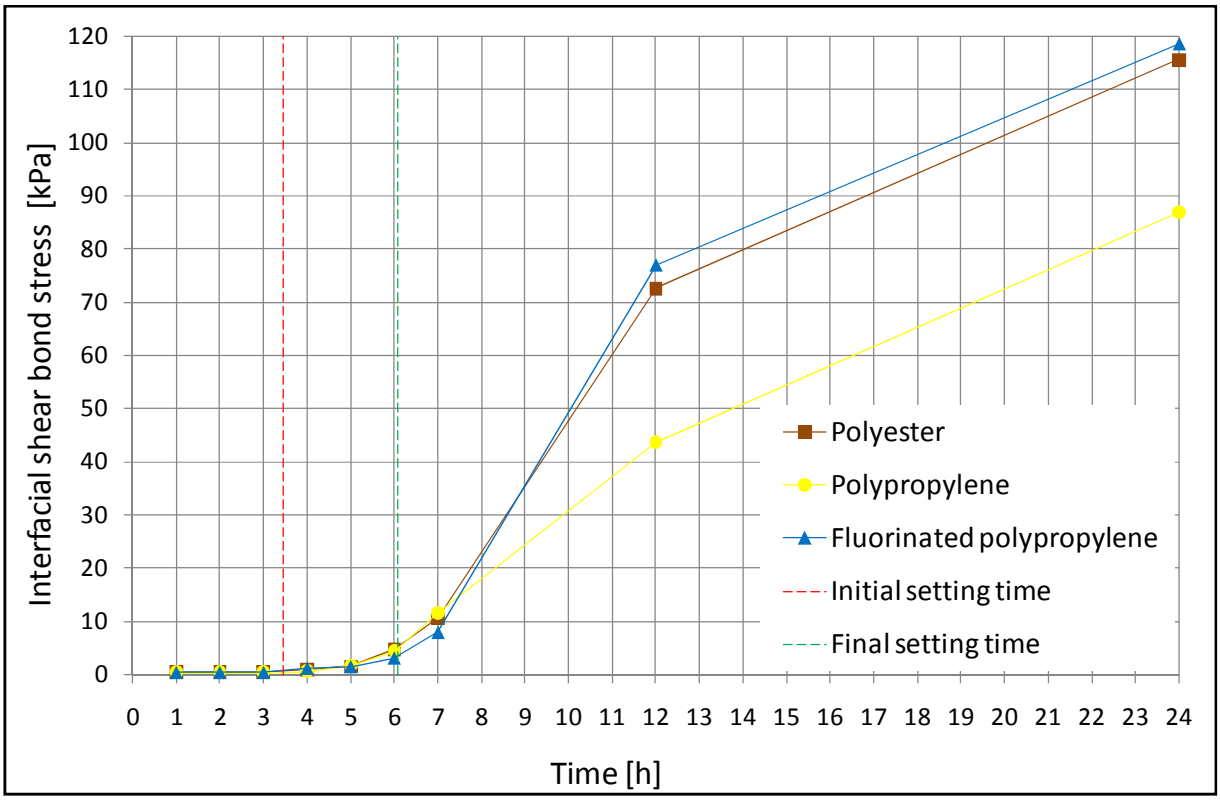

Figure 4.19: Interfacial shear bond stress of fibres from M1S up to 24 hours

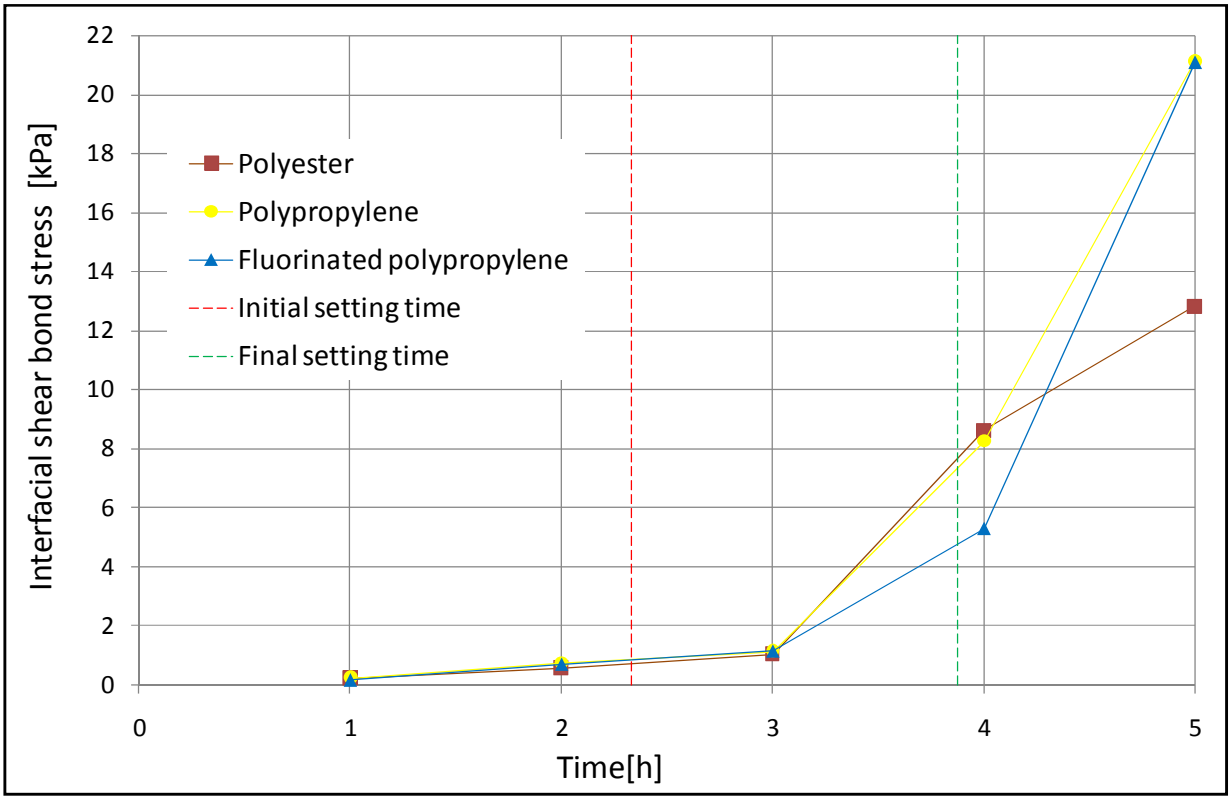

Figure 4.20: Interfacial shear bond stress of fibres from M2S up to 5 hours

4.3. *Concluding summary*

In this section the results of the PSC experiments and the single fibre pullout experiments were given. For the PSC experiments a single graph of a specimen from a specific mix was given for all the mixes with and without fibres. These graphs summarises all the experimental information available for a specific specimen. Summaries of the crack growth and bleeding for all the mixes were also given. The results of the single fibre pullout experiments were given in terms of average maximum pullout force and interfacial shear bond stress.

The results given in this chapter are discussed in detail in the following chapter.

5. Discussion of experimental results

This chapter contains the discussion of the experimental results given in Chapter 4. The objectives of the plastic shrinkage cracking (PSC) experiments were to determine when PSC occurs and to understand some of the factors which influence PSC. The objective of the single fibre pullout tests was to give a measure of the influence of fibres on PCS with time. A link between the PSC experiments and the single fibre pullout test is also proposed.

5.1. *Plastic shrinkage cracking (PSC) experiments*

In the following sections the validity of the theses and observations as stated in Section 3.1.3 are discussed. The main objective was to determine when PSC starts and ends. This is followed by more observations that can be made from the results.

Figure 5.1 shows a schematic graph that indicates all the important events during the early ages of concrete. Table B1 in Appendix B summarises the results of these events for all the tests.

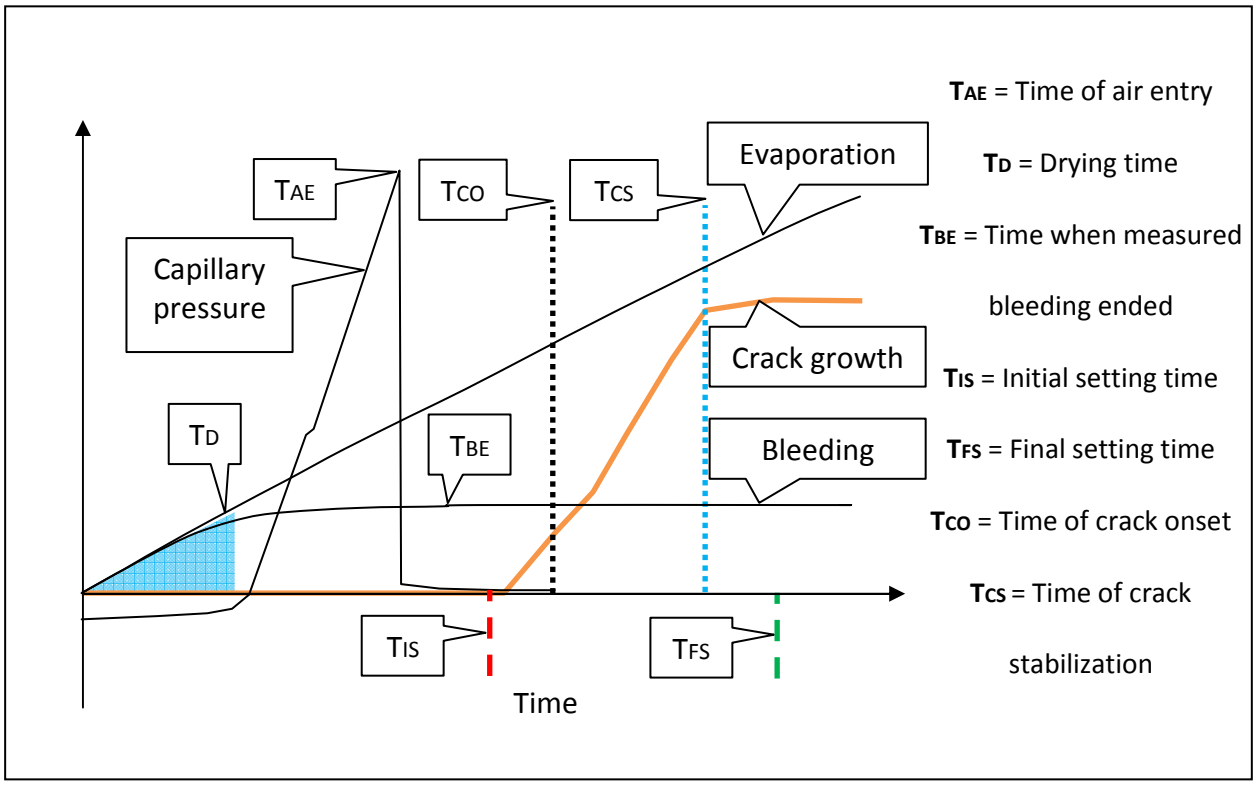

Figure 5.1: Schematic graph of important events during the early ages of concrete

5.1.1. Drying time (T_D)

Thesis 1 states: PSC can only occur once the total volume of water evaporated from the concrete surface exceeds the volume of bleeding water at the surface.

This event is called the drying time and is indicated on Figure 4.1 with a marker labelled T_D. The figure shows the results of M1S and M1B at Climates 1 and 2. The initial positive capillary pressure before the onset of the drying time can be explained as the hydrostatic pressure acting on the imbedded sensor tip.

It is shown in Figure 4.1 that the capillary pressure only starts developing once the drying time is reached. This was confirmed for two different environmental conditions and it is especially clear for Climate 2 which gave the lowest evaporation rate. Since the mechanism that causes PSC is capillary pressure, as discussed in Section 2.3.1, it can be concluded that PSC is only possible once the drying time is reached.

Thesis 1 is thus confirmed.

The drying time signifies the start of capillary pressure build-up in the concrete and therefore the possibility of PSC. In other words, until the drying time is not reached in a concrete element, no PSC is possible.

5.1.2. Time of air entry (T_{AE})

Thesis 2 states: No plastic shrinkage cracks will form before air entry has occurred.

The time of crack onset marks the time when the first crack is observed and is indicated on the graph of each specimen on which PSC test were conducted. Figures 4.1 and 4.2 show that no cracks were observed before the time of air entry. The same observation is made for all the PSC tests as shown in Figures 5.2 and 5.3 which graphically summarise all the important times for experiments where cracking occurred.

Thesis 2 is thus confirmed.

Although the event of air entry signifies the initiation of cracking and the crack location, as explained in Section 2.4.2, the cracks are often too small to be observed with the naked eye at the time of air entry and only become visible after considerable horizontal shrinkage of the concrete paste.

It should be mentioned that air entry remains a local event and may occur at variable times and locations throughout a large fresh concrete element, for example a slab. However, no plastic shrinkage crack can form at any location within a concrete element before air entry has occurred at this location.

5.1.3. Initial setting time (T_{IS})

Observation 1 states: The time of crack onset is near or just after the initial set of concrete.

Figures 5.2 to 5.4 graphically summarise the important events of all the mixes. Each column of the graphs show the following: the time when measured bleeding ended, the initial and final setting times for the specific mix as well as the time of air entry, crack onset and stabilization for both specimens of the specific mix.

In Figure 5.2, M1A at Climate 1 only shows one data point for the time of air entry, since the capillary pressure measurement for the other specimen malfunctioned. Also, M1B at Climate 1 only shows data points for the time of crack onset and stabilization for one of the specimens, this is because only one of the specimens cracked.

Figures 5.2 and 5.3 show that for mixes where cracking occurred the time of crack onset correlates closely to the initial set of the concrete. In fact, the figures show the close relation between the time of crack onset, air entry and the initial set of concrete.

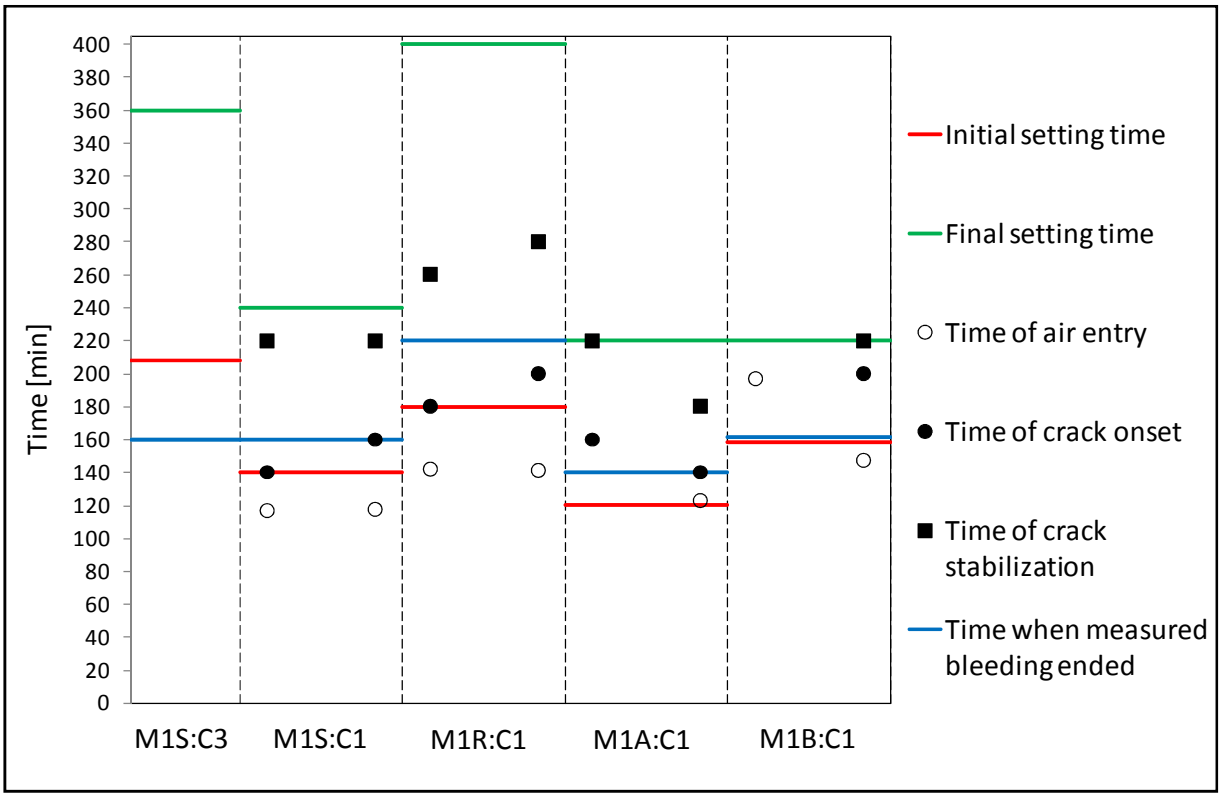

Figure 5.2: Important times of the variations of Mix 1 without fibres where cracking occurred

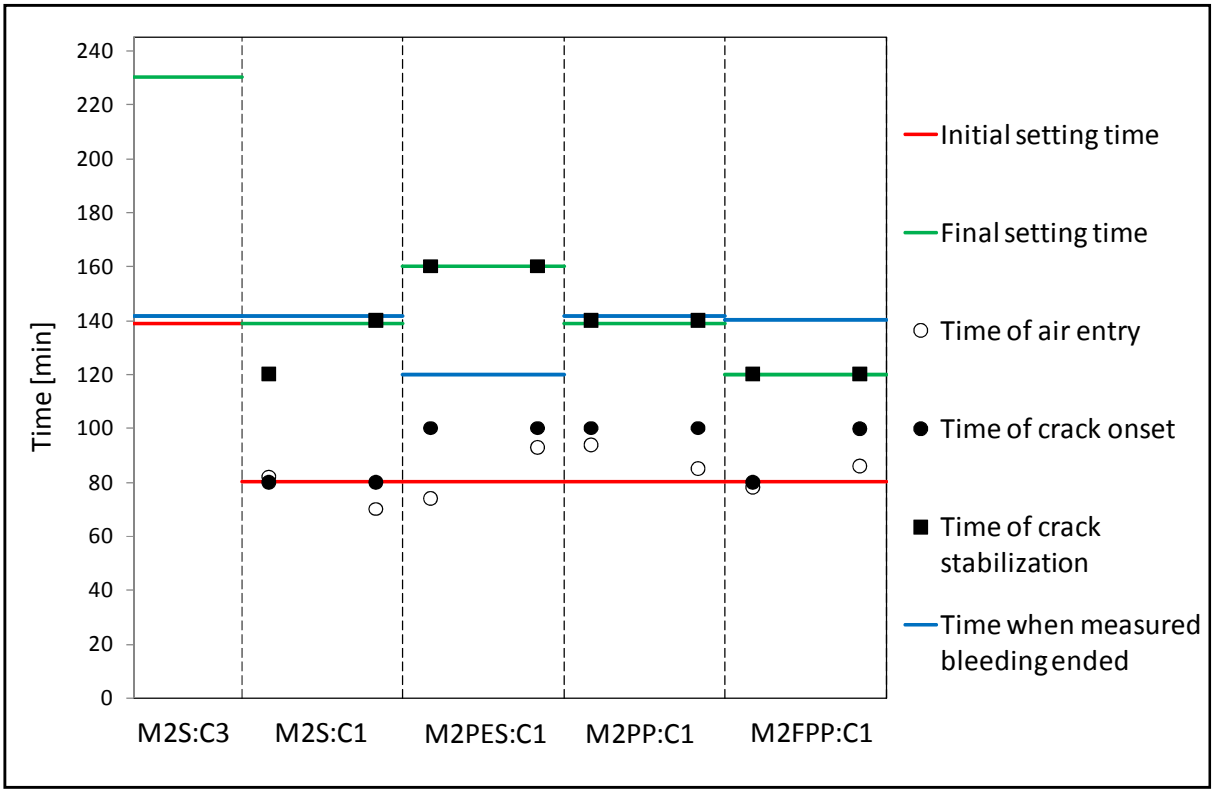

Figure 5.3: Important times of the standard Mix 2 with and without fibres where cracking occurred

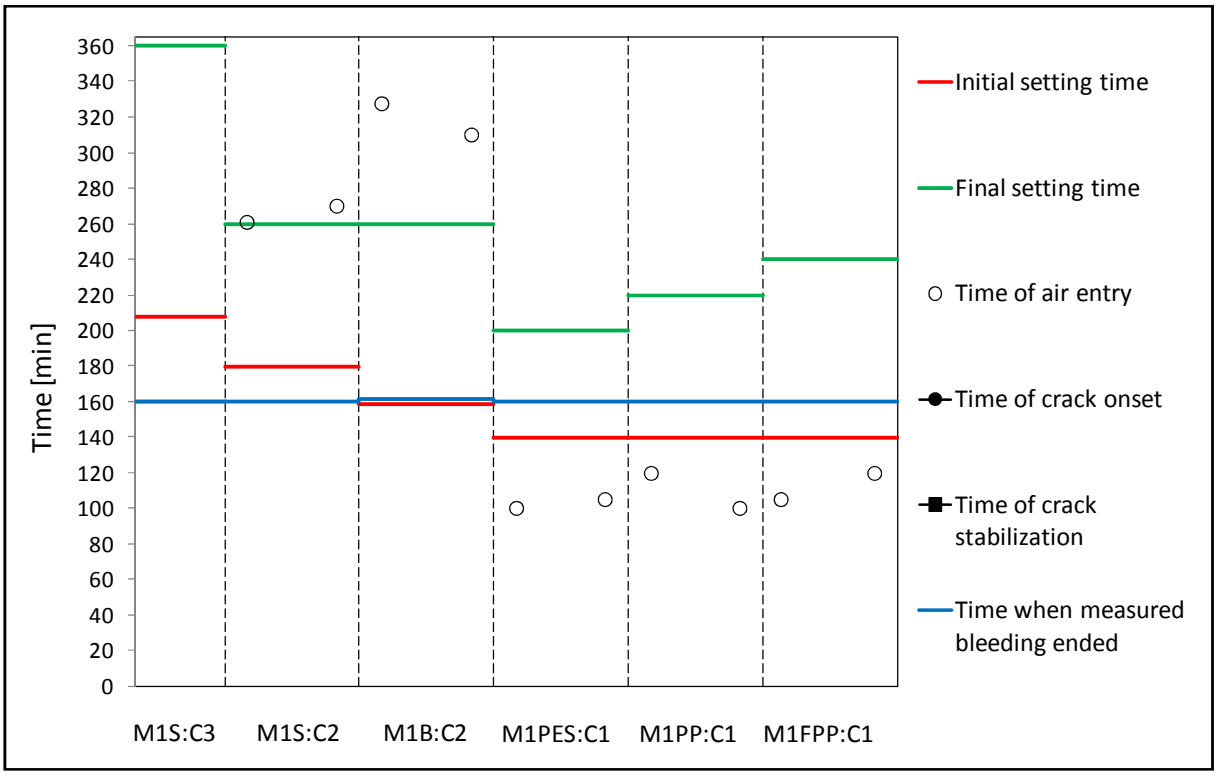

Figure 5.4: Important times of the variations of Mix 1 where no cracking occurred

To understand the correlation between the mentioned times it is necessary to consider two aspect of fresh concrete which were identified in the background study.

- In Section 2.4.2 it is stated that the time of air entry coincides with the time of maximum settlement (Slowik et al., 2008:504).

- In Section 2.4.1.3 it is stated that bleeding is caused by the settlement of solid particles and that the end of bleeding can be either mechanically or at the end of the dormant period (Powers, 1968:533-535). Mechanically ceased bleeding occurs when the particles have reached the maximum possible settlement and the particles become physically restraint by each other from any further settlement. Bleeding that ceases at the dormant period occurs when the particle settlement is haltered by the filling of interparticle gaps by hydration products. The dormant period ends when the paste is no longer plastic (Powers, 1968:491) and corresponds with the end of the stiffening stage of fresh concrete as explained in Section 2.4.5. Since the end of the stiffening stage can be identified by the initial set of concrete, the author believes that the initial setting time can also be used to identify the time when bleeding stops

due to hydration. This is however only possible if the concrete paste reaches the initial setting time before the bleeding ceases mechanically.

Keeping these aspects in mind, it would be reasonable to assume that the point of maximum settlement would coincide with the point when bleeding ceases, since bleeding is caused by settlement. To confirm this statement the time of air entry, which coincides with the time of maximum settlement, must also coincide with the time when bleeding ends. Before comparing the time of air entry with the time when bleeding ends to confirm this statement, it is first necessary to determine the actual time when bleeding ended. This is needed since the bleeding measurements and the PSC experiment were conducted at different climates.

As explained before bleeding can either end due to mechanical restraint or due to hydration which can be identified by the initial setting time of concrete. The times when measured bleeding ended as well as the initial setting times are shown in Figures 5.2 to 5.4. The bleeding measurements were conducted at Climate 3 and stopped bleeding before the reach of the initial setting time for the variations of Mix 1. Therefore the bleeding stopped due to mechanical restraint and not hydration for the bleeding measurements at Climate 3. For the more severe Climates 1 and 2 which were used for the PSC experiments, it was found that the initial setting time was almost always reached before the bleeding measurements at Climate 3 ended. This observation results in the assumption that bleeding ceased due to hydration and not mechanical restraint for the variations of Mix 1 at Climates 1 and 2. The same observation can be made for the variations of Mix 2 at Climate 1 where the initial setting times are reached before the bleeding measurements ended at Climate 3. In other words, for the majority of the PSC tests the bleeding ceased due to hydration and not mechanical restraint. The time when bleeding ends for the PSC experiments as shown in Figures 5.2 to 5.4 should therefore be taken as the minimum of the initial setting time and time when measured bleeding ended for each mix.

The initial setting time is therefore taken as the time when bleeding ends for nearly all tests. The initial setting time relates closely to the time of air entry for all tests as shown in Figures 5.2 to 5.4 except for M1S and M1B at Climate 2 where no cracking was observed. The

statement that the point of maximum settlement would coincide with the point when bleeding ceases seems therefore to be feasible and is discussed further in Section 5.1.5.

It can be concluded that the initial setting time gives an approximate point in time from where no more vertical settlement or bleeding will occur especially for concrete mixes under extreme environmental conditions. As discussed in Section 2.4.2 the time of maximum vertical settlement not only corresponds to the time of air entry which is required for crack forming, but also the time when the horizontal component of the capillary force start having a pronounced effect. The initial setting time therefore gives a point in time when significant horizontal shrinkage starts and therefore cracking can be expected if capillary pressure is present.

This explains why plastic shrinkage cracks starts forming close to the initial setting time of the concrete. The knowledge that the initial setting time defines a point in time when plastic shrinkage cracks can be expected to occur if capillary pressure is present could be utilized to prevent or reduce PSC.

Observation 1 is thus confirmed.

5.1.4. Final setting time (T_{FS})

Observation 2 states:

- *No plastic shrinkage cracks will start after the final set of concrete.*
- *The time where PSC stops is somewhere between the initial and final set of concrete and coincides with the time of crack growth stabilization.*

The time of crack stabilization is defined as the time where a clear decrease in the rate of crack area growth can be identified.

It is shown in Figures 5.2 and 5.3 that all the cracks started before the final setting time. Furthermore, no new cracks started for at least 40 minutes after the final setting time has been reached as shown in Figure 5.4. This supports the observation that no pure plastic shrinkage cracks will form after the final set of concrete.

The first part of Observation 2 is thus confirmed.

Figures 4.6 and 4.7 show the average crack area and rate of crack area growth with time respectively of the variations of Mix 1 without fibres and Table 5.1 summarises the average crack areas at specific times. The results in the table indicate that for the aforementioned mixes, except M1R, close to 80 % of the crack area at 40 minutes past the final setting time was already formed at the time of crack stabilization. For M1R no measurement of crack area was performed at 40 minutes past the final setting time. It is assumed that the crack area for M1R would also be stable at 40 minutes past the final setting time since the crack area has basically remained unchanged for 130 minutes when the final setting time is reached as shown in Figure 4.6.

Figures 4.8 and 4.9 show the average crack area and rate of crack area growth with time respectively of the standard Mix 2 with and without fibres and Table 5.2 summarises the average crack areas at specific times. The results indicate that more than 80 % of the crack area at 5 hours after casting was already formed at the time of crack stabilization. This is at least 2 hours after the final setting times have been reached which varied between 2 to 3 hours for the mentioned mixes. At 24 hours more that 70 % of the crack area has already been formed at the time of crack stabilization.

The results suggest that the majority of the crack growth occurs before the time of crack stabilization. The rate of the crack growth after the time of crack stabilization is insignificant if compared with the rate of the crack growth before the time of crack stabilization as shown in Figure 4.2. This figure clearly shows that the majority of the crack growth occurs in the period between the initial setting time of concrete and time of crack stabilization. The same result is found for all the mixes where cracking occurred.

Table 5.1: Crack area at specific times of the variations of Mix 1 without fibres

Mix		**M1S**	**M1R**	**M1A**	**M1B**
Crack area at specific times [mm²]	**T_{CS}**	35.3	11.6	37.4	4.05
	$T_{FS+40min}$	35.2	NM	47.6	4.50
Crack area at time of crack stabilization as [%] of crack area at 40 min past the final setting time	**T_{CS}/ $T_{FS+40min}$**	100	NM	78.6	90.0
Note: NM means not measured					

Table 5.2: Crack area at specific times of the standard Mix 2 with and without fibres

Mix		M2S	M2PES	M2PP	M2FPP
Crack area at specific times [mm²]	T_{CS}	81.9	50.5	38.2	29.3
	T_{FS}	87.1	50.5	38.2	29.3
	T_{5h}	100	56.9	42.0	32.3
	T_{24h}	115	69.4	46.6	35.1
Crack area at time of crack stabilization as [%] of crack area at final setting time as well as 5h and 24h after casting	T_{CS}/T_{FS}	93.9	100	100	100
	T_{CS}/T_{5h}	81.8	88.8	91.0	90.7
	T_{CS}/T_{24h}	71.1	72.8	82.0	83.5

The crack growth after the time of crack stabilization may include cracks due to capillary pressure (PSC) as well as other types of shrinkage like thermal gradient and drying shrinkage. However, it is difficult to distinguish between the types of cracks that forms after the time of crack stabilization, but due to the rate of the crack growth as well as the plastic state of the concrete paste before the time of crack stabilization, it can be concluded that only pure plastic shrinkage cracks occur up to the time of crack stabilization.

It cannot be confirmed that PSC ends at the time of crack stabilization, but the event of crack stabilization indicates a point in time where the majority of the pure PSC has occurred.

The second part of Observation 2 is thus partly confirmed.

In conclusion, the final setting time of concrete serves as a good indication of when PSC ends, because no pure plastic shrinkage crack will start after the final setting time of concrete and the time when the majority of the pure PSC has occurred (time of crack stabilization) usually ends before the final setting time is reached. This knowledge can be utilized to prevent or reduce PSC. Furthermore, it serves as useful information on the behaviour and nature of a typical plastic shrinkage crack, which can be used to create a model of PSC. Also, cracking of concrete is unavoidable and continues throughout the lifespan of a concrete element, through various types of shrinkage. Distinguishing between the different types of shrinkage and the time when they play a dominate role is important information if these shrinkage types and the effect they have on a structure are to be fully understood. Therefore the information that PSC starts and stabilizes rapidly between the initial and final setting times of concrete, is not only useful for the fundamental

understanding of PSC, but also defines a time period when PSC should be considered. After this period other types of shrinkage start having an effect. This allows other researchers to define a time when the effect of PSC must be considered in possible shrinkage measurements.

5.1.5. Importance of bleeding

The statement made in Section 5.1.3 that the time when bleeding ends corresponds to the time of maximum settlement is discussed in this section with the help of the results of all the mixes as shown in Figures 5.2 to 5.4.

Variations of Mix 1

The initial setting time of M1S under bleeding measurement conditions (Climate 3) is 208 minutes, which is more than the time of 160 minutes when the bleeding measurements stopped. This means that M1S at Climate 3 stopped bleeding due to mechanical restraint and not hydration. The initial setting time of M1S at Climate 1 is 140 minutes, which indicates that bleeding stopped due to hydration and not mechanical restraint.

It is however still reasonable to assume that most of the bleeding of M1S at Climate 1 probably occurred without the interference of hydration as for Climate 3 as the difference between the times when bleeding stopped due to hydration and mechanical restraint is only 20 minutes. The same assumption can be made for all the variations of Mix 1 at Climate 1. Under this assumption Table 5.3 shows the bleeding amount at the time of air entry as a percentage of the total amount of bleeding stopped due to mechanical restraint. For all the variations of Mix 1 at Climate 1 more than 92 % of the bleeding has already occurred by the time of air entry. This observation indicates that the time when bleeding stops due to mechanical restraints approximately corresponds with the time of air entry and therefore maximum settlement.

Variations of Mix 2

The initial setting time and time when bleeding ends for M2S at Climate 3 conditions, is 140 minutes. The initial setting time of the standard Mix 2 with and without fibres at Climate 1 is 80 minutes, which is much earlier than measured at Climate 3. Bleeding therefore stops due

to hydration for these mixes at Climate 1. The initial setting time of 80 minutes can be assumed to be the time when bleeding stops and corresponds closely with the time of air entry as shown in Figure 5.3. This observation indicates that the time when bleeding stops due to hydration approximately corresponds with the time of air entry and therefore maximum settlement.

From this discussion it can be concluded that the time when bleeding ends, either to mechanical restraint or hydration, can be used as an indicator or warning that plastic shrinkage cracks can be expected.

Table 5.3: Bleeding amount when bleeding stopped mechanically and when air entered

Fibres	Climate	Mix name : Specimen	Total bleeding [g] amount when		B_{AE}/B_{MEC}
			bleeding stopped mechanically	air entered	
			B_{MEC}	B_{AE}	
No fibres	1	M1S : S1	7.95	7.87	99%
		M1S : S2	7.95	7.88	99%
		M1R : S1	5.05	4.76	94%
		M1R : S2	5.05	4.76	94%
		M1A : S1	6.20	6.20	100%
		M1A : S2	6.20	6.12	99%
		M1B : S1	8.95	8.95	100%
		M1B : S2	8.95	8.92	100%
	2	M1S : S1	7.95	7.95	100%
		M1S : S2	7.95	7.95	100%
		M1B : S1	8.95	8.95	100%
		M1B : S2	8.95	8.95	100%
With fibres	1	M1PES : S1	4.60	4.25	92%
		M1PES : S2	4.60	4.30	93%
		M1PP : S1	7.35	7.20	98%
		M1PP : S2	7.35	6.80	93%
		M1FPP : S1	6.70	6.15	92%
		M1FPP : S2	6.70	6.45	96%

5.1.6. Influence of bleeding on crack area

Figures 4.10 and 4.11 show the bleeding results of all the mixes without fibres. These measurements do not account for the additional bleeding that results from the vertical component of the capillary pressure as discussed in Section 2.4.1.3. This additional bleeding starts at the drying time that signifies the start of the capillary pressure build-up and ends with the air entry pressure, which corresponds with the maximum settlement. Figures 4.6 and 4.8 show the crack area for all the mixes that showed cracking and Tables 5.1 and 5.2 summarise the crack areas at specific times. The following discussion only considers the mixes without fibres.

M1B with the highest amount of bleeding showed the smallest crack area and M2S with the least amount of bleeding showed the largest crack area. It is clear that bleeding has a significant influence on PSC. In general, the more bleeding a concrete has the less the PSC. However, too much bleeding is also unwanted since this may lead to surface laitance. Surface laitance is when the surface of the concrete becomes dusty when hardened, due to excessive bleeding water at the surface, which decrease the strength of the top surface (Illston et al., 2001:137).

An unexpected result was that of M1R which included a set retarder. The crack area of this mix was three times less than that of M1S and M1A, even though M1R showed less bleeding. This is surprising since it is commonly believed that the longer a paste remains plastic the more vulnerable it is to PSC. A possible explanation for this result is found when the bleeding characteristics of M1R are considered. M1R bleeds 60 minutes longer and more persistent than the other mixes even though the total amount of bleeding was less. These prolonged and persistent bleeding characteristics resulted in a concrete mix that could relieve the capillary pressure build-up more often and effective through additional vertical settlement which results in extra bleeding water at the surface of the concrete. The additional vertical settlement is caused by the vertical component of the capillary pressure.

Although the aforementioned explanation is still a theory which requires further investigation, it does lead to the idea that PSC can also be reduced by altering the bleeding

characteristics of a mix. In general, the theory states that a mix which exhibits prolonged and persistent bleeding characteristics can counteract the capillary pressure build-up and therefore PSC through additional bleeding when needed.

5.1.7. Influence of wind

Figure 4.1 shows the results of two different mixes tested at two different wind speeds. The higher wind speed of Climate 1 (33 km/h) resulted in an average concrete water evaporation rate of 1 kg/m²/h while the lower wind speed of Climate 2 (4 km/h) resulted in an average concrete water evaporation rate of 0.4 kg/m²/h. The temperature and the relative humidity are the same for both climates. The different evaporation rates influences the drying times of the mixes, which is defined as the time when PSC becomes a possibility. Both M1S and M1B showed an increase in drying time from the higher to lower wind speed of approximately 85 minutes. This increase in drying time delayed the start of PSC enough to cause no cracking. It is clear that the wind has a big influence on the PSC due to the sensitivity of the evaporation rate to the wind speed.

5.1.8. Bleeding of LV-FRC

Figures 4.12 and 4.13 show the bleeding results of the standard Mixes 1 and 2 with and without fibres. For M1S the addition of fibres clearly decreased the total amount of bleeding and therefore settlement. Polyester fibres showed the biggest reduction in the total amount of bleeding. This is believed to be due to the hydrophilic nature of the polyester fibres, which absorbs water. It is concluded that polyester fibres absorb more water than the other fibres, especially considering that the polyester fibres were added at a lower volume fraction than the other fibres (see Table 3.5). The fluorinated polypropylene fibres showed less bleeding than the untreated polypropylene fibres for M1S. A possible explanation is the increased hydrophilicity (potential to absorb water) of the fluorinated polypropylene fibres through the fluorination process, compared to untreated polypropylene fibres.

No clear distinction could be made between the bleeding results for the standard Mix 2 with and without fibres, except that the polyester fibres resulted in the least amount of bleeding, which supports the results of the standard Mix 1 with and without fibres.

In general, it seems that fibres reduce the total amount and rate of bleeding. This increases the rate of capillary pressure build-up as shown in Figure 5.5. The figure shows the capillary pressure build-up of the standard Mixes 1 and 2 with and without fibres at Climate 1. It is clear that the mixes with fibres have a higher rate of capillary pressure build-up than without fibres. This is due to the decrease bleeding characteristic of the mixes with fibres.

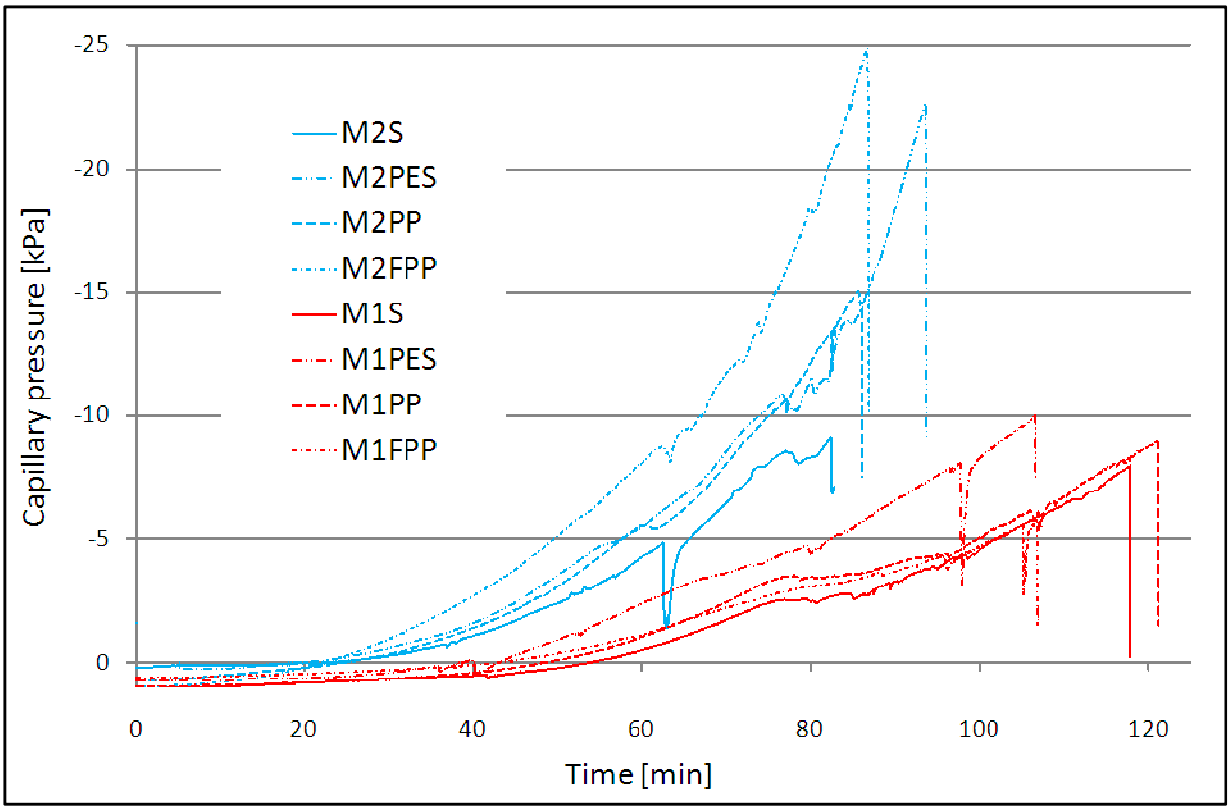

Figure 5.5: Capillary pressure of the standard Mixes 1 and 2 with and without fibres at Climate 1

5.1.9. Post-cracking behaviour of LV-FRC

Figures 4.4 and 4.5 as well as Figures 4.8 and 4.9 show the effect of fibres on crack growth for the standard Mixes 1 and 2 with and without fibres.

The addition of fibres to M1S led to no cracking. To avoid the same result for the second mix, an additional restraint was added to the PSC moulds for tests as shown in Figure 4.3. The extent to which the fibres types reduced the crack area, maximum crack width and crack length of M2S are summarised in Figures 5.6 to 5.8. The values were calculated as the

average of the two specimens for each mix. The figures show all the crack data of all the variations of Mix 2 normalised to the crack value of M2S as control after 5 hours.

The results indicated that the fluorinated polypropylene fibres resulted in the largest reduction of crack area, maximum size and length. Untreated polypropylene fibres resulted in the second largest crack reduction followed by polyester fibres. It should be mentioned that polyester fibres were added at a lower volume fraction, i.e. 35 % less per volume.

Figures 5.6 to 5.8 also show that the fibres result in a larger crack area and width reduction, compared to the length reduction. This indicates that fibres mainly resist crack growth by reducing the width of the cracks. The fibres therefore have minimum influence on the length of the crack, which is influenced by other factors for example, the specimen boundary conditions and the corresponding level of restraint. It can be concluded that fibres mainly give resistance to crack widening once the crack has already been formed.

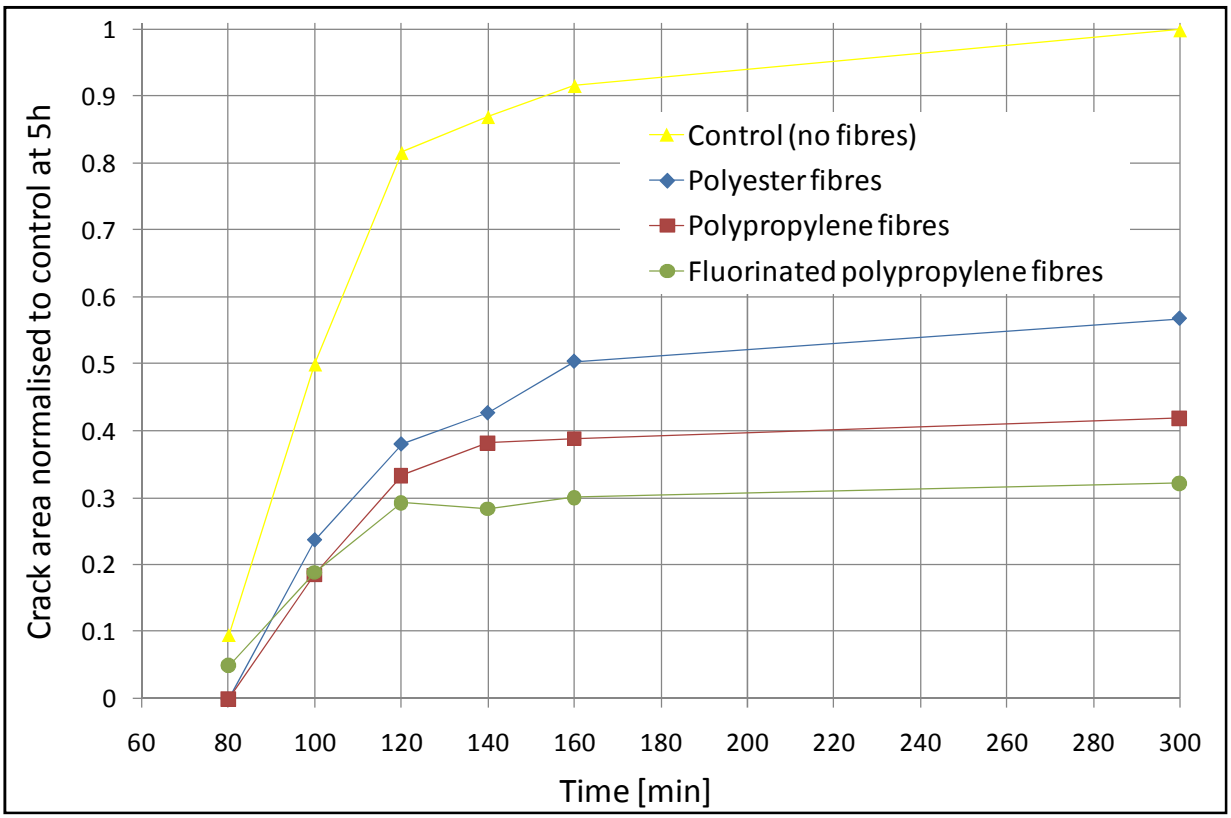

Figure 5.6: Normalised crack area for the standard Mix 2 with and without fibres at Climate 1

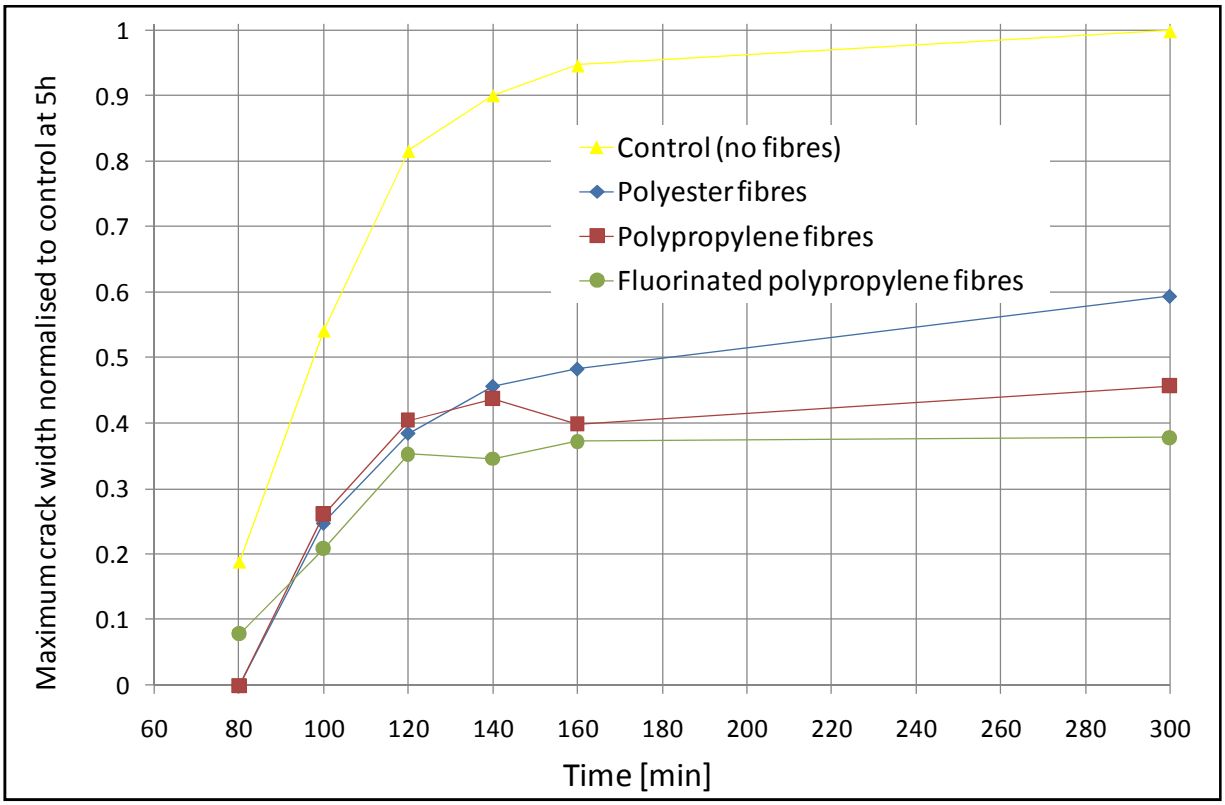

Figure 5.7: Normalised maximum crack width for the standard Mix 2 with and without fibres at Climate 1

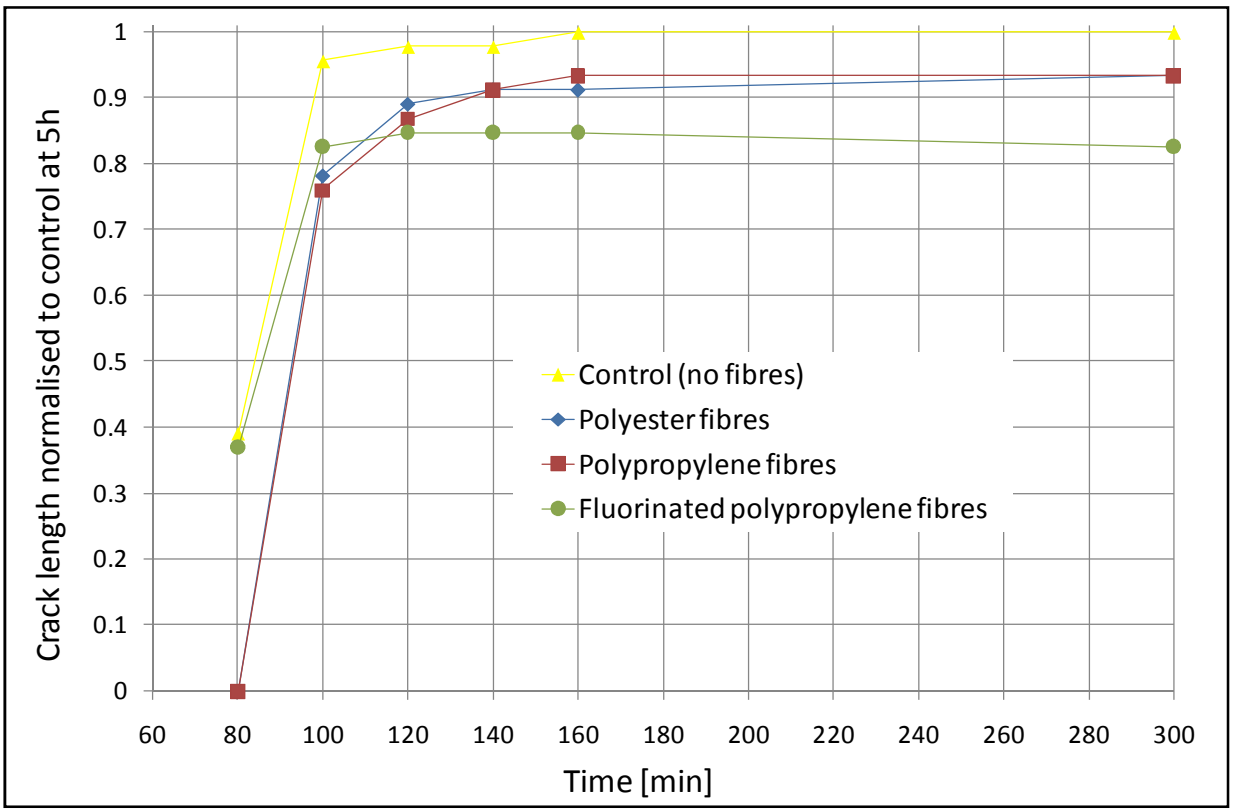

Figure 5.8: Normalised crack length for the standard Mix 2 with and without fibres at Climate 1

Figure 5.9 shows the crack area growth during each measured time interval of the standard Mix 2 with and without fibres as percentage of the total crack area of each mix as measured after 24 hours. This indicates that the majority of the crack growth was measured after a 100 and 120 minutes. The cracks formed during this period are considered to be pure plastic shrinkage cracks as discussed in Section 5.1.4. Since the majority of the crack growth occurs during this period, the majority of the crack reduction due to fibres must occur during this same period. Table 5.4 shows the percentage of crack growth reduction by adding fibres to the standard Mix 2 measured over a 20-minute interval. The results indicate that the percentage of crack growth reduction of a specific fibre type remains fairly constant over this period.

In conclusion, is seems that a certain fibre type added to a certain concrete at a certain volume fraction gives a consistent resistance to crack propagation during the critical period when the majority of the pure plastic shrinkage cracks occurs. This critical period is between the initial setting time of concrete and the time of crack stabilization.

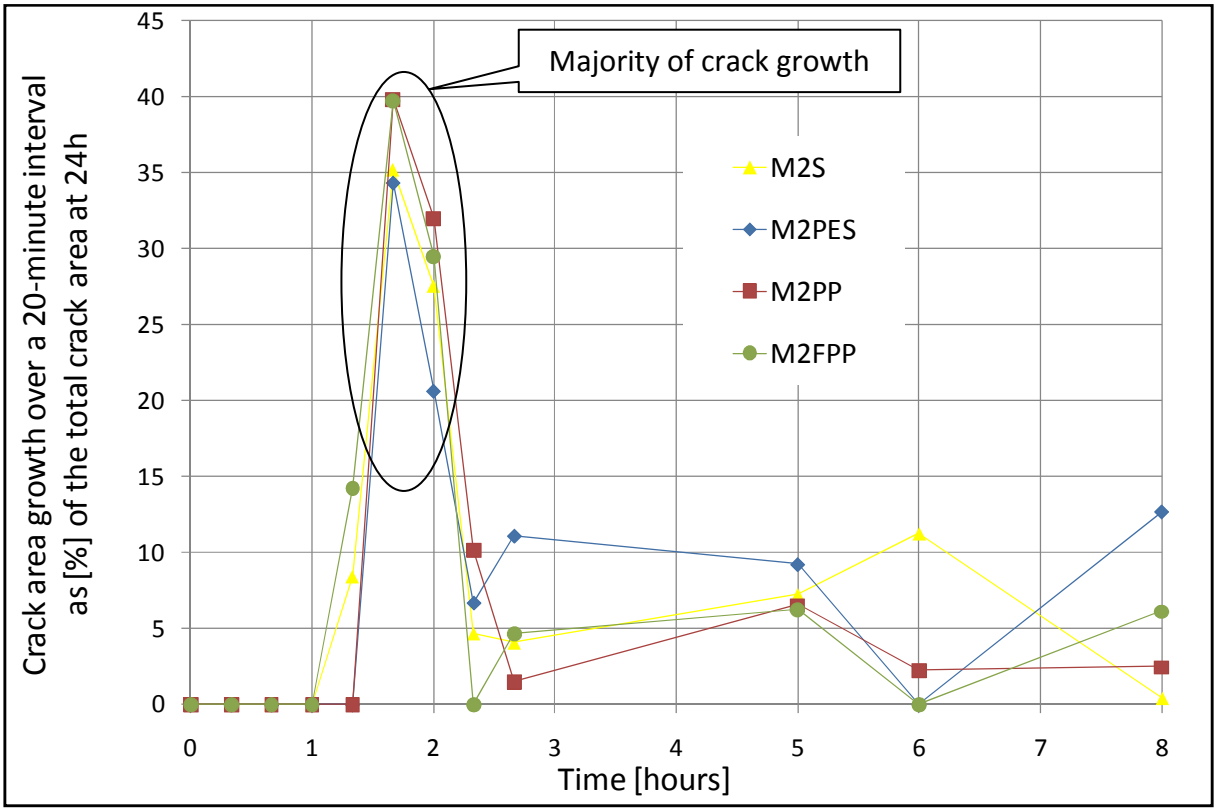

Figure 5.9: Crack area growth over a 20-minute interval as % of the total crack area at 24h of the standard Mix 2 with and without fibres at Climate 1

Table 5.4: Crack growth reduction over critical period due to fibre addition to M2S

Value	Time	Mix 2				Crack growth reduction [%]		
		M2S	M2PES	M2PP	M2FPP	PES	PP	FPP
Crack growth measured over a 20-minute interval [mm²]	T_{100min}	40.5	23.8	18.6	14.0	41.0	54.0	66.0
	T_{120min}	31.7	14.3	14.9	10.4	55.0	53.0	67.0

5.2. *Fibre pullout experiments*

In the following sections the results of the single fibre pullout test are discussed. The main objective of these tests were to determine the interfacial shear bond stress as a function of time between the fibre and the concrete paste, since this is the main factor controlling the performance of a fibre reinforced concrete with regards to crack propagation (Hannant, 1978:3).

Figures 4.15 to 4.17 show the results of the average pullout force required to fully debond the fibre from the concrete paste as well as the coefficient of variance (COV) of the data. The results were used to calculate the interfacial shear bond stress as shown in Section 4.2.2.

In general, the COV of the results are high due to the limited amount of tests and the nature of the fresh concrete paste. The COV gradually decreases with time. This is expected since the initial pullout forces from the fresh concrete paste are extremely low. The closer to zero the measured values in a data set the more sensitive the COV becomes to any slight variation even though the standard deviation of the data increases with time (see Tables C1 and C2). As the pullout force increase with time the COV becomes less sensitive to variations. The behaviour of the COV with time is due to the method of calculation (COV = standard deviation/average) and the extremely low forces measured during the first few hours after the concrete has been cast.

Figures 4.18 to 4.20 show the results of the interfacial shear bond stress between the fibre and the concrete paste for each fibre type and mix. The following discussions are based on the interfacial shear bond stress results.

5.2.1. Cracking resistance

The resistance of fibres with regard to cracking is dependent on the magnitude of the interfacial shear bond stress between the fibres and the concrete paste. The higher this value at a specific time the more resistance the fibre gives to crack widening.

The results in Figures 4.18 to 4.20 show a significant increase in interfacial shear bond stress from the initial setting time of the concrete paste if compared to the values before the initial setting time. This increase gradually becomes more pronounced with time and continued to increases until well after the final setting time has been reached.

In conclusion, the fibres gave pronounced increased resistance from the initial setting time of concrete, which was identified in Section 5.1.3 as the time when plastic shrinkage cracks are most likely to start. Therefore if cracking occurs in a concrete element where fibres are present, the fibre will bridge the cracks and provide additional resistance to further crack widening. This explains why fibres are effective in reducing PSC.

5.2.2. The time of cracking

The magnitude of the resistance that fibres give to crack widening once cracking has been initiated is time-dependent. The later cracking occurs the higher the interfacial shear bond stress between the fibre and the concrete paste due to the increased degree of hydration.
Thus, for PSC, the later cracking is initiated by air entry, the higher the resistance to crack widening if fibres are present. However, as discussed in Section 5.1.9, the resistance to crack growth for a specific fibre seems to remain consistent during the critical period after cracking has been initiated.

5.2.3. Influence of concrete paste properties

The properties of the concrete paste influence the magnitude of the interfacial shear bond stress with time. The results show that the ranges of these values are between 3.3 kPa and 4.9 kPa for M1S and between 4.9 kPa and 7.8 kPa for M2S at the final setting time of these mixes. The higher values for M2S can be explained by comparing the material composition of each mix. M2S, compared to M1S, has a higher fine content in terms of cement and fine aggregate as well as no added plasticiser, which together with the

lower water-cement ratio results in a higher rate of hydration. This means that M2S results in more solid contact points between the fibre and the concrete paste due to the higher fine content. Furthermore, these contact points increase faster due to the higher rate of hydration. In general, a mix with a higher fine content and rate of hydration results in an increased bond between the fibre and the concrete paste. This increases a mix resistance to crack widening.

However, the same material properties that causes an increased bond between the fibre and the concrete paste also increase the magnitude of the capillary pressure build-up as discussed in Sections 2.4.1.3 and 2.4.3. Figure 5.5 shows the capillary pressure build-up of the standard Mixes 1 and 2 with and without fibres. The figure shows that the second mix has higher rates of capillary pressure build-up than the first mix for the same climate due to the difference in material properties.

Since the second mix was designed for and resulted in pronounced PSC, it can be concluded that for PSC the influence of increased fibre bond with the concrete paste is of minor importance when compared to the influence of the increased capillary pressure build-up caused by the material properties.

5.2.4. Pullout mechanisms of fibres

The main mechanism which influences the bond between fibres used in this study and the concrete paste are adhesion and friction. Although it was not the objective of this study to investigate these mechanisms, several close-up pictures of fibres that have been pulled out from M2S at different times were taken with an electron microscope as shown in Figure 5.10.

The figure shows increasing frictional skid marks on the surface of the fibre with time. This does not give information on which mechanism plays the dominate roll. However, it does indicate that the frictional bond between the fibre and the concrete paste increases with time.

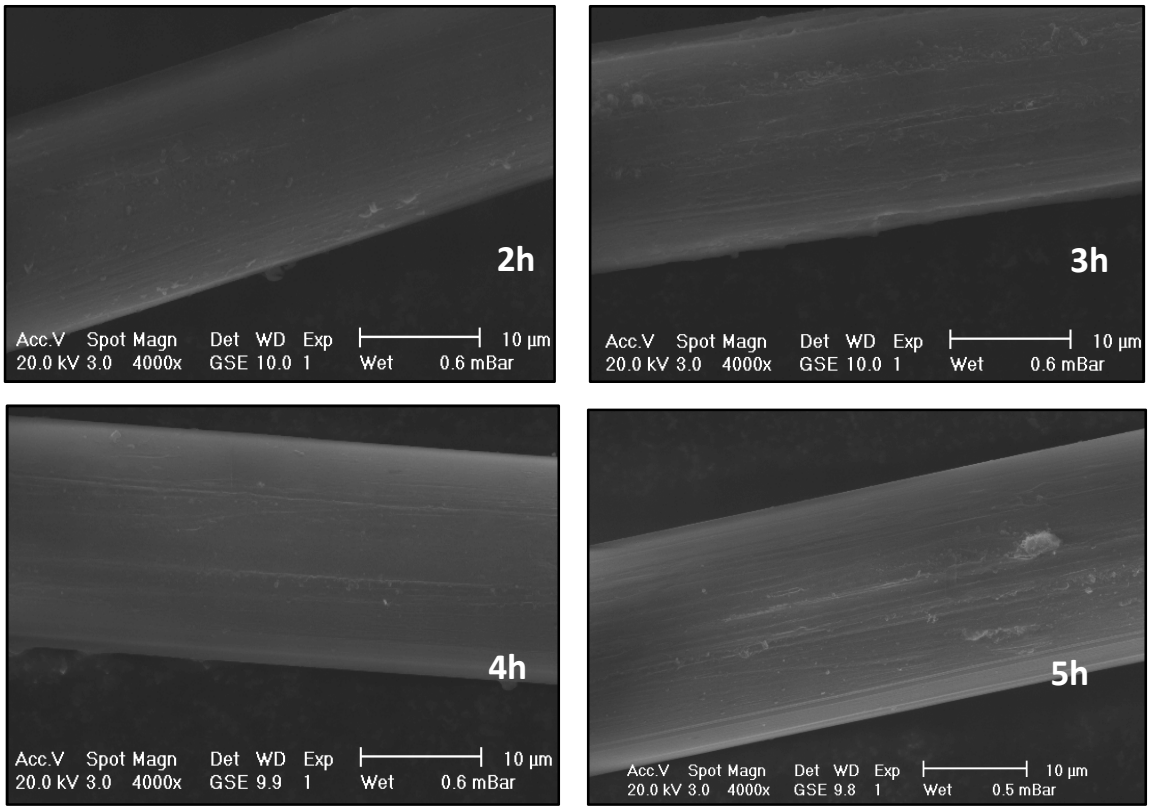

Figure 5.10: Electron microscope pictures of pulled out fibres

5.2.5. Influence of fibre properties

Fibre properties such as diameter, length, shape and surface properties have a significant influence on the pullout characteristics of the fibres. The properties of the different fibres used for the experiments did not differ significantly and the performance of the fibre types was similar. This made it difficult to distinguish between the fibre types. In general, all the fibres performed similar for both mixes within the period when PSC is expected (between initial and final setting times).

5.2.6. Proposed link between PSC and single fibre pullout experiments

Although the single fibre pullout test succeeded in the determination of the interfacial shear bond stress as a function of time between the fibre and the concrete paste, it still does not give an indication of the actual stress that fibres can bridge across a crack. The same problem exists for the PSC experiments, which measured the crack reduction potential of the fibres in terms of crack area. A link between these tests is needed to determine the stress which can be carried by fibres over a crack.

Equation 2.3 discussed in Section 2.4.1.3 is proposed as a possible link between the results of the single fibre pullout experiments and the PSC experiments. This equation gives the mechanical stress that can be bridged across a unit crack area by fibres. It combines the volume fraction, length and diameter of fibres used in the PSC experiments with the interfacial shear bond stress calculated in the single fibre pullout experiments. The bridging stresses can be used as an indication of how much resistance the fibres give at certain times against crack growth.

Figures 5.11 and 5.12 shows the bridging stress over a unit crack area carried by fibres for M1S and M2S, as calculated with Equation 2.3.

The validity of the proposed equation is unknown and must be investigated as follows:

- Conduct an in depth parameter study through experiments to determine the influence of the fibre properties in terms of fibre length, volume fraction and diameter on the proposed equation.
- The reliability and consistency of the interfacial shear bond stress must be improved through more tests.
- Measurements of the actual stress across a crack due to PSC as well as measurements of the actual stress that fibres can bridge across a crack must be conducted. These measurements must be compared with the values calculated with the proposed equation.

In conclusion, this study only identified Equation 2.3 as a possible link between the single fibre pullout and the PSC experiments. The verification of this equation is not part of this study.

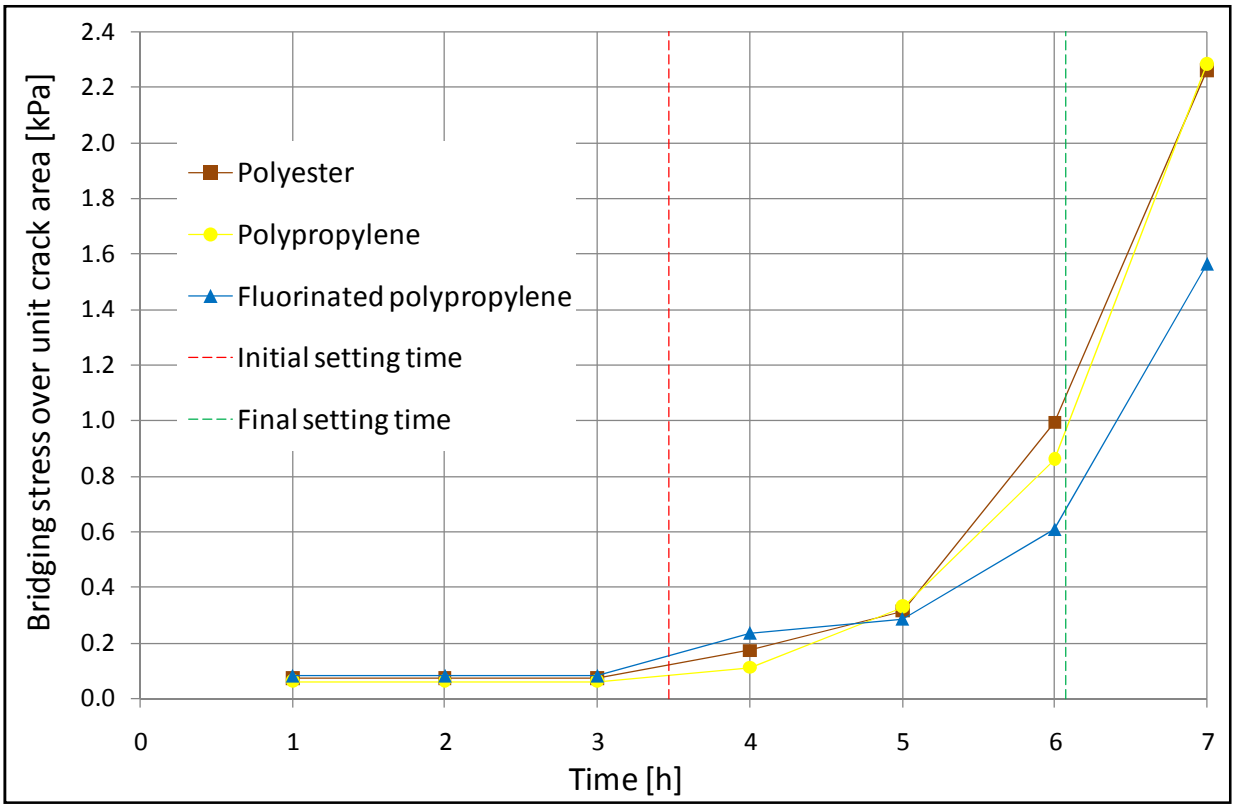

Figure 5.11: Bridging stress over unit crack area by fibres for M1S

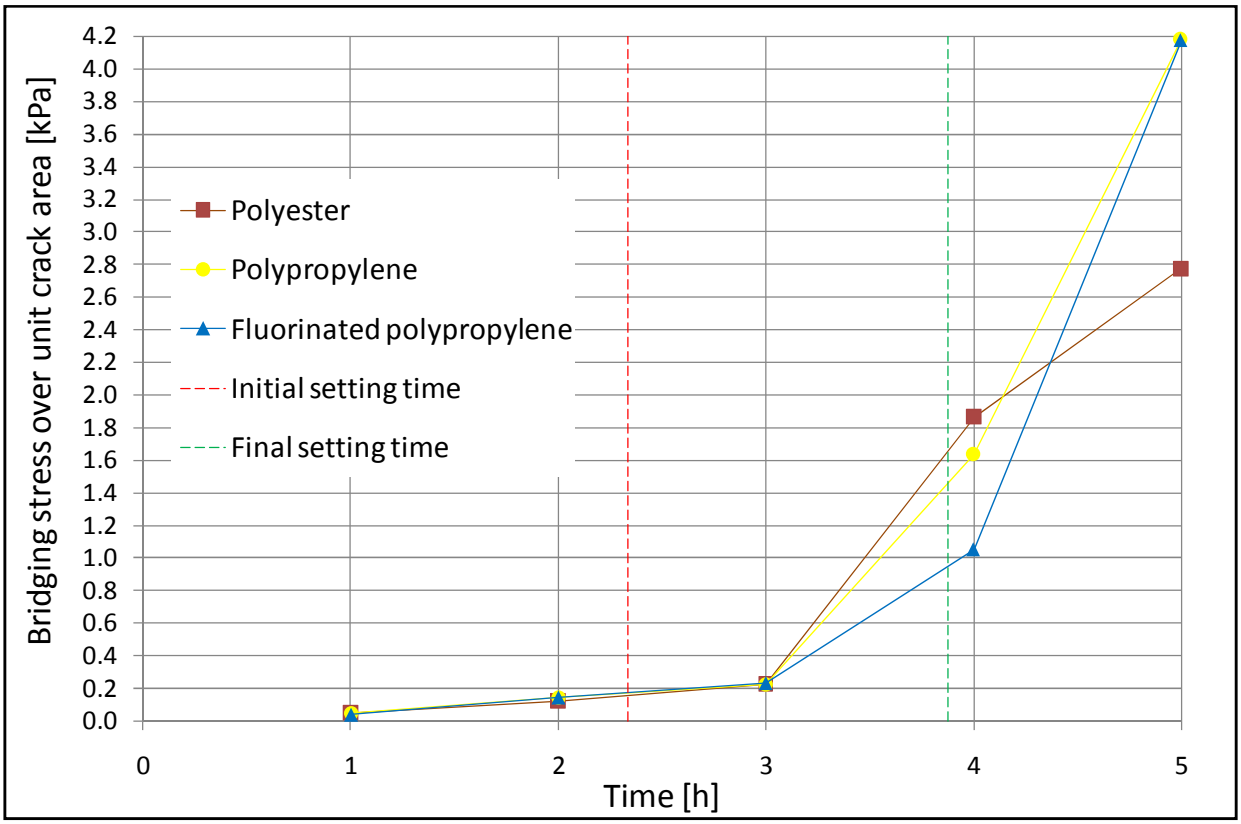

Figure 5.12: Bridging stress over unit crack area by fibres for M2S

5.3. *Fibre types*

It is difficult to recommend a certain fibre type above another for the prevention of PSC, especially since all the fibres reduced PSC to great effect. From the PSC results the fluorinated polypropylene fibre preformed the best in crack reduction, but the polyester fibres also performed well at a lower volume fraction. The effect of volume fraction on PSC for these fibres is still unknown. The results of crack bridging stress indicated that the polyester fibres would be best in reducing PSC, but the polyester fibres also resulted in the largest bleeding reduction, which will increase the potential for PSC. Furthermore, the untreated polypropylene fibres also gave good crack reduction as well as the least amount of bleeding reduction. It is therefore not clear which fibre would be best suited in reducing PSC for all conditions. The only conclusion that can be drawn is that the fibres reduce PSC.

5.4. *Concluding summary*

This chapter discussed the results of the PSC and the single fibre pullout experiments. It identified specific times when PSC are expected to start and end. It also confirmed the potential of the fibres to reduce PSC and identified the reason why fibres reduce PSC.

6. Conclusions and future prospects

The main objectives of this study was to provide the fundamental understanding of the phenomena of plastic shrinkage cracking (PSC) in conventional concrete as well as the principles involved for the improved performance of the low volume fibre reinforced concrete (LV-FRC) with regards to PSC.

The following significant conclusions in terms of PSC in conventional and LV-FRC can be drawn from this study:

- No PSC is possible before the total volume of water evaporated from the concrete surface does not exceed the total volume of bleeding water at the concrete surface. This is called the drying time. Furthermore, no plastic shrinkage crack will form at any location within a concrete element before air entry has occurred at this location. Both these events will only occur in environmental conditions with high evaporation rates. Thus, for conditions with low evaporation rates, these events will either occur to late or not at all, which significantly reduces the risk for PSC.

- If the environmental conditions are favourable for PSC, the majority of the plastic shrinkage cracks can be expected to start after the initial setting time of concrete and end before the final setting time of concrete. This is the critical time period where PSC is most likely to occur and can easily be determined for any mix. Any preventative measure for PSC would be most effective during this period. Furthermore, no new plastic shrinkage cracks will start after the final set of concrete has been reached.

- Bleeding has a significant influence on PSC. For conditions with high evaporation rates, the time when bleeding is no longer significant serves as a warning that PSC can be expected. Furthermore, mixes with a high bleeding capacity is less prone to PSC.

- The low volume of polymeric, synthetic fibres added to concrete in this study reduced bleeding which increases the risk for PSC. Despite this, all the fibres used reduced PSC to great effect. Once cracking has occurred, the fibres mainly reduce crack widening. Furthermore, the added resistance to cracking due to fibres seem to be consistent during the critical time period (between initial and final setting times) for a specific fibre type and volume fraction. The single fibre pullout tests also revealed that the interfacial shear bond stress between the fibre and the concrete paste which is mainly responsible for the resistance that fibres give to crack widening increases significantly from the initial set of concrete. This increase in crack widening resistance corresponds to the time when PSC are most likely to start, which explains why fibres are generally effective in reducing PSC.

From the knowledge gain during this study, the following are identified as important aspects that require further investigation:

- The influence of different levels of restraint on PSC needs to be investigated.

- The idea that PSC can be prevented by modifying the bleeding characteristics of the concrete mix has merit and should be investigated. This investigation requires the development of a method for measuring bleeding that accounts for the additional settlement due to the capillary pressure.

- The magnitude and the effect with time of the mechanisms that influence the pullout resistance of fibres need to be investigated. These mechanisms are adhesion and friction for the fibres used in this study.

- The validity of the proposed equation which calculates the stress that can be bridged by fibres over a unit crack area needs to be investigated.

- A practical model that uses the fundamental knowledge gained from this study needs to be developed. This model will use the knowledge of the times when PSC are

expected to start and end as well as the knowledge of the factors that influences the magnitude and likelihood of PSC. The aforementioned equation will also form an integral part of the model. This model can be used to develop the guidelines needed for the design and prevention of PSC in conventional concrete and LV-FRC.

7. References

Addis, Brian. 1998. *Fundamentals of Concrete*. Midrand: Cement and Concrete Institute.

Addis, B. & Owens, G. (eds). 2001. Fulton's concrete technology. 8th ed. Midrand: Cement & Concrete Institute.

Ahmadi, B.H. 2000. Initial and final setting time of concrete in hot weather. *Materials and Structures*, 33:511-514, October.

ASTM C 1579. 2006. *Standard Test Method for Evaluating Plastic Shrinkage Cracking of Restrained Fiber Reinforced Concrete*. West Conshohocken: ASTM International.

Boghossian, & Wegner, L.D. 2008. Use of flax fibres to reduce plastic shrinkage cracking in concrete. *Cement & Concrete Composites*, 30:929-937.

Chryso SA. 2007. *General Catalogue 1ste Edition: 2007*. Boksburg: Chryso South Africa.

Combrinck, R. & Boshoff, W.B. 2010. Investigation of plastic shrinkage cracking in concrete. *Proceedings of the Fourth International Conference on Structural Engineering, Mechanics and Computation*, Cape Town, 6-8 September 2010, 224. London: CRC Press/Balkema.

Deif, A., Martín-Pérez, B., & Cousin, B. 2009. Experimental study of chloride penetration in an RC slab sustaining in-service loads. *Proceedings of the Eighth International Conference on Creep, Shrinkage and Durability of Concrete and Concrete Structures*, Ise-Shima, 30 September - 2 October 2008, 1107 -1113. London: CRC Press/Balkema.

Forrester, R.G. 2004, *"Crypsystem" Treatment Process Enhances Polypropylene Fibre Reinforcement Performance in Shotcrete and Concrete*. Magaliesburg: Omega Consulting Services.

Garcia, A., Castro-Fresno, D. & Polanco, J.A. 2008. Maturity Approach Applied to Concrete by Means of Vicat Tests. *ACI Materials Journal*, 105(5): 445-450, September-October.

Hannant, D.J. 1978. *Fibre Cements and Fibre Concretes*. New York: John Wiley & Sons.

Illstone, J.M. & Domone, P.L.J. (eds). 2001. *Construction Materials: their nature and behaviour*. 3rd ed. New York: Spon Press.

Josserand, L. & De Larrard, F. 2004. A method for concrete bleeding measurement. *Materials and Structures*, 37:666-670, December.

Kronlöf, A., Markku, L., & Sipari, P. 1995. Experimental study on the basic phenomena of shrinkage and cracking of fresh mortar. *Cement and Concrete Research*, 25:1747-1754.

Kwak, H.-G. & Ha, S.-J. 2006. Plastic shrinkage cracking in concrete slabs. Part II: numerical experiment and prediction of occurrence. *Magazine of Concrete Research*, 58(8):517-532, October.

Marais, L.R. & Perrie, B.D. 1993. *Concrete industrial floors on the ground*. Midrand: Portland Cement Institute.

Mehta, P.K. & Monteiro, P.J.M. 2006. *Concrete: microstructure, properties, and materials*. 3rd ed. New York: McGraw-Hill.

National Ready Mixed Concrete Association (NRMCA). 2006. *Concrete in Practice: CIP 5 Plastic Shrinkage Cracking*. [Brochure]. Clobo.

Powers, Treval C. 1968. *The Properties of Fresh Concrete*. New York: John Wiley & Sons, Inc.

Qi, C., Weiss, J. & Olek, J. 2003. Characterization of plastic shrinkage cracking in fibre reinforced concrete using image analysis and a modified Weibull function. *Materials and Structures*, 36:386-395, July.

SANS 1083*. 2002. *Aggregates from natural sources – Aggregates for concrete.* Edition 2.1. Pretoria: Standards South Africa.

SANS 50196-3. 2006. *Methods for testing cement Part 3: Determination of setting times and soundness.* 2nd ed. Pretoria: Standards South Africa.

SANS 5862-1. 2006. *Concrete tests – Consistence of freshly mixed concrete – Slump test.* 2nd ed. Pretoria: Standards South Africa.

Slowik, V., Schmidt, M. & Fritzsch, R. 2008. Capillary pressure in fresh cement-based materials and identification of the air entry value. *Cement & Concrete Composites*, 30:557-565.

Slowik, V., Neumann, A., Dorow, J. & Schmidt, M. 2009. Early age cracking and its influence on the durability of concrete structures. *Proceedings of the Eighth International Conference on Creep, Shrinkage and Durability of Concrete and Concrete Structures*, Ise-Shima, 30 September - 2 October 2008, 471-477 . London: CRC Press/Balkema.

Slowik, V., Schmidt, M., Hubner, T. & Villmann, B. 2009. Simulation of capillary shrinkage cracking in cement-like materials. *Cement & Concrete Composites*, 31:461-469.

Smit, H. 2009. *Die ontwerp en evaluering van 'n prototipe toetsmetode om plastiese krimp kraakvorming onder Suid-Afrikaanse klimaatstoestande te kwantifiseer*. University of Stellenbosch.

Suhr, S. & Schoner, W. 1990. Bleeding of Cement Pastes. *Properties of Fresh Concrete: Proceedings of the Colloquium organized on behalf of the Coordinating Committee for Concrete Technology of RILEM*, Hanover, 3-5 October 1990, 33-40. London: Chapman and Hall.

Tatman, N. 2008. Wind tunnel design and operation. Available online: http://www.radford.edu/~chem-web/Physics/images/nathan-tatman-thesis.pdf [19 January 2010]

Uno, P.J. 1998. Plastic Shrinkage Cracking and Evaporation Formulas. *ACI Materials Journal*, 95(4):365-375, July-August.

Van der Spuy, J. 2010. [Personal communication]. 9 February 2010.

Wittmann, F.H. 1976. On the Action of Capillary Pressure in Fresh Concrete. *Cement and Concrete Research*, 6(1):49-56.

Wongtanakitcharoen, T. 2005. *Effect of Randomly Distributed Fibres on Plastic Shrinkage Cracking of Cement Composites*. Michigan: The University of Michigan. (PHD-thesis).

Zeiml, M., Leithner, D., Lackner, R. & Mang, H.A. 2006. How do polypropylene fibres improve the spalling behaviour of in-situ concrete?. *Cement and Concrete Research*, 36:929-942.

Zheng, Z. & Feldman, D. 1995. Synthetic Fibre-Reinforced Concrete. *Prog. Polym. Sci*, 20:185-210.

Zietsman, C. 2010. [Personal communication]. 9 February 2010.

List of appendices

Appendix A: Climate chamber design and performance verification

This appendix contains information about the design and layout of the first climate chamber built by Smith (2009) as well as the improved climate chamber that was redesigned and rebuilt by the author. The problems encountered with the first climate chamber during preliminary experiments on plastic shrinkage cracking (PSC) and how these problems were dealt with in the improved design are discussed. The performance of the improved climate chamber during the experiments is also evaluated.

A.1. First climate chamber layout and design (Smith, 2009)

The layout of the first climate chamber is shown in Figure A1.

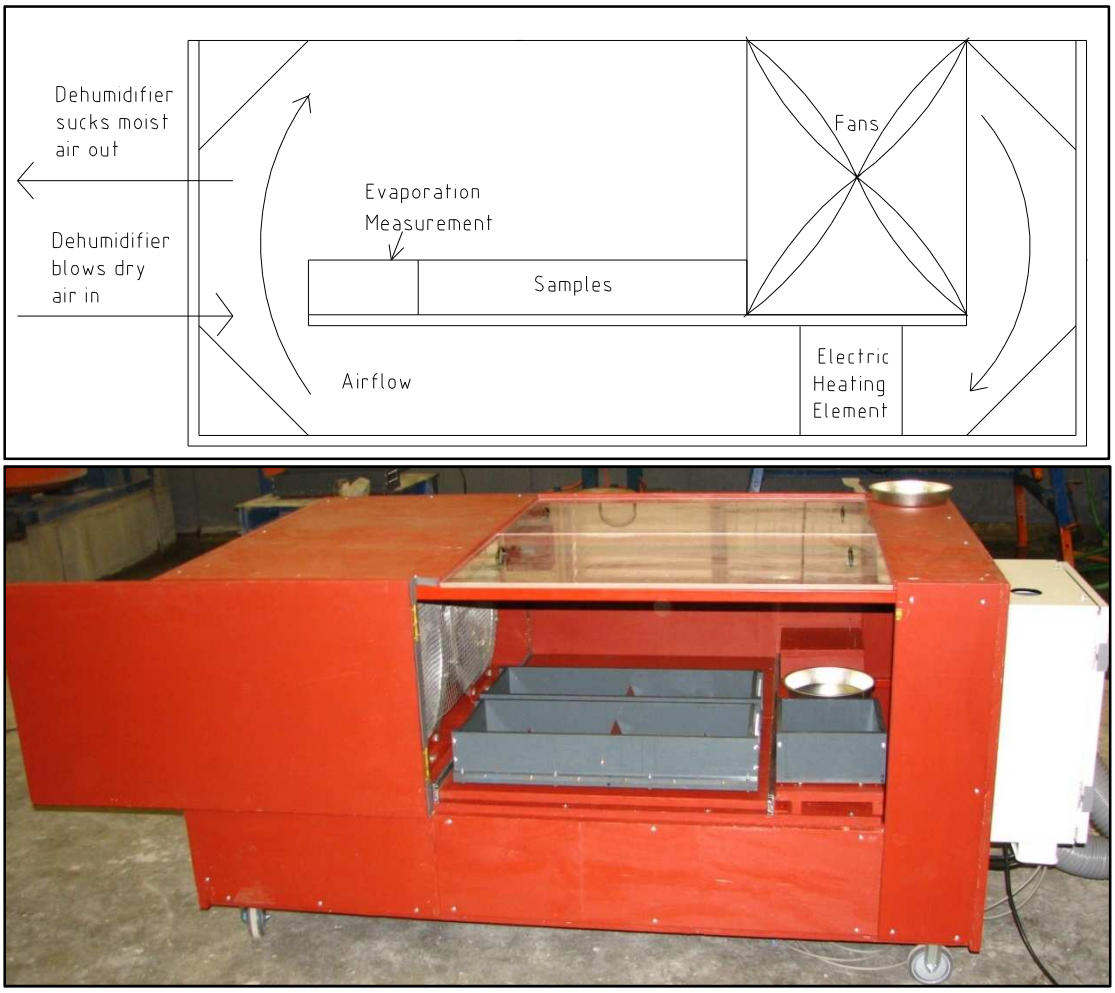

Figure A1: First climate chamber layout (Smith, 2009)

The 45° edges in the corners of the climate chamber directed the air flow created by the fans in a clockwise direction. The fans could be set to a variety of speeds which resulted in equivalent wind speeds over the samples. The temperature and the relative humidity could be controlled electronically with a heating element and dehumidifier respectively. The dehumidifier sucks moist air out of the chamber and pumps in dry air. The climate chamber therefore created the ideal environment for testing fresh concrete specimens under severe controlled climatic conditions which includes high wind speeds, high temperature and low relative humidity.

The climate chamber could accommodate four rectangular PVC moulds (PSC measurements), two square PVC moulds (concrete water evaporation measurements) and two circular metal pans (water evaporation measurements). The full details of the old design can be seen in the report by Smith (2009). The main focus of the design was to ensure that the capacity and size of the heating element, dehumidifier and fans were sufficient to control the environmental conditions inside the climate chamber. The end result was a climate chamber which could create a stable environmental condition in terms of temperature and relative humidity.

A.2. Problems with first climate chamber

During preliminary experiments on PSC conducted in the first climate chamber by the author in several aerodynamic and practical problems were encountered.

A.2.1. Aerodynamic Problems

The air flow inside the climate chamber was non-uniform and turbulent due the following unsound aerodynamic properties:

The climate chamber had no clearly defined path of air flow, but rather allowed multi-directional air flow. In principal air always flows from a high pressure (blow side of fan) to low pressure (suction side of fan) using the path of least resistance. Since the fans were not sealed on the sides it created two main paths for the air to travel form high to low pressure. The air could either flow directly back to the suction side of fans through the holes at the

side of the fans or it could be forced into the much smaller space beneath the samples from where it can circulate back to the suction side of the fans. This caused large volumes of air circulated directly back to the suction side of the fans, since the path beneath the sample had a lot of resistance. The resistance of the flow path beneath the samples was caused by the following factors:

- The large volume of air which was force into a smaller space caused a bottleneck effect or type of traffic jam at the beginning of the flow path beneath the samples.
- The air was forced to make a 180° turn in a small space without much guidance; furthermore the majority of the air was obstructed by a 90° wall.
- The air that managed to enter the flow path beneath the samples had an increase in speed due to the smaller volume but then also decreased in speed as it entered the bigger volume above the samples (principal of continuity).
- The fans were operating in reverse. This caused inefficiency because the fans were not working in their intended design direction.
- A great deal of turbulence was caused by the sharp edges and turns as well as the friction caused by the rough wood surface.
- The position of the dehumidifier intake caused a flow of air opposite to the intended wind direction. This caused additional turbulence especially during low wind speed tests.

A.2.2. Practical Problems

The evaporation specimens inside the chamber had to be weighed manually every 20 minutes which was not only labour intensive and time consuming, but also caused human errors in measurements which led to inaccurate results. The weighing process also disturbed the environmental conditions because the chamber had to be opened constantly for measurements. This included evaporation, crack growth and setting time measurements.

A.3. Guidelines for improving climate chamber

To address the problems associated with the first climate chamber a decision was made to redesign and rebuild the climate chamber. The objectives of the new design were to achieve a uniform wind speed over the test samples and incorporate new electronic testing equipment for measurements. The equipment included electronic scales for measuring evaporation as well as temperature and capillary pressure sensors in the concrete specimens. The existing fans, heating elements, dehumidifier, control box, electrical systems and moulds were reused in the new climate chamber.

Mr. Cobus Zietsman (2010), the Head Technical Officer of the Mechanical Engineering Department of Stellenbosch University who has years of practical experience with wind tunnels, and Mr. Johan van der Spuy (2010), a senior lecturer at the Thermo-Fluid Division also at the Mechanical Engineering Department of Stellenbosch University both gave advice and guidelines of how to correct the aerodynamic problems. They highlighted the following points to consider for the new design:

- The samples should be on the suction side of fans where the air flow is less turbulent and more uniform.

- The suction side of the fan should have a diffuser. A diffuser is a compartment which slowly expands along its length, which allows the fluid pressure to increase with decreasing velocity. The angle of the diffuser should not be more than 21° to minimize boundary layer separation which causes flow unsteadiness.

- Fans should always be used in their intended turning direction for maximum efficiency.

- Normal axial fans put an amount of swirl in the exit flow, this can be corrected by installing pre-rotation vanes upstream of the fans.

- Axial fans should be sealed at the sides to avoid any direct air circulation from the blow to the suction side of the fan.

- Changes in flow direction should be as smooth and efficient as possible. Use 180° turns curved continuously without any straight parts as far as possible.

- The use of screens just before the tests section will decrease vortex sizes and increase air flow uniformity. A screen is basically a sieve.

- Placing an air mixer just downstream of the heating element will cause an even air temperature distribution.

- Turning vanes can be used in the 180° turns to avoid uneven air density distribution due to the centrifugal force present in a bend. The position of these turning vanes may differ for different wind speeds and should be determined with a numerical model of the entire system.

A.4. Improved design and layout

A detailed numerical model was needed to predict and simulated the flow and flow efficiency of the climate chamber accurately. Due to limited time and knowledge no such numerical model was used for the design of the climate chamber, instead good guidelines, advice and some engineering judgement was used for the design. A discussion of the design and layout for the improved climate chamber as shown in Figure A2 follows:

A.4.1. Material

The entire wind tunnel except the test compartment is rolled out of 1.5 mm thick galvanized steel sheeting, which gives negligible friction. The sheeting is galvanized to prevent corrosion. The test compartment with moulds is lined with PVC and the covers are made of transparent Perspex. The supporting frame is made of 25 x 25 x 2 mm mild steel tubing and the entire frame is covered with plywood for insulation. The steel tubing is painted with a

rust inhibiting primer for protection against corrosion and the wood is painted with a waterproofing system from Plascon.

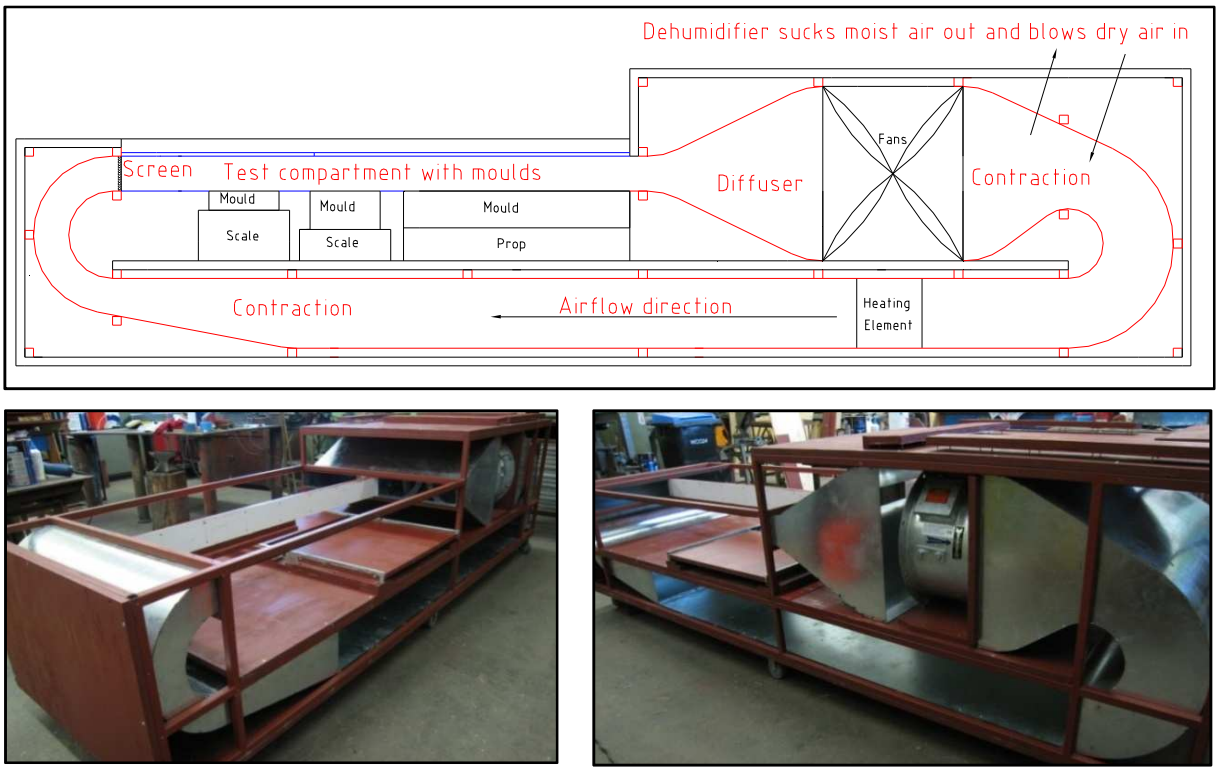

Figure A2: Improved climate chamber layout

A.4.2. Diffuser

The diffuser is located between the test compartment and the fans and because of limited space the angles are 26°, which is still in range of the prescribed 21°. The function of the diffuser is to recover pressure from the kinetic motion of the air in the test compartment which thereby reduces the power required to drive the wind tunnel (Tatman, 2008:11).

A.4.3. Fans

The fans no longer work in reverse, but blow in their intended design direction towards the contraction. This causes wind flow clockwise trough the wind tunnel. The fans are also sealed to ensure that no air flows directly back to the suction side. No pre-rotation fanes were included to reduce the swirl caused by the fans, because different shape pre-rotation fanes would be required for each fan speed.

A.4.4. 180° turns

The 180° turns are curved continuously with no straight sections which increase the turn efficiency. No turning vanes were included due to complex construction and design issues.

A.4.5. Contractions

The first contraction is located directly after the fans and throttles the air into the first 180° turn. The second contraction is just before the second 180° turn which is followed by the test compartment. Contractions are normally put just before the test region of a wind tunnel to increase the mean velocity and minimize inconsistencies in flow uniformity (Tatman, 2008:10).

A.4.6. Screen

Screens are typically put before the test section of a wind tunnel to increase flow uniformity. The screen must have an open-area ratio (β) of smaller that 0.57. With $\beta = (1-d/L)^2$, where d is the diameter of the wire and L is the length between each wire (Tatman, 2008:9). This requires the d/L-ratio to be less than 0.245. Figure A3 shows the plastic screen used at the beginning of the test compartment, the d/L- ratio is 0.15, with d = 1.5 mm and L = 10 mm. The d/L-ratio of the installed screen therefore complies with the requirements.

Figure A3: Plastic screen used at the beginning of the test compartment

A.4.7. Test compartment

The test compartment contains all the moulds and can be viewed through Perspex covers. The rest of the test compartment is lined with PVC except for the surfaces of the specimens themselves. Figure A4 shows the test compartment with specimens during a test.

Figure A4: Test compartment with Perspex covers and PVC lining inside

A.4.8. Dehumidifier

The in- and outtake of the dehumidifier are located in the middle of the wind tunnel at the top of the first contraction after the fans as shown in Figure A2. The moist air gets sucked out directly downstream of the fans and the dry air is pumped in directly downstream of the air intake. This results in minimal disturbance of the air flow and also maintains the air flow direction.

A.4.9. Heating element

No air mixer was place downstream of the heating element due to the additional air resistance that it may create. It can be considered if there is a problem with an uneven temperature distribution in the air flow.

A.4.10. Measuring devices

The sensors that measure the temperature and the relative humidity in the climate chamber are located in the middle of the chamber at the beginning of the test compartment. The electronic measuring scales, concrete temperature and pressure sensors can be fitted to the concrete specimens located in the test compartment. Electronic measurements results in less manual labour and minimum disturbance of the environmental conditions.

A.5. Improved climate chamber performance during experiments

An assessment of the performance of certain aspects of the improved climate chamber and measuring equipment follows:

A.5.1. Wind

Wind speed measurements were taken at 18 different points uniformly distributed over the test compartment. Six of these points were located at the beginning of the test compartment as well as six in the middle and six at the end of the compartment. The measurements were repeated for the entire range of fan speeds in increments of 5 Hz. The results of the measurements showed big improvement from the first climate chamber. The wind speed is relatively uniform over the entire test compartment with the biggest coefficient of variance (COV) of 16% at a fan speed of 5 Hz.

The wind speed at maximum fan capacity is nearly 70 km/h, which is more than double the wind speed the first climate chamber could reach. The results of the measurements are shown in Table A1. The relationship between the average wind speed over the 18 points and fan speed is linear with an R-squared value of 0.9986, as shown in Figure A5. The graph or the trend line in Figure A5 can be used to estimate the wind speed in the test compartment for a selected fan speed.

Table A1: Wind speed measurements

Fan speed [Hz]	*μ = Average wind speed [km/h]*	σ = Standard deviation [km/h]	COV [%]
0	*0.0*	0.0	0.0
5	*4.0*	0.7	16.5
10	*11.5*	1.5	12.8
15	*18.1*	2.4	13.4
20	*26.1*	3.0	11.6
25	*33.4*	4.4	13.2
30	*40.7*	4.6	11.4
35	*47.5*	5.4	11.4
40	*54.3*	5.8	10.6
45	*61.3*	7.2	11.7
50	*69.3*	6.1	8.7

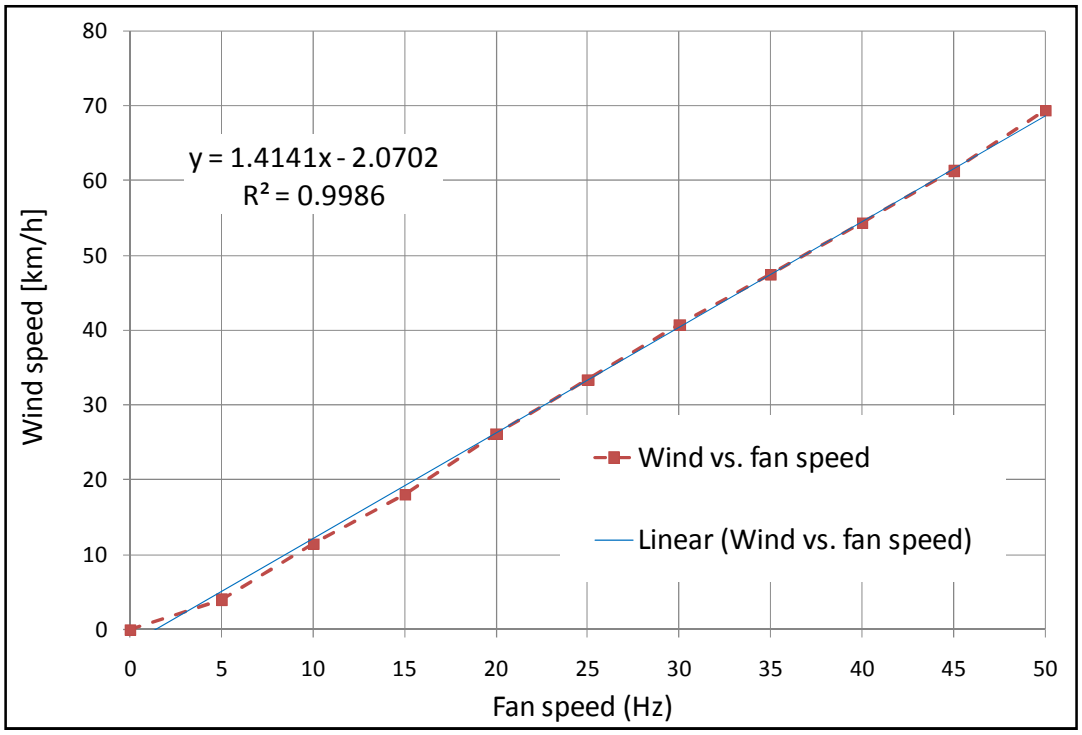

Figure A5: Graph of fan speed [Hz] vs. wind speed [km/h]

A.5.2. Temperature and relative humidity

Figures A6 to A8 show the results of measurements of temperature and relative humidity at the beginning of the test compartment in the climate chamber. The climate chamber manages to control the temperature and relative humidity effectively to preset values for high and low wind speeds.

The change in temperature and relative humidity after 60 minutes in Figure A6 was due to the placement of a second mix in the climate chamber, which disturbed the environmental conditions. The disturbance was only noticed for high wind speeds. At low wind speeds the environmental conditions were more stable as shown in Figure A7, which also had a second mix placed in the climate chamber after 60 minutes.

It can be concluded that the opening of the climate chamber at high wind speed causes more disturbance of the conditions, because the fans at higher wind speeds draws in more air from the outside environment and pushes out more air from inside the climate chamber. It was also observed that the relative humidity decreases below the preset values if the mix has minimum bleeding characteristics as sown in Figure A8 and can be prevented by placing additional water in the climate chamber.

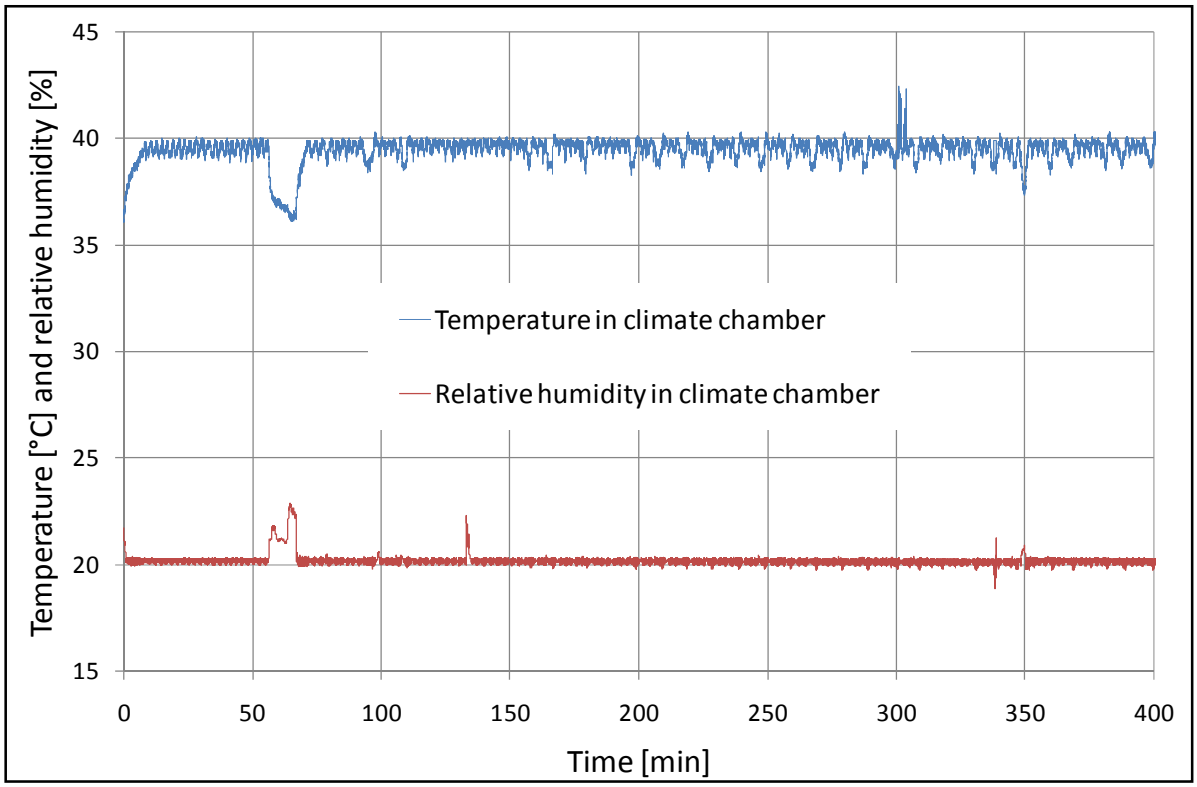

Figure A6: Climate chamber temperature and relative humidity for a mix with normal bleeding under high wind speed

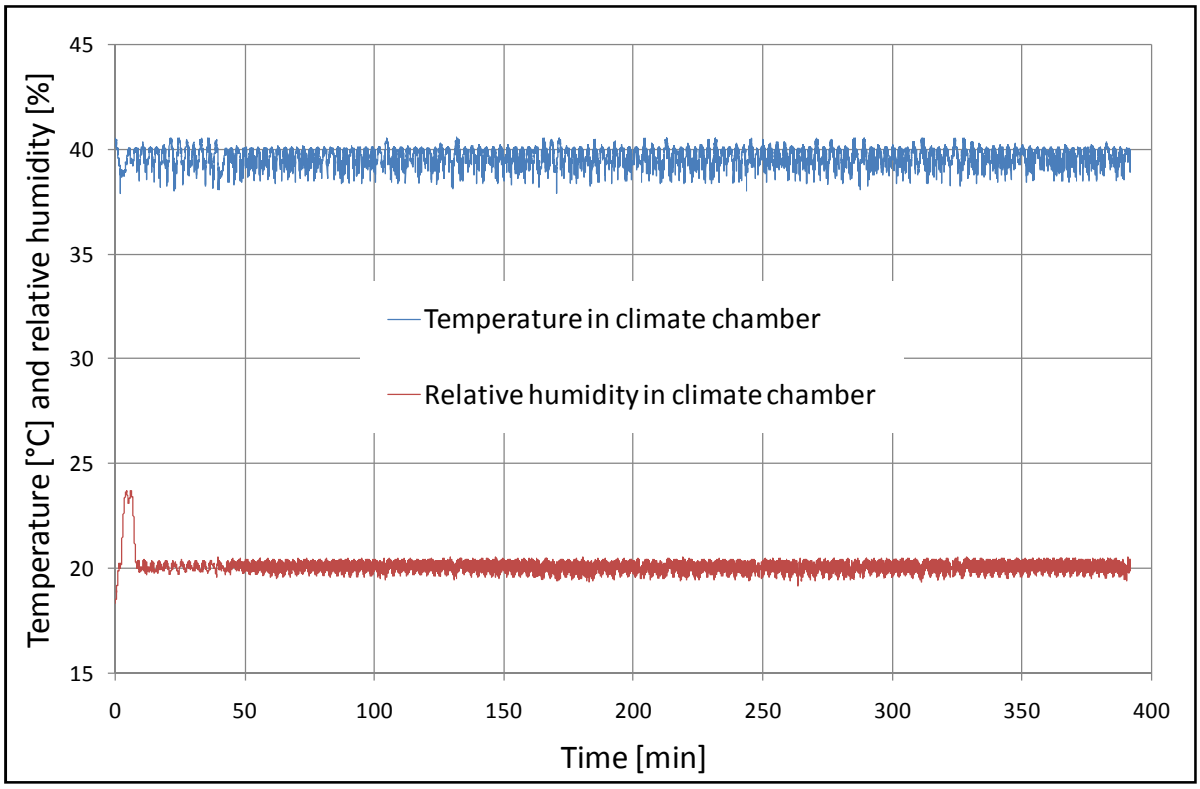

Figure A7: Climate chamber temperature and relative humidity for a mix with normal bleeding under low wind speed

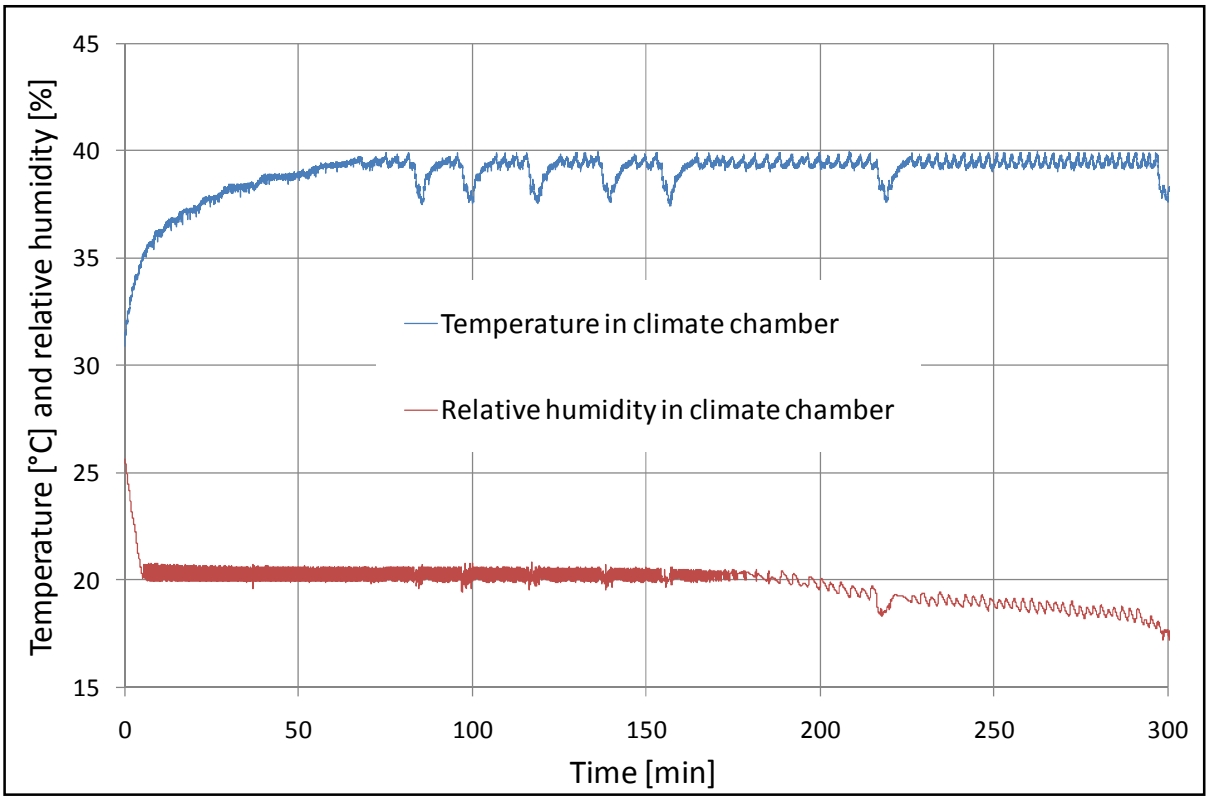

Figure A8: Climate chamber temperature and relative humidity for a mix with minimum bleeding under high wind speed

A.5.3. Concrete Temperature

Figures A9 and A10 show the results of temperature measurements inside the concrete specimens at high and low wind speeds respectively. In general the temperature reached after 400 minutes at the high wind speed was on average 5 °C more than the temperature reached at the lower wind speed. The higher wind speed results in a faster increase of the concrete temperature.

This difference in concrete temperature is the main reason for the quicker setting time of the mixes at higher wind speeds, since an increase in temperature increases the setting times.

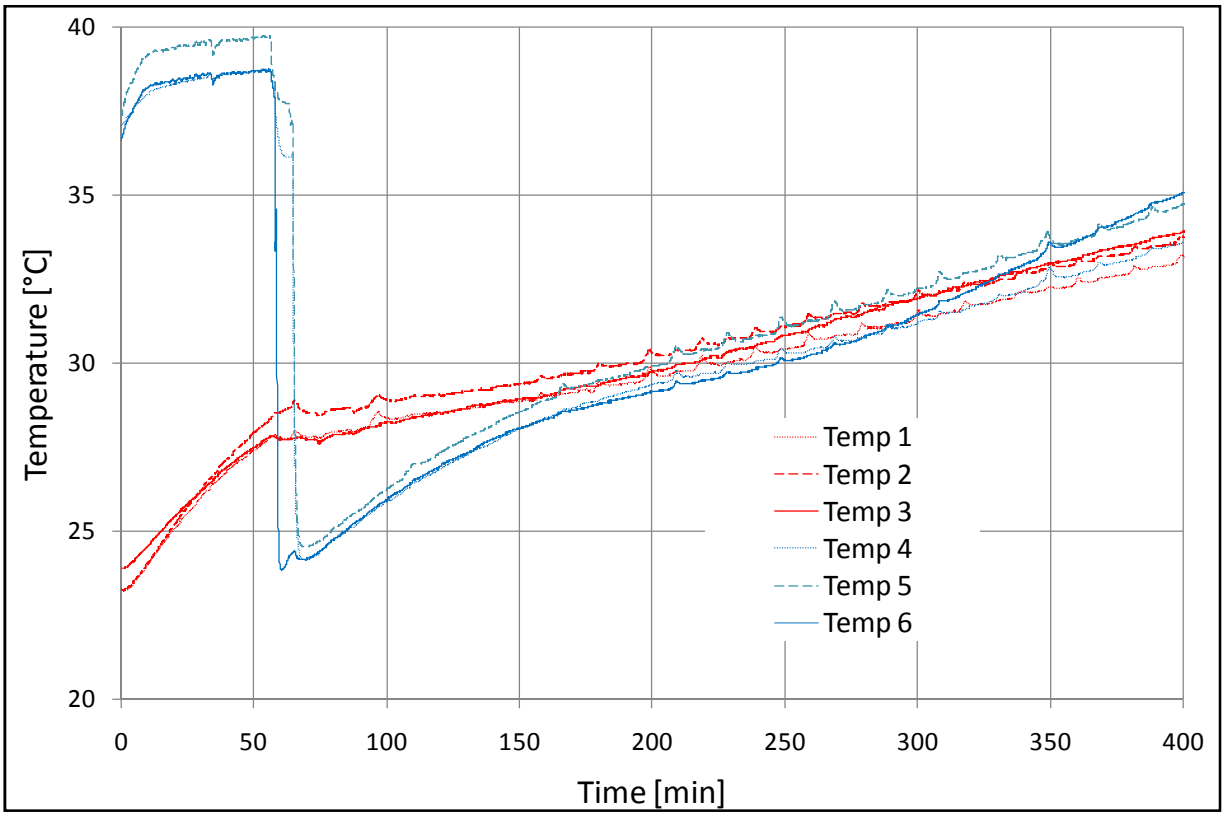

Figure A9: Temperature in concrete for a mix with enough bleeding under high wind speed

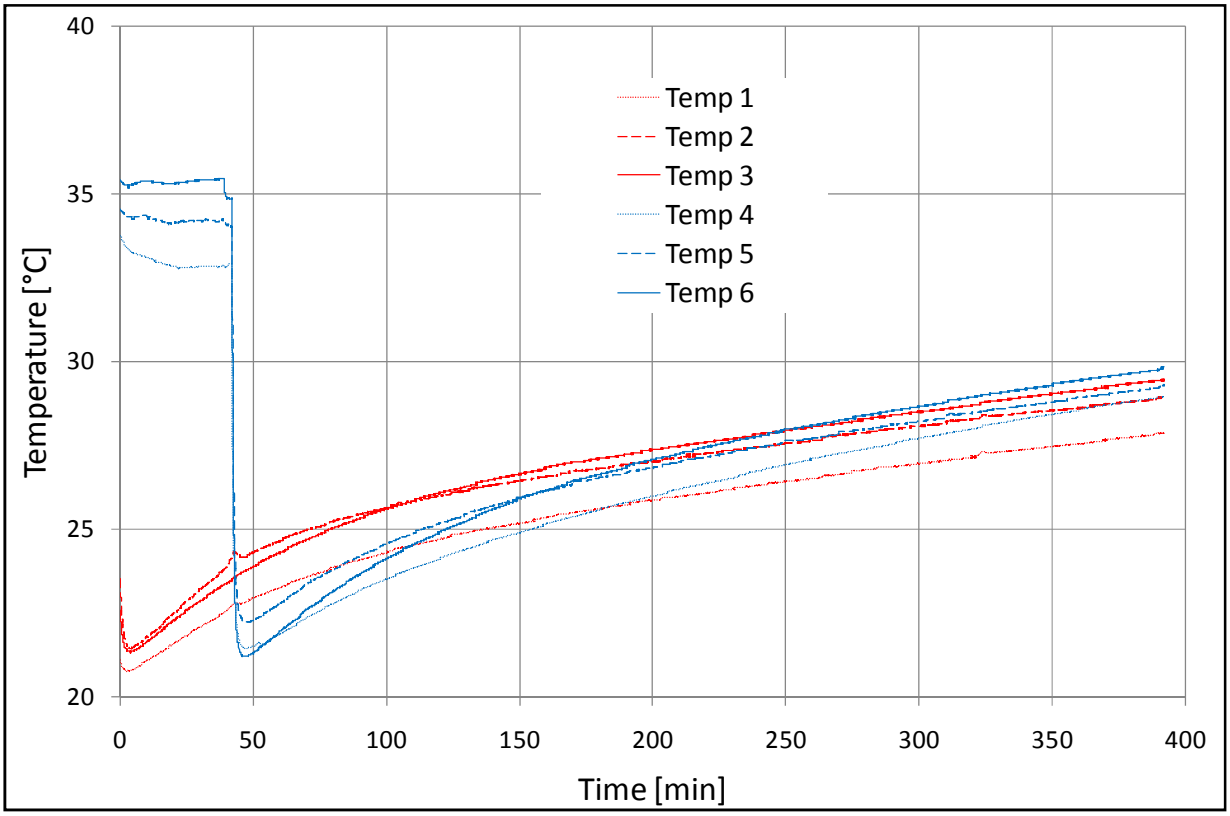

Figure A10: Temperature in concrete for a mix with enough bleeding under low wind speed

A.5.4. Scales

The result of a single electronic scale used for measuring the concrete evaporation at high wind speed is shown in Figure A11. The results show a clear increase in weight every time the climate chamber is opened to conduct crack measurements. This increase was accounted for by using the average weight of the specimen in 20 minutes intervals, as shown by the moving average line in Figure A11.

These average values were used to determine the cumulative evaporation amounts, which led to satisfactory results, as shown in Figure A12. The figure shows the calculated cumulative evaporation using the aforementioned average values for two different mixes at different climates. It also shows the cumulative evaporation using the equation proposed by Uno (1998:368) as well as the pan evaporation for both climates. All the mentioned cumulative evaporation amounts for the specific climates and mixes show similar trends.

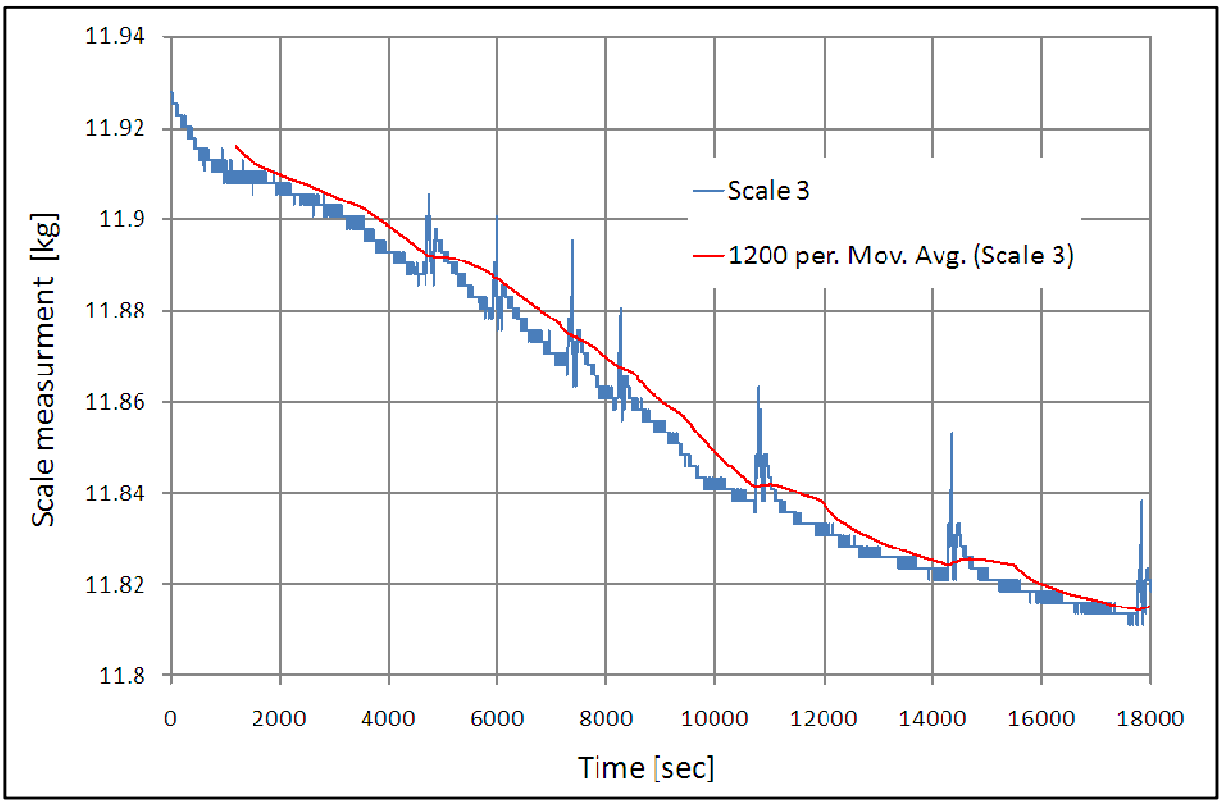

Figure A11: Scale measurements of concrete evaporation

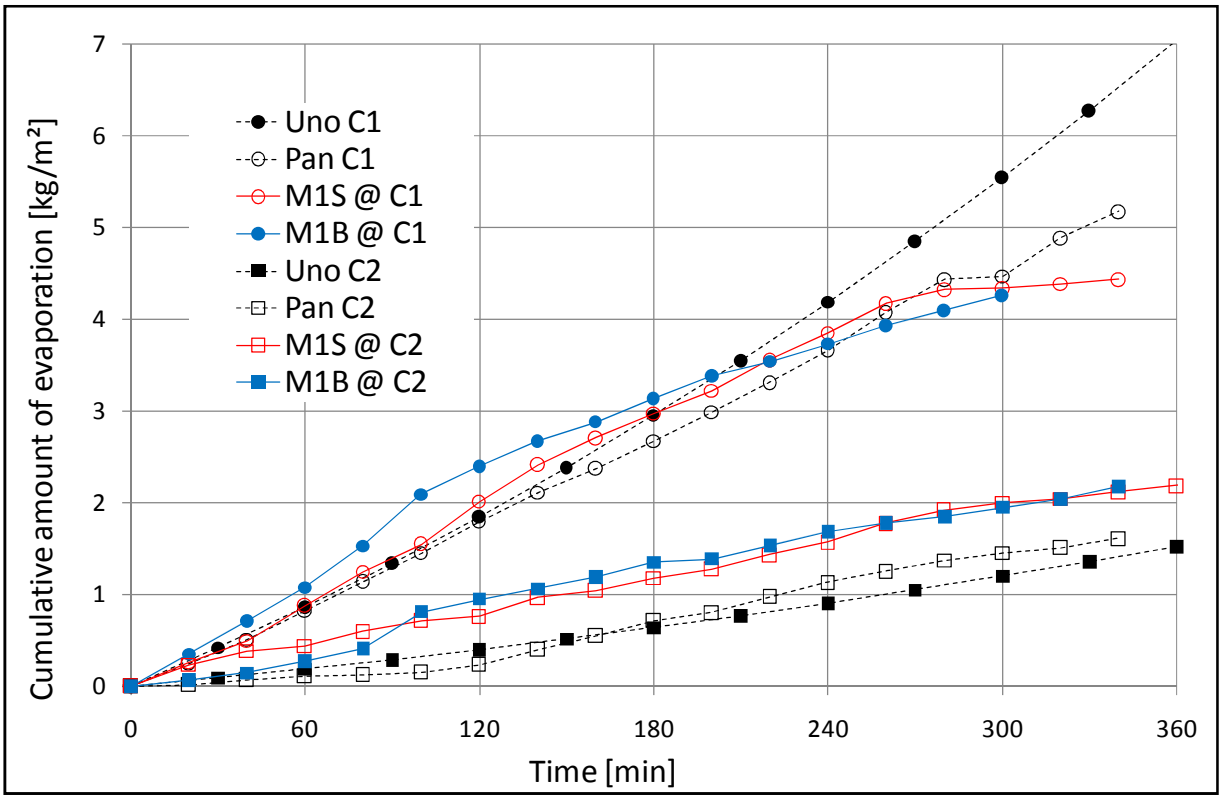

Figure A12: Cumulative evaporation amounts at Climates 1 and 2

A.5.5. Capillary pressure

Figure A13 shows two examples of capillary pressure measurements. The initial positive pressure is due to the hydrostatic pressure acting on the sensor tip. Air entry is characterized with a significant drop in pressure after a period of consistent pressure build-up. The inconsistencies before air entry can be explained as the pressure relieve when the concrete paste debonds from the frictionless sides of the PSC moulds which occurs mainly in the transverse direction.

The measurement of capillary pressure remains a local measurement and can be influenced by inconsistencies near the sensor tip which may disturb the connection of the sensor with the capillary pore system. Inconsistencies are caused by large aggregates blocking the sensor tip and also small particles or air bubbles which may have entered the sensor tip. Despite this, good measurements of capillary pressure all in the range of -5 to -30 kPa were obtained. This is the same magnitude as measured by Slowik (2008:563-564) for concrete paste.

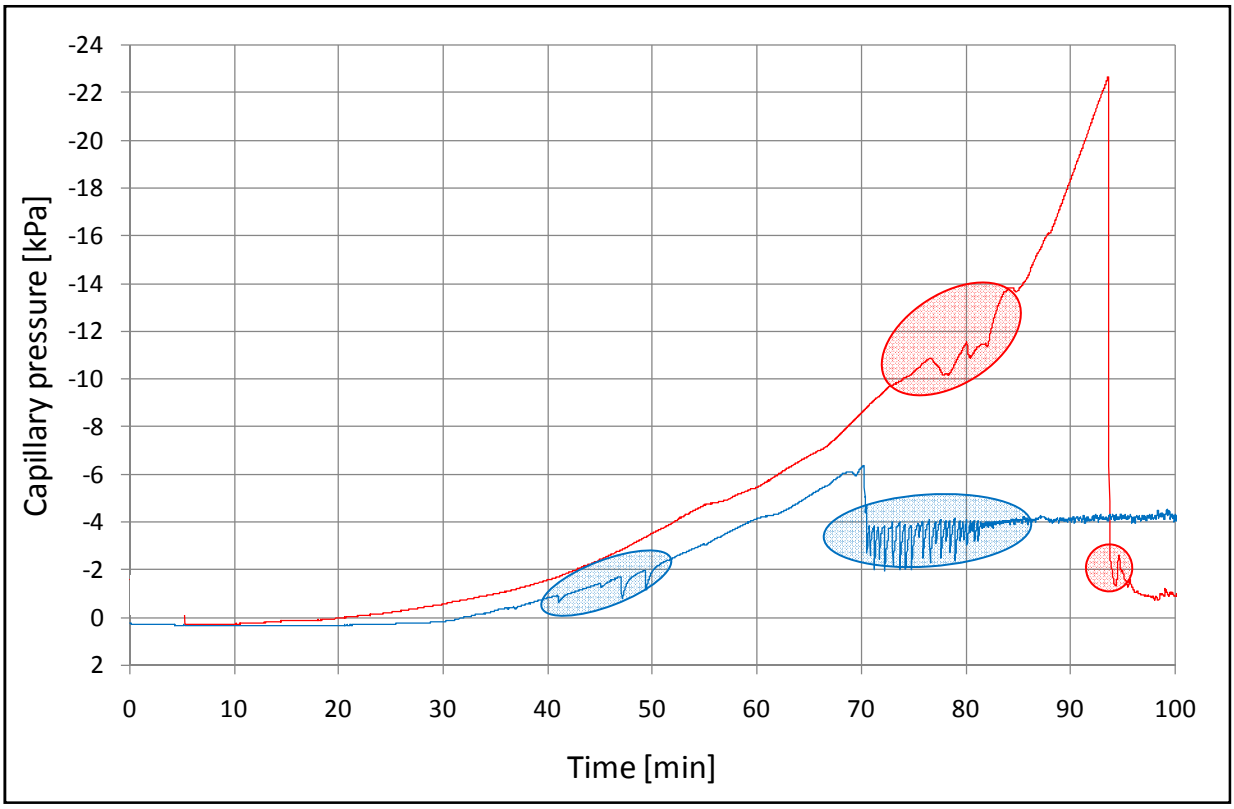

Figure A13: Typical capillary pressure measurements

A.5.6. Crack measurements

The method of crack measurement requires the opening of the climate chamber to take pictures. This causes disturbance of the conditions especially for high wind speeds as seen in Figures A8 and A11. A method of measurement which causes fewer disturbances is sought after.

A.5.7. Plastic shrinkage cracking (PSC) moulds

The rectangular moulds shown in Figure A1 were used for the measurement of the PSC. The experiments with the variations of Mix 1 showed considerable debonding (see Figure A14) form the sides of the moulds in the longitudinal direction of the moulds, which may have resulted in additional crack growth. The results also showed no measureable cracks when fibres were added to M1S. To avoid the same result for the variations of Mix 2 an additional restraint was added in the form of a round steel bar, at each end of the mould as shown in Figure A15. The added restraint resulted in minimal debonding from the sides of the moulds at the longitudinal edges and caused visible cracks with and without fibres.

Figure A14: Debonding of concrete form mould side

Figure A15: PSC mould with additional restraint

Appendix B: Plastic shrinkage cracking test results

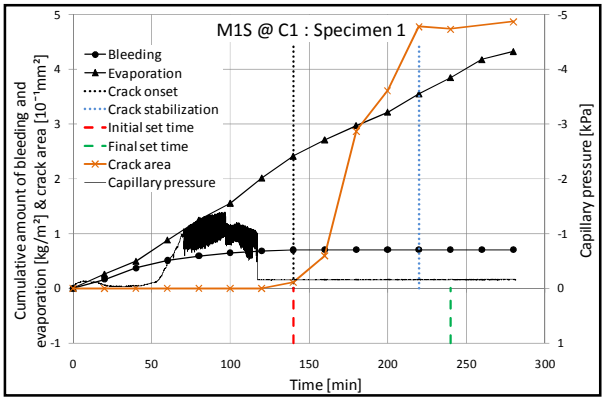

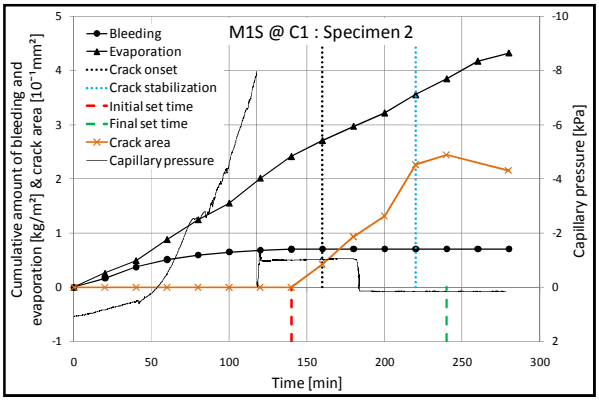

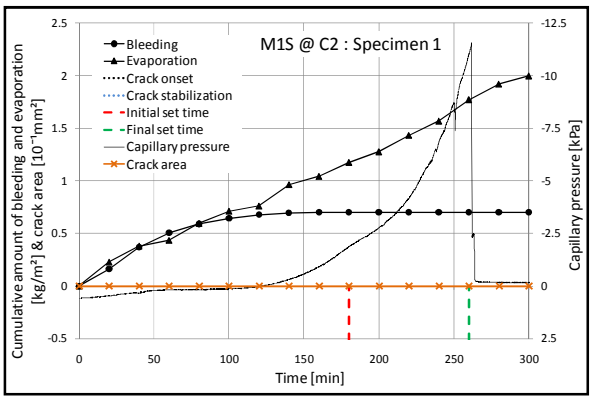

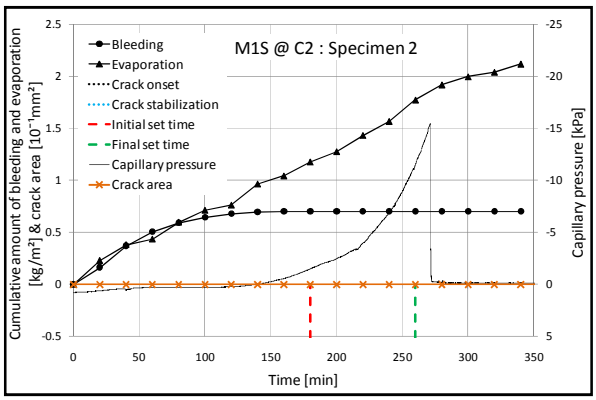

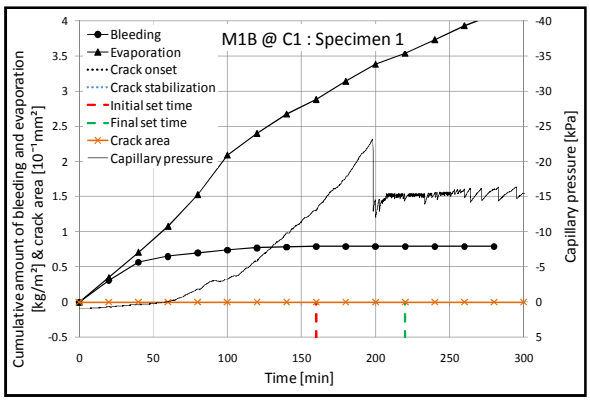

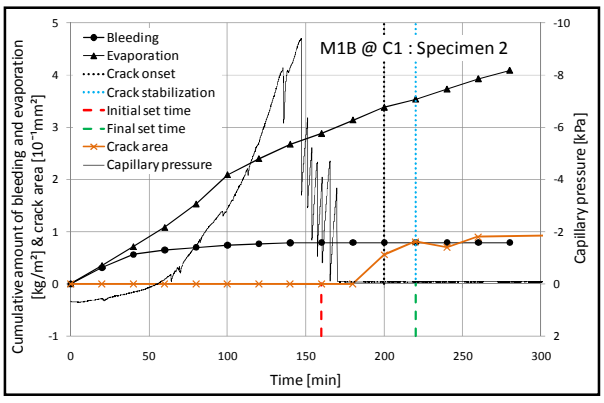

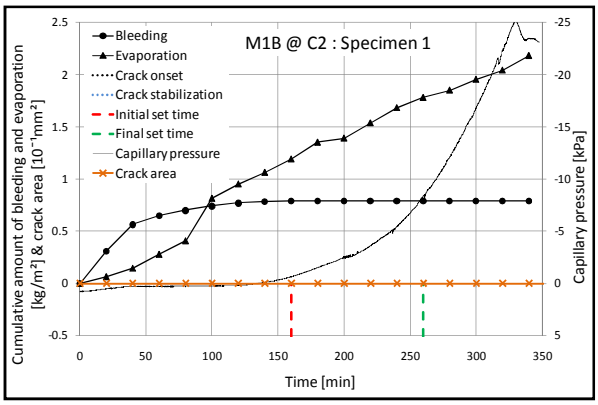

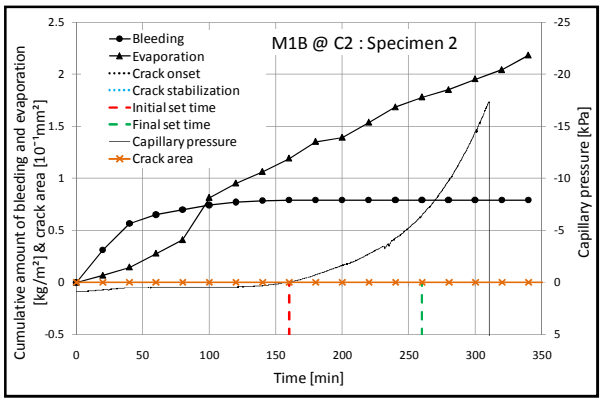

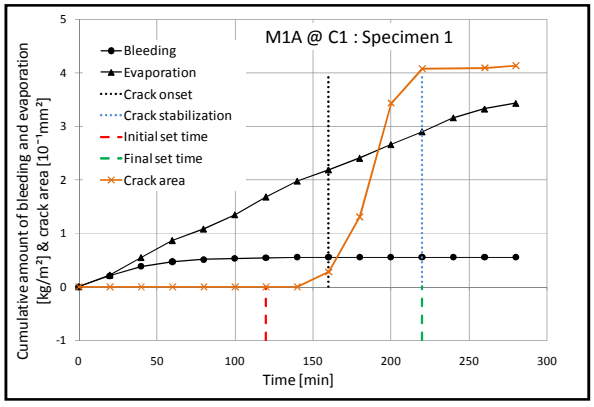
M1A @ C1 : Specimen 1
Bleeding
Evaporation
Crack onset
Crack stabilization
Initial set time
Final set time
Crack area
Cumulative amount of bleeding and evaporation [kg/m²] & crack area [10⁻¹mm²]
Time [min]

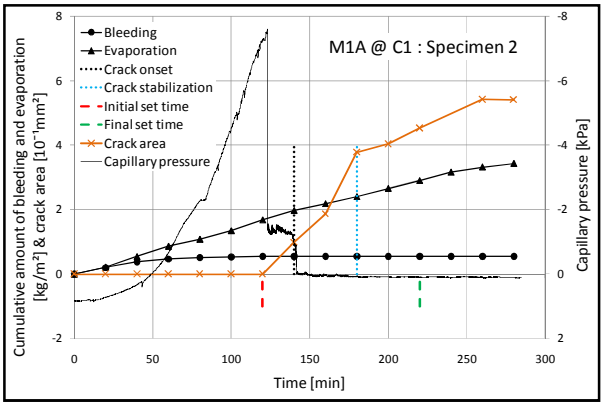
M1A @ C1 : Specimen 2
Bleeding
Evaporation
Crack onset
Crack stabilization
Initial set time
Final set time
Crack area
Capillary pressure
Cumulative amount of bleeding and evaporation [kg/m²] & crack area [10⁻¹mm²]
Capillary pressure [kPa]
Time [min]

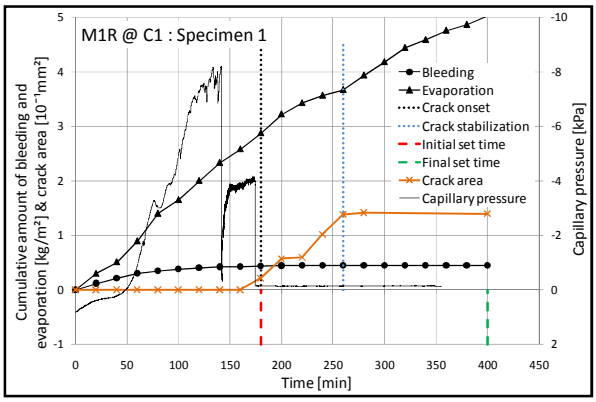
M1R @ C1 : Specimen 1
Bleeding
Evaporation
Crack onset
Crack stabilization
Initial set time
Final set time
Crack area
Capillary pressure
Cumulative amount of bleeding and evaporation [kg/m²] & crack area [10⁻¹mm²]
Capillary pressure [kPa]
Time [min]

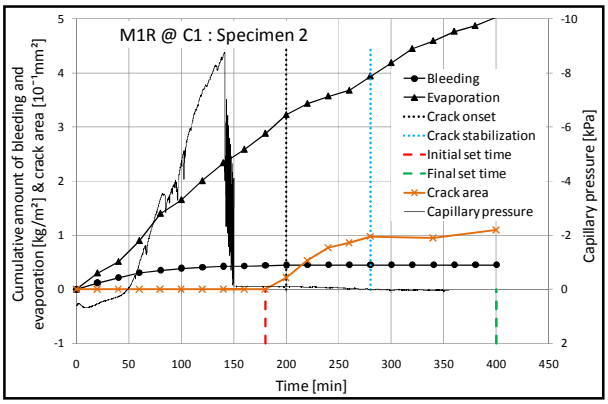
M1R @ C1 : Specimen 2
Bleeding
Evaporation
Crack onset
Crack stabilization
Initial set time
Final set time
Crack area
Capillary pressure
Cumulative amount of bleeding and evaporation [kg/m²] & crack area [10⁻¹mm²]
Capillary pressure [kPa]
Time [min]

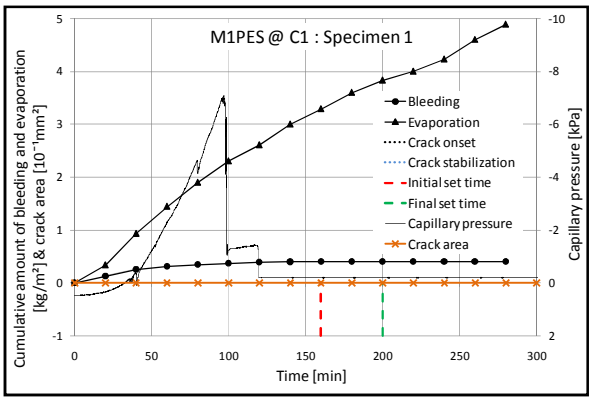
M1PES @ C1 : Specimen 1
Bleeding
Evaporation
Crack onset
Crack stabilization
Initial set time
Final set time
Capillary pressure
Crack area
Cumulative amount of bleeding and evaporation [kg/m²] & crack area [10⁻¹mm²]
Capillary pressure [kPa]
Time [min]

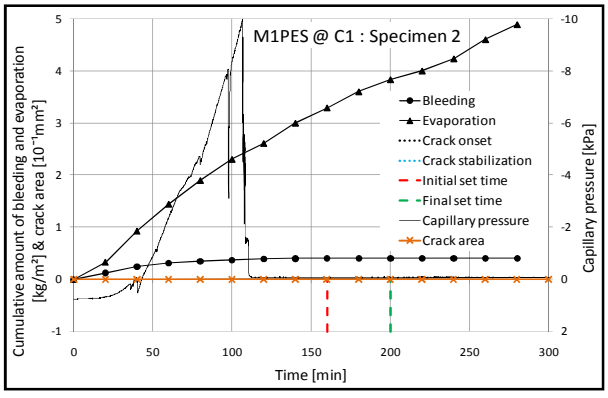
M1PES @ C1 : Specimen 2
Bleeding
Evaporation
Crack onset
Crack stabilization
Initial set time
Final set time
Capillary pressure
Crack area
Cumulative amount of bleeding and evaporation [kg/m²] & crack area [10⁻¹mm²]
Capillary pressure [kPa]
Time [min]

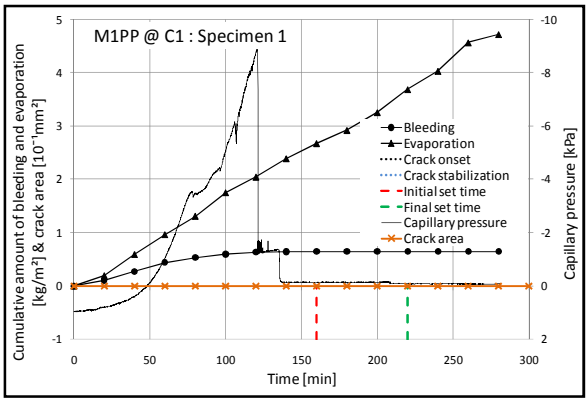
M1PP @ C1 : Specimen 1
Bleeding
Evaporation
Crack onset
Crack stabilization
Initial set time
Final set time
Capillary pressure
Crack area
Cumulative amount of bleeding and evaporation [kg/m²] & crack area [10⁻¹mm²]
Capillary pressure [kPa]
Time [min]

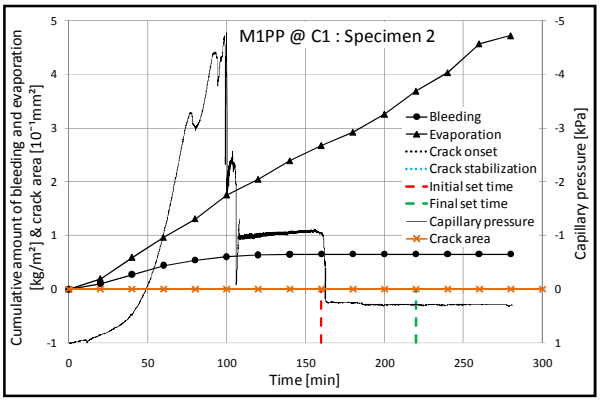
M1PP @ C1 : Specimen 2
Bleeding
Evaporation
Crack onset
Crack stabilization
Initial set time
Final set time
Capillary pressure
Crack area
Cumulative amount of bleeding and evaporation [kg/m²] & crack area [10⁻¹mm²]
Capillary pressure [kPa]
Time [min]

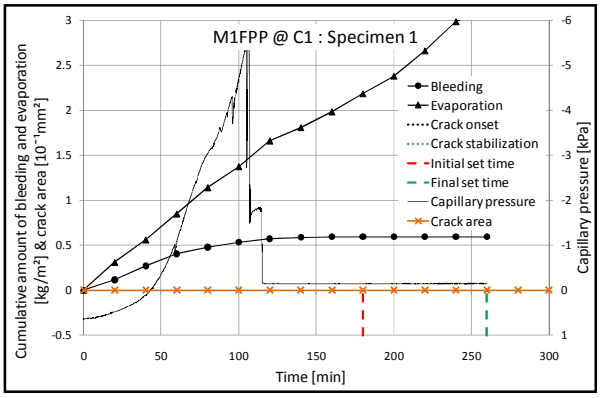
M1FPP @ C1 : Specimen 1
Cumulative amount of bleeding and evaporation [kg/m²] & crack area [10⁻¹mm²]
Capillary pressure [kPa]
Time [min]
Bleeding
Evaporation
Crack onset
Crack stabilization
Initial set time
Final set time
Capillary pressure
Crack area

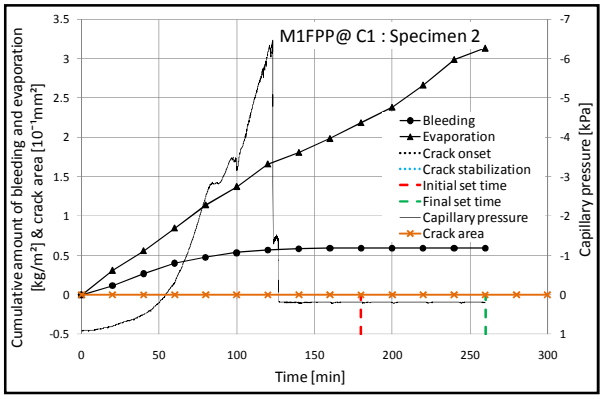
M1FPP@ C1 : Specimen 2
Cumulative amount of bleeding and evaporation [kg/m²] & crack area [10⁻¹mm²]
Capillary pressure [kPa]
Time [min]
Bleeding
Evaporation
Crack onset
Crack stabilization
Initial set time
Final set time
Capillary pressure
Crack area

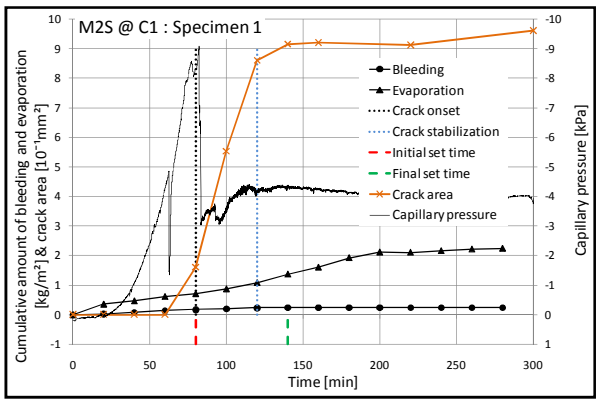
M2S @ C1 : Specimen 1
Cumulative amount of bleeding and evaporation [kg/m²] & crack area [10⁻¹mm²]
Capillary pressure [kPa]
Time [min]
Bleeding
Evaporation
Crack onset
Crack stabilization
Initial set time
Final set time
Crack area
Capillary pressure

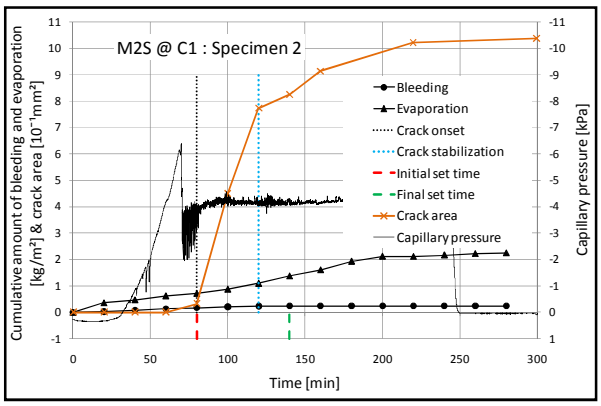
M2S @ C1 : Specimen 2
Cumulative amount of bleeding and evaporation [kg/m²] & crack area [10⁻¹mm²]
Capillary pressure [kPa]
Time [min]
Bleeding
Evaporation
Crack onset
Crack stabilization
Initial set time
Final set time
Crack area
Capillary pressure

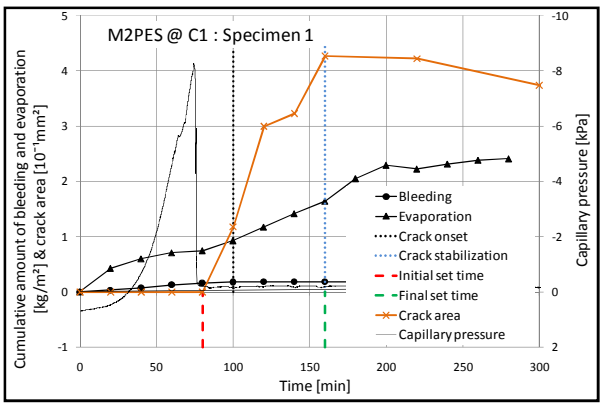
M2PES @ C1 : Specimen 1
Cumulative amount of bleeding and evaporation [kg/m²] & crack area [10⁻¹mm²]
Capillary pressure [kPa]
Time [min]
Bleeding
Evaporation
Crack onset
Crack stabilization
Initial set time
Final set time
Crack area
Capillary pressure

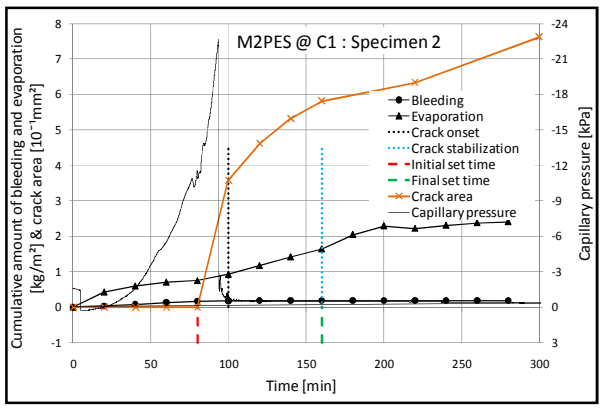
M2PES @ C1 : Specimen 2
Cumulative amount of bleeding and evaporation [kg/m²] & crack area [10⁻¹mm²]
Capillary pressure [kPa]
Time [min]
Bleeding
Evaporation
Crack onset
Crack stabilization
Initial set time
Final set time
Crack area
Capillary pressure

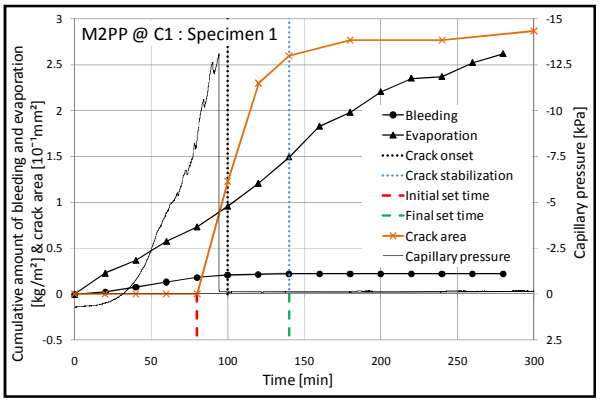
M2PP @ C1 : Specimen 1
Cumulative amount of bleeding and evaporation [kg/m²] & crack area [10⁻¹mm²]
Capillary pressure [kPa]
Time [min]
Bleeding
Evaporation
Crack onset
Crack stabilization
Initial set time
Final set time
Crack area
Capillary pressure

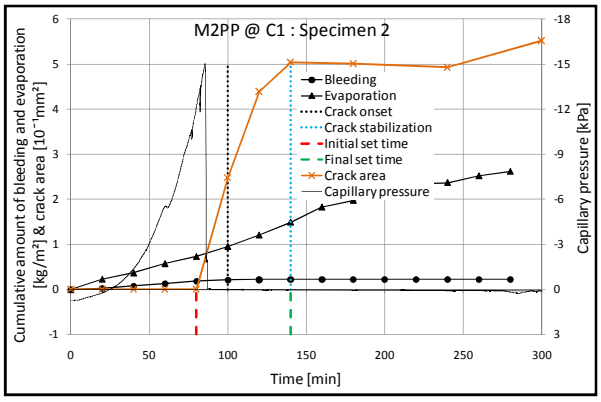
M2PP @ C1 : Specimen 2
Cumulative amount of bleeding and evaporation [kg/m²] & crack area [10⁻¹mm²]
Capillary pressure [kPa]
Time [min]
Bleeding
Evaporation
Crack onset
Crack stabilization
Initial set time
Final set time
Crack area
Capillary pressure

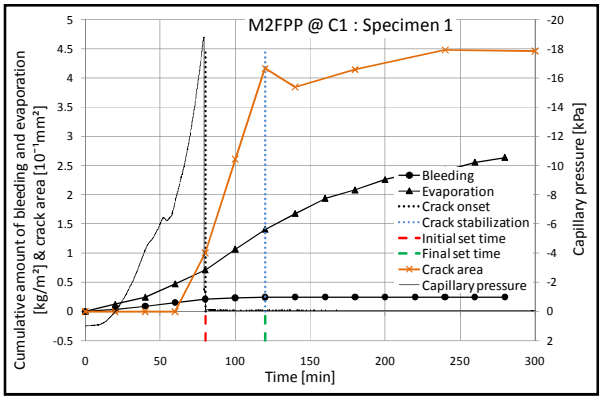

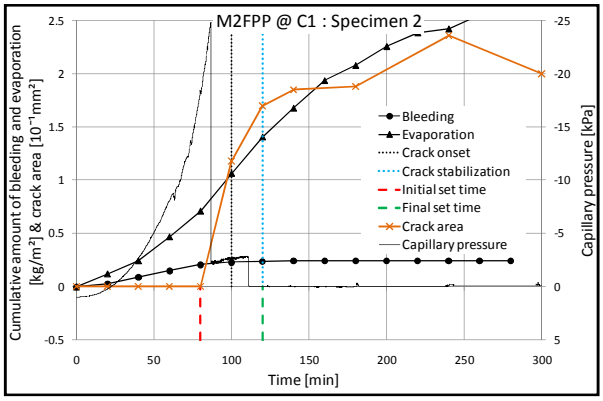

Table B1: Summary of the important times of all the PSC tests

Mix : Climate : Specimen	Time in minutes of							Total bleeding [g] amount at		[%]
	No bleeding	Air entry	Crack onset	Crack Stabilization	Initial set	Final set	Drying	End	Air entry	B_{AE}/B_{TOT}
	T_{NB}	T_{AE}	T_{CO}	T_{CS}	T_{IS}	T_{FS}	T_{D}	B_{TOT}	B_{AE}	
M1S : C3	160	-	-	-	208	360	-	-	-	-
M1S : C1 : S1	160	117	140	220	140	240	53	7.95	7.87	99
M1S : C1 : S2	160	118	160	220	140	240	47	7.95	7.88	99
M1R : C1 : S1	220	142	180	260	180	400	44	5.05	4.76	94
M1R : C1 : S2	220	141	200	280	180	400	42	5.05	4.76	94
M1A : C1 : S1	140	271	180	220	100	220	51	6.20	6.20	100
M1A : C1 : S2	140	123	140	220	100	220	45	6.20	6.12	99
M1B : C1 : S1	160	197	-	-	160	220	61	8.95	8.95	100
M1B : C1 : S2	160	147	200	220	160	220	55	8.95	8.92	100
M1S : C2 : S1	160	261	-	-	180	260	125	7.95	7.95	100
M1S : C2 : S2	160	270	-	-	180	260	140	7.95	7.95	100
M1B : C2 : S1	160	328	-	-	160	260	144	8.95	8.95	100
M1B : C2 : S2	160	310	-	-	160	260	150	8.95	8.95	100
M1PES : C1 : S1	160	100	-	-	140	200	35	4.60	4.25	92
M1PES : C1 : S2	160	105	-	-	140	200	37	4.60	4.30	93
M1PP : C1 : S1	160	120	-	-	140	220	39	7.35	7.20	98
M1PP : C1 : S2	160	100	-	-	140	220	38	7.35	6.80	93
M1FPP : C1 : S1	160	105	-	-	140	240	40	6.70	6.15	92
M1FPP : C1 : S2	160	120	-	-	140	240	44	6.70	6.45	96
M2S : C3	140	-	-	-	140	230	-	-	-	-
M2S : C1 : S1	140	82	80	120	80	140	20	2.70	1.99	74
M2S : C1 : S2	140	70	80	140	80	140	27	2.70	1.73	64
M2PES : C1 : S1	120	74	100	160	80	160	28	2.05	1.68	82
M2PES : C1 : S2	120	93	100	160	80	160	27	2.05	1.95	95
M2PP : C1 : S1	140	94	100	140	80	140	27	2.50	2.26	90
M2PP : C1 : S2	140	85	100	140	80	140	28	2.50	2.13	85
M2FPP : C1 : S1	140	78	80	120	80	120	15	2.75	2.29	83
M2FPP : C1 : S2	140	86	100	120	80	120	23	2.75	2.43	88

Appendix C: Single fibre pullout test results

Table C1: Summary of fibre pullout results from M1S

Time [hours]		1,2,3h	4h	5h	6h	7h	12h	24h
Polyester (PES) Le = Embedded length [mm] = 20 L = Length [mm] = 12 duc = Uncut diameter [µm] = 18 Vf = Volume fraction [%] = 0.065 dc = Cut diameter [µm] = 18	Pullout force [mN]	0.32	1.14	2.05	4.70	x	72.0	156
		0.04	0.84	1.00	4.80	x	88.0	124
		0.25	1.10	3.75	4.65	12.5	86.0	112
		0.45	0.75	1.06	7.70	8.7	-	-
		0.43	1.00	0.95	4.00	21.3	-	-
		0.78	1.06	2.06	7.60	9.3	-	-
		x	0.42	0.62	2.80	7.2	-	-
Number of results from pullout force data		6	7	7	7	5	3	3
Standard deviation of pullout force data [mN]		0.25	0.25	1.08	1.82	5.7	8.7	22.7
F = Average pullout force [mN]		0.38	0.90	1.64	5.18	11.8	82.0	131
COV = Coefficient of variance of pullout force data [%]		65.1	28.3	66.1	35.2	48.0	10.6	17.4
τ = Interfacial shear bond stress [kPa] = F/(πdLe)		0.33	0.80	1.45	4.58	10.4	72.5	116
σc = Bridging stress over crack [kPa] = 0.5τVf(L/d)		0.07	0.17	0.31	0.99	2.30	15.7	25.0
Polypropylene (PP) Le = Embedded length [mm] = 20 L = Length [mm] = 12 duc = Uncut diameter [µm] = 20 Vf = Volume fraction [%] = 0.099 dc = Cut diameter [µm] = 30	Pullout force [mN]	0.50	0.72	3.50	4.40	6.70	62.5	75.5
		0.17	0.59	2.00	7.20	10.2	45.2	130
		0.37	1.00	1.45	5.70	20.4	56.8	122
		0.83	0.51	x	8.50	14.0	-	-
		0.23	0.96	x	6.05	15.9	-	-
		0.22	x	0.90	3.70	16.0	-	-
		x	0.41	2.60	2.65	18.2	-	-
Number of results from pullout force data		6	6	5	7	7	3	3
Standard deviation of pullout force data [mN]		0.25	0.24	1.01	2.03	4.7	8.8	29.4
F = Average pullout force [mN]		0.39	0.70	2.09	5.46	14.5	54.8	109
COV = Coefficient of variance of pullout force data [%]		64.3	34.5	48.3	37.3	32.4	16.1	27.0
τ = Interfacial shear bond stress [kPa] = F/(πdLe)		0.31	0.56	1.66	4.34	11.5	43.6	86.9
σc = Bridging stress over crack [kPa] = 0.5τVf(L/d)		0.06	0.11	0.33	0.86	2.3	8.6	17.2
Fluorinated polypropylene (FPP) Le = Embedded length [mm] = 20 L = Length [mm] = 12 duc = Uncut diameter [µm] = 20 Vf = Volume fraction [%] = 0.099 dc = Cut diameter [µm] = 30	Pullout force [mN]	0.27	0.58	1.80	6.05	13.5	100	134
		0.50	2.60	2.83	3.20	14.5	103	178
		0.28	2.43	3.63	4.50	7.4	87.0	135
		0.42	2.24	1.73	3.20	6.70	-	-
		1.43	0.46	1.09	4.00	9.70	-	-
		0.28	1.70	0.84	3.26	6.90	-	-
		x	0.55	0.87	2.85	10.7	-	-
Number of results from pullout force data		6	7	7	7	7	3	3
Standard deviation of pullout force data [mN]		0.45	0.96	1.06	1.12	3.20	8.50	24.8
F = Average pullout force [mN]		0.53	1.51	1.83	3.87	9.90	96.7	149
COV = Coefficient of variance of pullout force data [%]		85.0	63.4	57.8	28.9	32.0	8.80	16.7
τ = Interfacial shear bond stress [kPa] = F/(πdLe)		0.42	1.20	1.45	3.08	7.90	76.9	118
σc = Bridging stress over crack [kPa] = 0.5τVf(L/d)		0.08	0.24	0.29	0.61	1.60	15.2	23.5
Note: (x) means faulty measurement; (-) means not measured.								

Table C2: Summary of fibre pullout results from M2S

Time [hours]		1h	2h	3h	4h	5h
Polyester (PES) L_e = Embedded length [mm] = 20 L = Length [mm] = 12 d_{uc} = Uncut diameter [μm] = 18 V_f = Volume fraction [%] = 0.065 d_c = Cut diameter [μm] = 18	Pullout force [mN]	0.15	0.58	2.68	9.50	19.3
		0.46	0.91	0.84	11.7	x
		0.23	x	0.98	13.7	13.0
		0.28	0.81	0.87	6.20	13.3
		0.13	0.26	0.54	7.60	12.4
Number of results from pullout force data		5	4	5	5	4
Standard deviation of pullout force data [mN]		0.13	0.29	0.85	3.03	3.22
F = Average pullout force [mN]		0.25	0.64	1.18	9.74	14.5
COV = Coefficient of variance of pullout force data [%]		53.5	45.1	72.2	31.1	22.2
τ = Interfacial shear bond stress [kPa] = $F/(\pi d L_e)$		0.22	0.57	1.05	8.61	12.8
σ_c = Bridging stress over crack [kPa] = $0.5\tau V_f(L/d)$		0.05	0.12	0.23	1.87	2.78
Polypropylene (PP) L_e = Embedded length [mm] = 20 L = Length [mm] = 12 d_{uc} = Uncut diameter [μm] = 20 V_f = Volume fraction [%] = 0.099 d_c = Cut diameter [μm] = 30	Pullout force [mN]	0.17	0.39	2.31	16.8	23.1
		0.21	0.42	1.75	9.80	x
		0.18	2.37	1.15	10.3	26.7
		0.68	0.97	0.99	7.80	29.8
		0.17	0.42	0.84	7.10	x
Number of results from pullout force data		5	5	5	5	3
Standard deviation of pullout force data [mN]		0.22	0.85	0.61	3.84	3.35
F = Average pullout force [mN]		0.28	0.91	1.41	10.4	26.5
COV = Coefficient of variance of pullout force data [%]		79.1	92.9	43.4	37.1	12.6
τ = Interfacial shear bond stress [kPa] = $F/(\pi d L_e)$		0.22	0.73	1.12	8.24	21.1
σ_c = Bridging stress over crack [kPa] = $0.5\tau V_f(L/d)$		0.04	0.14	0.22	1.63	4.18
Fluorinated polypropylene (FPP) L_e = Embedded length [mm] = 20 L = Length [mm] = 12 d_{uc} = Uncut diameter [μm] = 20 V_f = Volume fraction [%] = 0.099 d_c = Cut diameter [μm] = 30	Pullout force [mN]	0.22	0.35	0.55	9.20	30.3
		0.19	0.29	0.96	4.80	18.5
		0.21	2.06	2.62	7.40	28.5
		0.27	0.58	1.63	6.10	27.1
		0.22	1.19	1.49	5.80	28.0
Number of results from pullout force data		5	5	5	5	5
Standard deviation of pullout force data [mN]		0.03	0.74	0.78	1.70	4.61
F = Average pullout force [mN]		0.22	0.89	1.45	6.66	26.5
COV = Coefficient of variance of pullout force data [%]		13.3	83.1	54.0	25.5	17.4
τ = Interfacial shear bond stress [kPa] = $F/(\pi d L_e)$		0.18	0.71	1.15	5.30	21.1
σ_c = Bridging stress over crack [kPa] = $0.5\tau V_f(L/d)$		0.03	0.14	0.23	1.05	4.17
Note: (x) means faulty measurement; (-) means not measured.						